A multidimensional omics analysis of the DNA damage response in *Caenorhabditis elegans*

Inaugural-Dissertation

der Mathematisch-Naturwissenschaftlichen Fakultät

der Universität zu Köln

zur

Erlangung des Doktorgrades

vorgelegt von

Diletta Edifizi

aus Padova, Italien

Köln, May 2017

A multidimensional omics analysis of the DNA damage response in *Caenorhabditis elegans*

Inaugural-Dissertation

zur

Erlangung des Doktorgrades

der Mathematisch-Naturwissenschaftlichen Fakultät

der Universität zu Köln

vorgelegt von

Diletta Edifizi

aus Padova, Italien

Köln, May 2017

The work described in this dissertation was conducted from March 2013 to March 2017 under the supervision of Prof. Dr. Björn Schumacher at the Institute for Genetics, University of Cologne, Zülpicher Straße 47a, D-50674, Cologne, Germany and CECAD Research Center, University of Cologne, Joseph-Stelzmann Straße 26, D-50931, Cologne, Germany.

Diese Arbeit wurde durchgeführt zwischen März 2013 und März 2017 unter der Anleitung von Prof. Dr. Björn Schumacher am Institut für Genetik der Universität zu Köln, Zülpicher Straße 47a, D-50674, Köln, Deutschland und am CECAD Forschungszentrum, Universität zu Köln, Joseph-Stelzmann Straße 26, D-50931, Köln, Deutschland.

Parts of this work have been published:
Teile dieser Arbeit wurden bereits verffentlicht:

Diletta Edifizi and Björn Schumacher
Genome Instability in Development and Aging: Insights from Nucleotide Excision Repair in Humans, Mice, and Worms
Biomolecules 2015, 5, 1855-1869; — doi: 10.3390/biom5031855

Berichterstatter:	Prof. Dr. Björn Schumacher
	Prof. Dr. Markus Krüger
Prüfungsvorsitzender:	Prof. Dr. Siegfried Roth
Tag der mündlichen Prüfung:	30 May 2017

There are no ideal conditions to write, study,

work or think, but it is only

the will, the passion and the stubbornness

to push a man to pursue

his own project.

K.Lorenz

Summary

DNA damage comprises a causal factor for ageing and ageing-associated diseases. Defects in genome maintenance pathways give rise to a variety of human congenital syndromes that are characterized by growth retardation, cancer susceptibility, and accelerated ageing. The specific consequences of unrepaired DNA damage in human diseases are particularly apparent in syndromes caused by distinct nucleotide excision repair (NER) defects; however, with yet poorly understood genotype-phenotype correlations and highly complex disease phenotypes. It is established that the equivalent mutations in the simple metazoan *Caenorhabditis elegans* reflect the distinct outcomes of DNA repair defects and allow investigation of the consequences of persistent DNA damage during animal development and ageing. Here, we conducted proteome, lipidome, and phosphoproteome analysis of NER-deficient animals in response to UV-B treatment to gain comprehensive insights into the full range of physiological adaptations to unrepaired DNA damage. We derive metabolic changes indicative of a tissue maintenance program and implicate an autophagy-mediated protoestatic response. We assign central roles for the IIS regulator DAF-2, and the EGF- and AMPK-like signalling pathways in orchestrating the adaptive response to DNA damage. Our results provide new insights into the DNA damage responses in the organismal context.

Zusammenfassung

DNA-Schäden zählen zu den grundlegenden Faktoren, die sowohl für das Entstehen von altersbedingten Krankheiten, als auch den Alterungsprozess selbst verantwortlich sind. Defekte in DNA-Schadensreparaturmechanismen verursachen zahlreiche kongenitale Syndrome im Menschen, die durch Wachstumshemmungen, ein erhöhtes Krebsrisiko sowie einen beschleunigten Alterungsprozess charakterisiert sind.

Die spezifischen Konsequenzen nichtreparierter DNA-Schäden, die während menschlicher Krankheiten auftreten können, sind besonders bei verschiedenen durch Defekte in Nukleotidexzisionsreparaturmechanismen ausgelösten Syndromen, wobei deren genauen Genotyp-Phänotyp-Korrelationen und hochkomplexen Krankheitsbilder noch immer unvollständig definiert sind.

Äquivalente Mutationen im mehrzelligen Modellorganismus *Caenorhabditis elegans* resultieren in ähnlichen DNA-Reparaturdefekten und erlauben daher eine eingehendere Untersuchung der Konsequenzen von bleibenden DNA-Schäden, die während der Entwicklung und des Alterungsprozesses des Tieres auftreten können.

In der vorliegenden Arbeit wurden UV-bestrahlte Würmer mit defizitärer Nukleotidexzisionsreparatur einer Proteom-, Lipidom-, und Phosphoproteomanalyse unterzogen, um einen umfassenden Überblick über die Gesamtheit der physiologischen Adaptionen an das Vorhandensein fortbestehender DNA Schäden zu erhalten.

Wir beobachten metabolische Veränderungen, die auf ein spezifisches Gewebeinstandhaltungsprogramm hindeuten und eine Autophagie-vermittelte, proteostatische Antwort implizieren. Wir bestimmen zentrale Rollen für den insulinähnlichen Signalwegsregulator DAF-2 und die EGF- und AMPK-hnlichen Signalwege in der Orchestrierung dieser DNA-Schadensantwort. Die Ergebnisse dieser Arbeit bieten neue Einblicke in die DNA-Schadensantworten im organismischen Kontext.

Abbreviations

°C	degree Celsius
6-4PP	6-4 pyrimidine pyrimidone photoproduct
μg	microgram
μl	microliter
μm	micrometer
ACN	acetonitrile
AD	Alzheimers disease
AGC	automatic gain control
AMPK	AMP-activated protein kinases
ATP	adenosine triphosphate
BER	base excision repair
BLAST	basic local alignment search tool
Ca2+	calcium
$CaCl_2$	calcium chloride
cAMP	cyclic AMP
C. elegans	*Caenorhabditis elegans*
Cer	ceramide

CDP-DAG	cytidine diphosphatediacylglycerol
CeTOR	*Caenorhabditis elegans* target of rapamycin
CGC	*Caenorhabditis* genetics center
CL	cardiolipin
cm	centimetre
CPD	cyclobutane pyrimidine dimer
CREB	cAMP- responsive element (CRE)-binding protein
CRTC-1	cAMP-regulated transcriptional co-activator
CS	Cockayne syndrome
CSA	Cockayne syndrome complementation group A
CSB	Cockayne syndrome complementation group B
CH_3COOH	acetic acid
CUL4A	cullin 4A
$CuSO_4$	copper sulfate
DAG	diacylglycerol
DAF-2	abnormal dauer formation 2
DAF-7	abnormal dauer formation 7
DAF-16/FOXO	abnormal dauer formation 16
DDB	DNA damage-binding protein
DDR	DNA damage response
DEW	Dewar valence isomers
DNA	deoxyribonucleic acid
DNA POL	DNA polymerase
dNTP	deoxynucleoside 5'-triphosphate
DSB	double-strand break

DTT	dithiothreitol
E. coli	*Escherichia coli*
EDTA	ethylenediaminetetraacetic acid
EGF	epidermal growth factor
EP	enriched peptone
ER	endoplasmic reticulum
ERCC1	excision repair cross-complementation group 1
EWL	entire worm lysate
FA	fatty acid
FDR	false discovery rate
GFP	green fluorescent protein
GG-NER	global-genome nucleotide excision repair
GlcCer	glucosylceramide
GO	gene ontology
GPCR	G protein-coupled receptor
GSEA	gene set enrichment analysis
GST	glutathione S-transferases
h	hours
H_2O	water
H_3PO_4	phosphoric acid
HCD	higher-energy collisional dissociation
HEPES	4-(2-hydroxyethyl)-1-piperazineethanesulfonic acid
HPTLC	high performance thin layer chromatography
HR	homologous recombination
IIS	insulin/insulin-like growth factor signalling

IP	immunoprecipitation
IR	ionizing radiation
kb	kilobases
KH_2PO_4	potassium dihydrogen phosphate
KOH	potassium hydroxide
KPO_4	potassium phosphate
KEGG	kyoto encyclopedia of genes and genomes
kV	kilovolt
L1-L4	larval stages 1 to 4
LB	lysogeny broth
LC-ESI-MS/MS	electrospray ionization-tandem mass spectrometry
LC-MS/MS	liquid chromatography-tandem mass spectrometry
Log	logarithm
Lys-C	endoproteinase
m/z	mass-to-charge ratio
M	molar
$MgCl_2$	magnesium chloride
$MgSO_4$	magnesium sulfate
m	minutes
ml	milliliter
mM	millimolar
mmBCFAs	monomethyl branched chain FAs
MMR	mismatch repair
mRNA	messenger RNA
MRM	multiple reaction monitoring

ms	milliseconds
MS	mass spectrometry
mJ/cm^2	millijoule/square centimeter
NaCl	sodium chloride
NaClO	sodium hypochloride
NER	nucleotide excision repair
NGM	nematode growth medium
NHEJ	non-homologous end joining repair
Na_2HPO_4	disodium phosphate
NH_4OH	ammonium hydroxide
nm	nanometer
p-value	probability value
PCNA	proliferating cell nuclear antigen
PCR	polymerase chain reaction
PC	phospahtidylcholine
PE	phosphatidylethanolamine
PG	phosphatidylglycerol
PI	phosphatidylinositol
PI3/AKT	phosphatidylinositol 3-kinase
PKC	protein kinase C
PIP2	phosphatidylinositol 4,5 bisphosphate
PLC	phospholipase C
pmol	picomole
ppm	parts per million
PS	phosphatidylserine

PTMs	post-translational modifications
r	Pearson correlation coefficient
RAD	radiation sensitive
rcf	relative centrifugal force
RNAP II	RNA polymerase II
RNP	ribonucleoprotein
RPA	replication protein A
rpm	revolutions per minute
ROC1	regulator of cullins 1
ROS	reactive oxygen species
s	seconds
S6K1	ribosomal protein S6 kinase beta-1
SD	standard deviation
Ser/S	serine
SFA	saturated fatty acid
SILAC	stable isotope labeling by aminoacids in cell culture
SL	sphingolipids
SM	sphingomyelin
SQST-1	sequestosome related
STAT	signal transducers and activators of transcription
SWI/SNF	switching defective/sucrose non-fermenter
TC-NER	transcription-coupled nucleotide excision repair
TFA	trifluoroacetic acid
TFIIH	transcription initiation factor IIH

Th	Thomson
Thr/T	threonine
TiO2	titanium dioxide
TLC	thin layer chromatography
TOR	target of rapamycin
TRIS	tris(hydroxymethyl)aminomethane
TTD	trichothiodystrophy
Tyr/Y	tyrosine
UFA	unsaturated fatty acid
UNC	uncoordinated
UPR	unfolded protein response
UPS	ubiquitin proteasome system
UV	ultraviolet
XP	xeroderma pigmentosum
XPA	xeroderma pigmentosum complementation group A
XPB	xeroderma pigmentosum complementation group B
XPC	xeroderma pigmentosum complementation group C
XPD	xeroderma pigmentosum complementation group D
XPE	xeroderma pigmentosum complementation group E
XPF	xeroderma pigmentosum complementation group F
XPG	xeroderma pigmentosum complementation group G

Contents

List of Figures

Chapter 1

Introduction

Global societies experience demographic changes with an increasing burden of ageing-associated diseases. Understanding the causes of ageing and the mechanisms driving the ageing process remains still one of the major scientific challenges. The maintenance of the genome throughout life is of particular importance, as the DNA damage accumulation is thought to comprise a driving factor for the ageing process [91, 238]. Indeed, DNA lesions are constantly formed amid genotoxic attacks by exogenous sources such as UV light (UV) and ionizing radiation (IR) or endogenous insults, such as reactive oxygen species (ROS) or metabolic by-products. To overcome the potential deleterious effects of genomic instability, cells have evolved specialized DNA repair systems, each repairing specific types of lesions. Base excision repair (BER) rapidly removes ROS and oxidized bases produced during metabolic processes [68]. Mismatch repair (MMR) swipes up mistakes missed by the replication machinery, through scanning the newly replicated strand [138]. The error-prone non-homologous endjoining (NHEJ) [142] and the accurate homologous recombination (HR) pathways [222] are key mechanisms for repairing DNA double strand breaks (DSBs). Bulky DNA lesions that disturb the normal double-helical structure of DNA, such as UV-induced 6-4 pyrimidine photoproducts (6-4PPs) [154] and cyclobutane pyrimidine dimers (CPDs) [211], are repaired by the nucleotide excision repair (NER) [**?**]. The bulky DNA lesions that disturb the normal double-helical structure of DNA, as UV-induced 6-4 pyrimidine photoproducts (6-4PPs) [154] and cyclobutane pyrimidine dimers (CPDs) [211], are repaired by the nucleotide excision repair (NER) [36]. Mutations in the above-mentioned DNA repair systems have been identified in human patients who suffer from elevated cancer susceptibility or premature ageing syndromes [209]. A clear

distinction between cancer susceptibility and premature ageing has been observed in patient groups that carry distinct mutations in NER. For this reason, mutations in NER have been highly instructive for understanding the links between unrepaired DNA damage, and cancer development and accelerated ageing.

1.1 Ultraviolet-induced DNA lesions

Sunlight is a primary energy source for life on earth, but can also pose a serious genotoxic threat for most living organisms due to the variety of its adverse effects [217]. UV radiation is a component of sunlight, and its electromagnetic spectrum can be subdivided into ranges depending on its wavelength: UV-A (400-315 nm), UV-B (315-280 nm) and UV-C (280-100 nm). UV-C is almost completely absorbed by the ozone layer and the atmosphere, along with most of the UV-B radiation [149]. UV-A is the most abundant but is less biologically relevant than UV-B, which is the best-absorbed radiation by the DNA [191]. UV radiation directly interacts with nucleotides to form mainly three types of mutagenic DNA lesions: CPDs [211], 6-4PPs [154], and Dewar valence isomers (DEWs) [225] **(Figure 1.1)**. CPDs are the most prevalent UV-induced DNA photoproducts, causing only a slight bend in the DNA helix, while the 6-4PPs induce a severe structural distortion of the DNA backbone at the site of the lesion [113]. 6-4PPs are easily converted into their related DEWs upon further exposure to UV-B radiation [192]. Some organisms that are highly exposed to sunlight, such as plants and marsupials, possess specialized photolyases that can directly revert either one of these lesions by splitting up the bulky bond [23]. Other organisms only employ the NER to repair the damage by excising a stretch of DNA surrounding the lesion and synthesizing a new undamaged strand [92].

1.2 The NER pathway

6-4PPs and CPDs, are removed by two distinct NER sub-pathways: global-genome (GG-) NER, which scans the entire genome for helix-distorting lesions, and transcription-coupled (TC-) NER, which is directed at locations of stalled transcriptional complexes in actively transcribed genes [152] **(Figure 1.2)**.

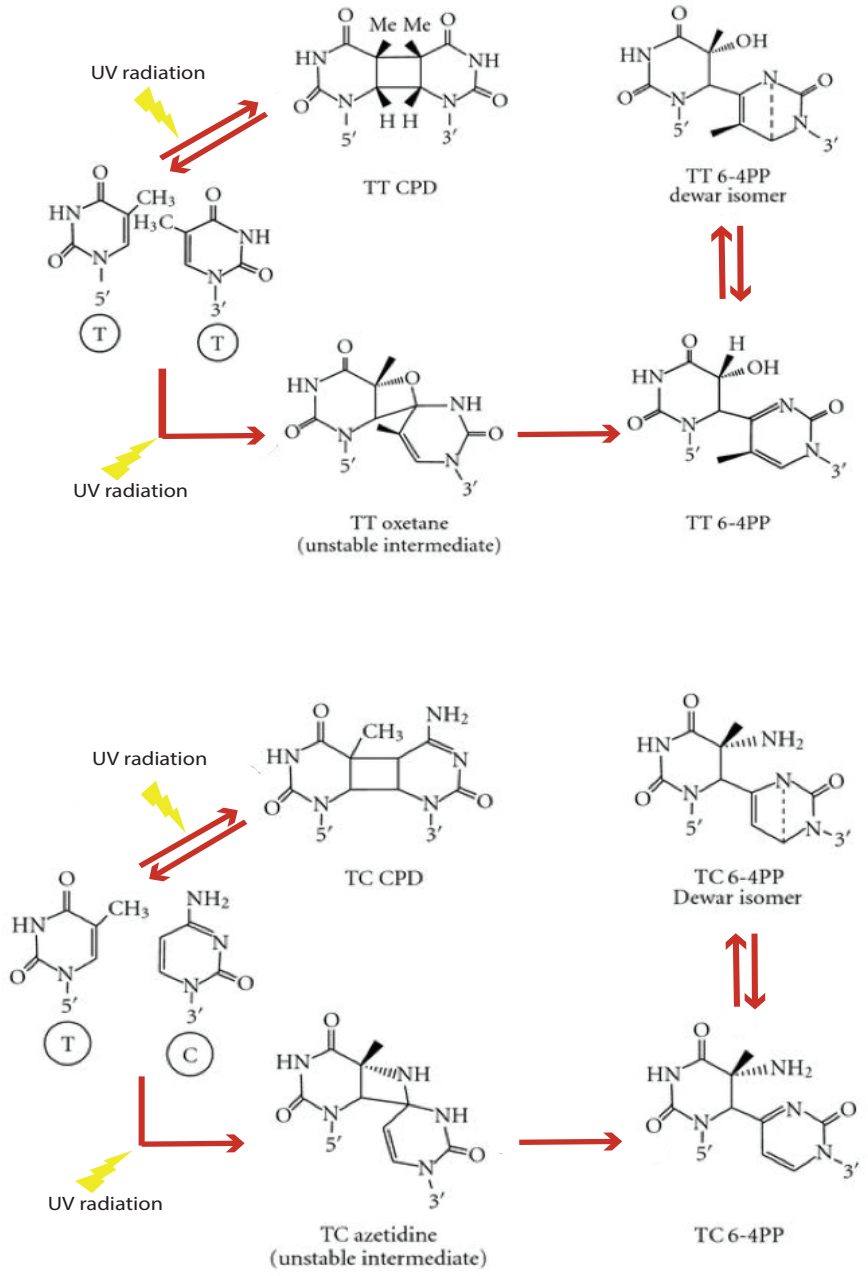

Figure 1.1: **Chemical structure of UV-induced DNA lesions.** The structure and formation of the three major classes of DNA lesions: CPDs, 6-4PPs and DEWs (modified from Rastogi,2010 [191]).

1.2.1 DNA damage recognition

GG-NER initiates with the detection of the DNA helix distortion by the damage sensor complex XPC-RAD23B [220]. The poor substrate specificity of XPC-RAD23B for CPDs requires the presence of the additional UV-DDB (UV DNA damage binding protein) complex, con-

sisting of DDB1 and DDB2/XPE [241, 67]. UV-DDB, together with CUL4A (cullin 4A) and ROC1 (regulator of cullins 1), forms a larger ubiquitin ligase complex [80] that ubiquitinates DDB2 and XPC in response to UV-irradiation, thereby increasing XPC's DNA-binding properties [221]. TC-NER is instead activated by the stalling of RNA polymerase II (RNAP II) at the site of a transcription-blocking DNA lesion. The TC-NER-mediated response is initiated by the recruitment of two TC-NER-specific proteins: CSA (Cockayne syndrome complementation group A) and CSB (Cockayne syndrome complementation group B) [69]. CSA encodes a WD40 repeat protein, involved in protein-protein interactions with CSB, and a subunit of RNAP II. It forms, along with DDB1, CUL4A, and ROC1, a complex exhibiting ubiquitin ligase activity [204]. CSB is a repair-coupling factor that belongs to the SWI/SNF family of ATP-dependent chromatin remodelers, and has additional nucleosome remodeling activity by binding to core histone proteins *in vitro* [35]. CSB stimulates transcription elongation by RNAP II [210], and together with CSA is required for further assembly of the TC-NER machinery. Cells carrying defective CSA or CSB lack the selective repair of transcribed genes, showing elevated UV-sensitivity [237].

1.2.2 DNA damage verification, strand incision and repair synthesis

Once a lesion is detected by the GG-NER or TC-NER machineries, the TFIIH (transcription initiation factor IIH) complex is recruited for DNA damage verification, to unwind, and subsequently to open the DNA helix using its core helicase subunits XPB and XPD [208]. After helix opening, XPA, XPG, and the replication protein A (RPA) are recruited to the repair site, with a consequent release of the XPC-RAD23 complex from the DNA [198]. XPA allows the assembly of the preincision complex, meanwhile RPA coats and protects the undamaged strand, aiding the positioning of the endonucleases ERCC1-XPF and XPG on the damaged strand [50]. The ERCC1-XPF endonuclease catalyzes the first incision at the 5-end, followed by the 3-end incision performed by XPG [218]. The free 3-hydroxyl group produced by the 5-excision is sufficient to start repair synthesis. Meanwhile the TFIIH-bound oligonucleotide carrying the lesion is released and subsequently degraded [108]. Distinct DNA polymerases (DNA Polδ, Polε, and Polκ) [183] are required for the repair synthesis, with the help of the replication clamp PCNA and the clamp loader RFC [214]. The DNA Polε requires the DNA ligase 1 for gap-filling synthesis in proliferating cells [168] **(Figure 1.2)**.

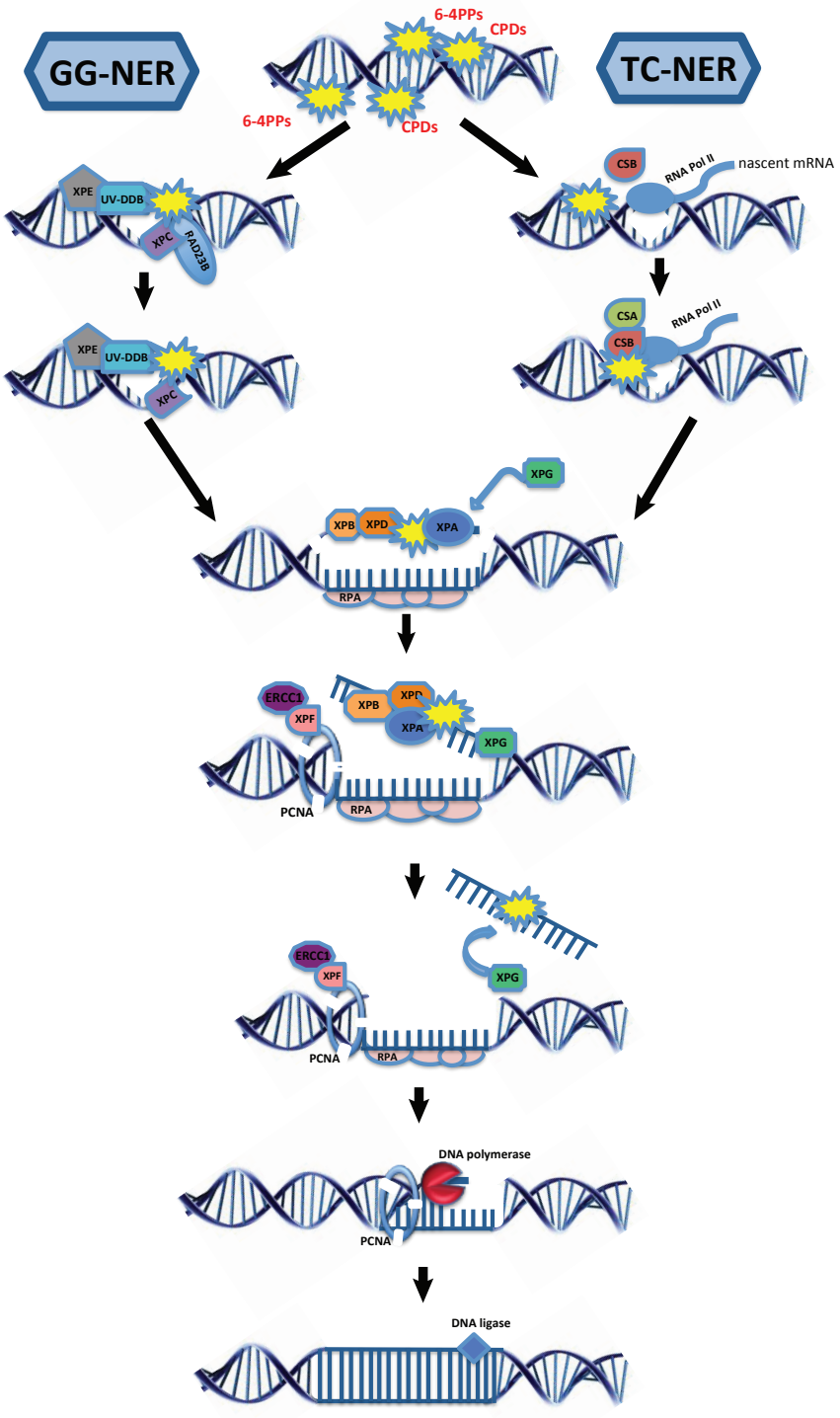

Figure 1.2: **Nucleotide excision repair sub-pathways.** GG-NER recognizes DNA lesions while scanning the whole genome, while TC-NER initiates repair when RNA polymerase II stalls at a lesion. Except the initial damage recognition part, the verification, dual excision, repair synthesis and ligation mechanisms are shared.

1.3 NER-deficiency syndromes in humans: cancer *versus* development and ageing

Congenital syndromes that are caused by heritable mutations in DNA repair and genome stability pathways, and that are manifested in cancer susceptibility and accelerated ageing, underline the importance of genome maintenance for withstanding ageing [62]. Important insights about the distinct consequences of genome instability have been provided by studying NER deficiency syndromes [209]. Xeroderma pigmenstosum (XP) is an autosomal recessive disease caused by mutations compromising only the GG-NER sub-pathway. Patients carrying mutations in *XPC* or *XPE* genes, involved in initial damage detection, show UV-induced pigmentation abnormalities and high skin cancer susceptibility [119]. Mutations impairing only the TC-NER sub-pathway (affecting *CSA* or *CSB* genes), cause instead the onset of Cockayne syndrome (CS), a disease characterized by severe mental retardation traits and accelerated ageing [131]. Mutations in NER factors such as XPA and XPD, which are employed by both GG- and TC-NER, can lead to XP (typically with neurodegenerative components) [54], rare cases of XP combined with CS, and trichothiodystrophy (TTD) [119]. TTD patients in addition to displaying photosensitivity, also suffer from prematurely aged appearance (progeria) [36].

1.4 Model organisms as a tool to study NER-deficiency syndromes

Due to the complexity of the physiological alterations occurring in human pathologies resulting from DNA repair defects, a number of model organisms including mice [5, 48, 47] and nematodes [126, 219, 19], have been extensively used to investigate the mechanisms responding to persistent DNA lesions in the context of development and ageing **(Figure 1.3)**.

Mouse models, carrying the same mutations in NER genes identified in human subjects with skin cancer susceptibility [51, 233, 206] or in CS and TTD patients [246, 226, 47, 234, 106], have been created to better understand the pathological outcomes of DNA repair defects. The complete inactivation of NER activity in *Xpa* mutant mice leads to high susceptibility to UV-induced carcinogenesis [51]. The same susceptibility is observed upon partial NER inactivation

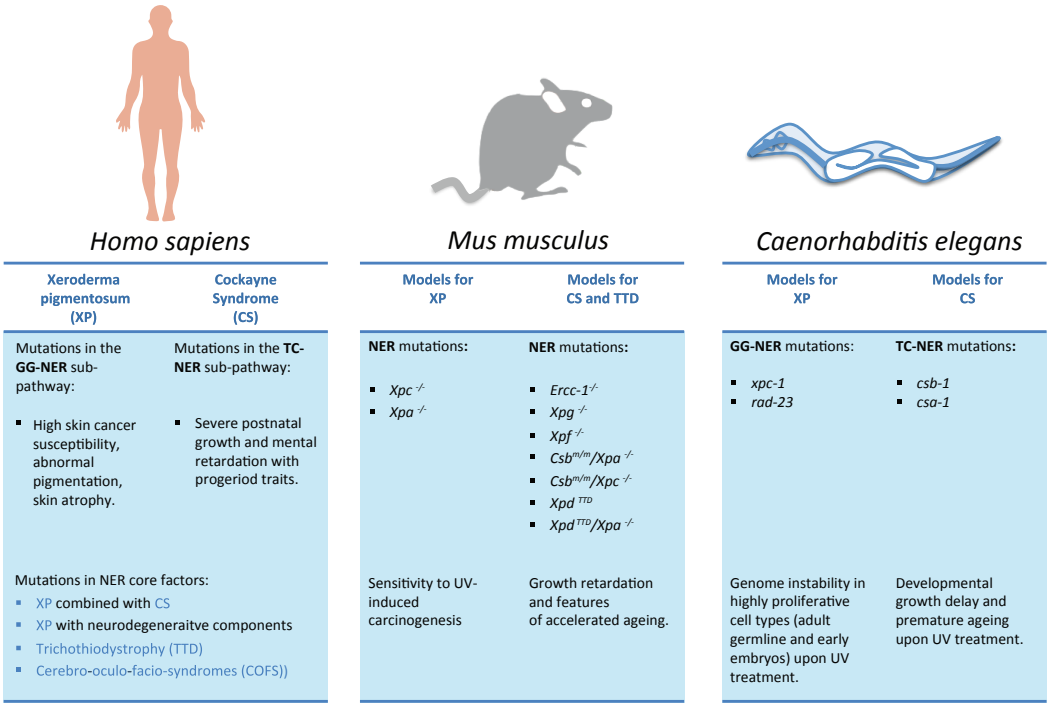

Figure 1.3: **Consequences of NER mutations in human patients in comparison to mice and *C. elegans*NER models.** In contrast to human patients, genetic inactivation of GG-NER (e.g., *Xpc*) or TC-NER (*Csb* or *Csa*) genes alone in mice have comparatively mild consequences and mainly elevate susceptibility to UV-induced carcinogenesis. However, when genetically combined, the mutations give rise to severe CS-like phenotypes such as retarded postnatal developmental growth and features of premature ageing.

in *Xpc* and *Csb* mutant mice, indicating distinct consequences compared to human patients in whom skin cancer susceptibility had been primarily linked to GG-NER [233, 206]. The mild progeroid phenotypes of *Csb* mutant mice were severely enhanced when either *Xpc* or *Xpa* were additionally inactivated [234]. Although the mouse models are highly instructive, the links between NER mutations and the pathological outcomes have remained poorly understood [131]. Therefore simpler metazoan systems might be utilized to shed new light on the response mechanisms to unrepaired DNA lesions in the context of development and ageing.

1.4.1 *C. elegans* as an in vivo model for NER-studies

The soil nematode *Caenorhabditis elegans* has been extensively used as a metazoan in vivo model [22] to study ageing [174, 39] and to better understand the consequences of DNA repair defects [125]. *C. elegans* is a microscopic (adults are about 1 mm long) and transparent

free-living nematode, that undergoes a deterministic developmental program and that can be easily genetically manipulated. Newly hatched larvae pass through four larval stages (L1 to L4) before reaching adulthood. The adult worm, in case of hermaphrodites, self-fertilize to generate offsprings within the first few days of adulthood [26]. *C. elegans* L1 larvae, in response to environmental stresses, such as crowding, starvation and heat stress, are able to arrest their development and enter in L1 diapause stage. This arrest is reversible, and characterized by an increased nematode stress resistance [14]. In *C. elegans* most of the major mammalian repair pathways, including NER, are evolutionarily conserved. NER in *C. elegans* is the major pathway involved in the DNA damage response caused by UV radiation [125]. Mutations in the two NER branches result in distinct outcomes of the UV response. Mutations in the GG-NER gene *xpc-1* lead to genome instability in proliferating cells, which in adult nematodes are restricted to the germline [124]. UV-treated GG-NER-deficient *xpc-1* mutant larvae complete somatic development, though they are unable to develop a germline [169]. In contrast, TC-NER-deficient *csb-1* or *csa-1* mutants undergo a somatic developmental arrest or delay upon UV exposure, without their germline being affected [169, 124, 219, 7]. Thus, GG-NER defects are linked to genome instability in proliferating cells, a hallmark of cancer development in humans, while TC-NER defects mirror the growth defects and accelerated decline in tissue functionality associated with CS [249, 196]. Completely NER-deficient *xpa-1* or *xpc-1;csb-1* double-mutants are UV-hypersensitive: even low UV doses cause both somatic and germline growth arrest [219, 124, 169]. Taken together, the phenotypic distinction of GG- and TC-NER mutants has established *C. elegans* as a useful genetic model for the study of NER deficiencies.

where GG-NER defects lead to genome instability in proliferating cells which in humans comprises a causal event in malignant transformation, while TC-NER defects lead to severe developmentalgrowth delays mirroring a primary CS-associated clinical feature.

1.4.2 Linking DNA damage to ageing and longevity

The conserved NER mechanisms acting during somatic development and tissue maintenance provide a unique opportunity to investigate DNA damage response mechanisms during metazoan development and ageing. In worms, as in mammals, highly conserved longevity assurance mechanisms are involved in counteracting the detrimental consequences of persistent DNA damage [62]. In NER-deficient mutants, the insulin/insulin-like growth factor signalling (IIS),

a conserved pathway regulating development, stress resistance and lifespan, is activated. The role of the IIS is to control the *C. elegans* development in response to environmental stresses through its effector, the transcription factor DAF-16/FOXO. Under normal conditions, DAF-16 is hyperphosphorylated by IIS signalling and sequestered in the cytosol in its inactive form. Only when IIS is turned off, for example during starvation, hypophosphorylated DAF-16 is activated and it translocates into the nucleus to modulate expression of genes involved in stress resistance and longevity [182]. The IIS pathway, through DAF-16, also responds in somatic tissues upon UV treatment to counteract DNA damage-driven ageing by elevating tolerance to persistent DNA damage [169, 28]. IIS attenuation in somatic tissues, leads to the activation of DAF-16, which overcomes the developmental delay and promotes tissue integrity in the presence of unrepaired DNA lesions. A plethora of DAF-16 target genes have already been identified, some of which regulated ROS scavengers, detoxification enzymes, chaperones, and a large number of functionally uncharacterized genes [172, 250]. The *bona fide* longevity assurance mechanisms of DAF-16 activity might antagonize DNA damage-driven growth retardation and ageing by elevating tolerance towards persistent or accumulating DNA damage, thus raising the threshold when the age-dependent accumulation of DNA damage leads to functional deterioration [169]. Strikingly, NER-deficient *csb-1;xpa-1* double mutant and *ercc-1* mutant mice, with growth defects and accelerated ageing phenotype, showed a similar dampening of the IIS-equivalent somatotropic axis [178, 234, 232]. Taken together, studies on NER mutants suggest the presence of highly conserved system-wide response mechanisms to genome instability during nematode and mammalian developmentand ageing [62].

1.5 High-throughput approaches to identify global response mechanisms upon stress

To date, high-throughput and quantitative mass-spectrometry (MS)-based approaches are largely used for detection of global protein dynamics in complex organismal mixtures [76]. In *C. elegans*, many transcriptome and proteome studies have been performed, allowing the identification of key regulators in response to stress [20, 169, 129, 188, 141], to IIS dampening [78, 83, 202, 59, 53, 242], and during ageing [242, 174, 141, 39]. Moreover, coupling large-scale proteome analyses [141, 129, 93, 242] and their post-translational modifications (PTMs),

[17, 147] with global transcriptome studies [20, 169], is a powerful approach to gain knowledge about the role of signalling pathways involved under normal and altered conditions [75]. MS-based lipidomic and metabolomics approaches [115, 102, 174, 39, 70, 53, 34] are recently emerging as high throughput technologies to advance our understanding about molecular biological processes and metabolic changes indicative of physiological adaptations upon specific conditions, such as stress [184, 89] or ageing [166, 97].

1.5.1 Role of lipids in cellular metabolism

In biological systems, fatty acids (FAs) play important roles in energy storage, membrane dynamics and structure, and signalling [240, 95]. Lipids undergo cycles of synthesis and degradation, fundamental to store and produce energy, generally defined as lipid metabolism. In the cell, lipids are usually stored as triacylglycerols in cytoplasmic organelles, called lipid droplets, which play a crucial role in the regulation of intracellular fat storage and energy metabolism [11, 243]. Upon increased energy demand, triacylglycerols are hydrolyzed by lipases to form the lipid intermediate diacylglycerol (DAG), working as second messenger to activate the downstream protein kinase C (PKC) [227], and free FAs, used as energy source [130]. Fatty acids not only work as energy storage, but also serve as structural components of membranes. The biosynthesis of complex straight chain FAs, starts in the cytosol from acetyl-CoA, which undergoes chain elongation and extension steps through the action of carboxylase and fatty acid synthases enzymes. Further cycles of elongation and desaturation of the previously formed short- and medium-chain FAs lead to the formation of saturated (SFAs) and unsaturated (UFAs) long-chain fatty acids, building blocks for the more complex sphingolipids (SL) and glycerophospholipids [258](**Figure 1.4**).

Both SLs and glycerophospholipids are highly conserved components of cell membranes. SLs are intermediates for the production of ceramide (Cer), a key product for the synthesis of glucosylceramide (GlcCer) [236, 258], having a role in stress responses upon DNA damage [261, 255, 256], and sphingomyelin (SM), which controls growth and ageing [46, 84]. Another major component of cellular membranes is the lipid class of glycerophospholipids [236, 90, 258], synthesized from the intermediate phosphatidic acid. The downstream products of phosphatidic acid, DAG and cytidine diphosphatediacylglycerol (CDP-DAG), are both intermediates for the synthesis of more complex glycerophospholipids: phosphatidylcholine

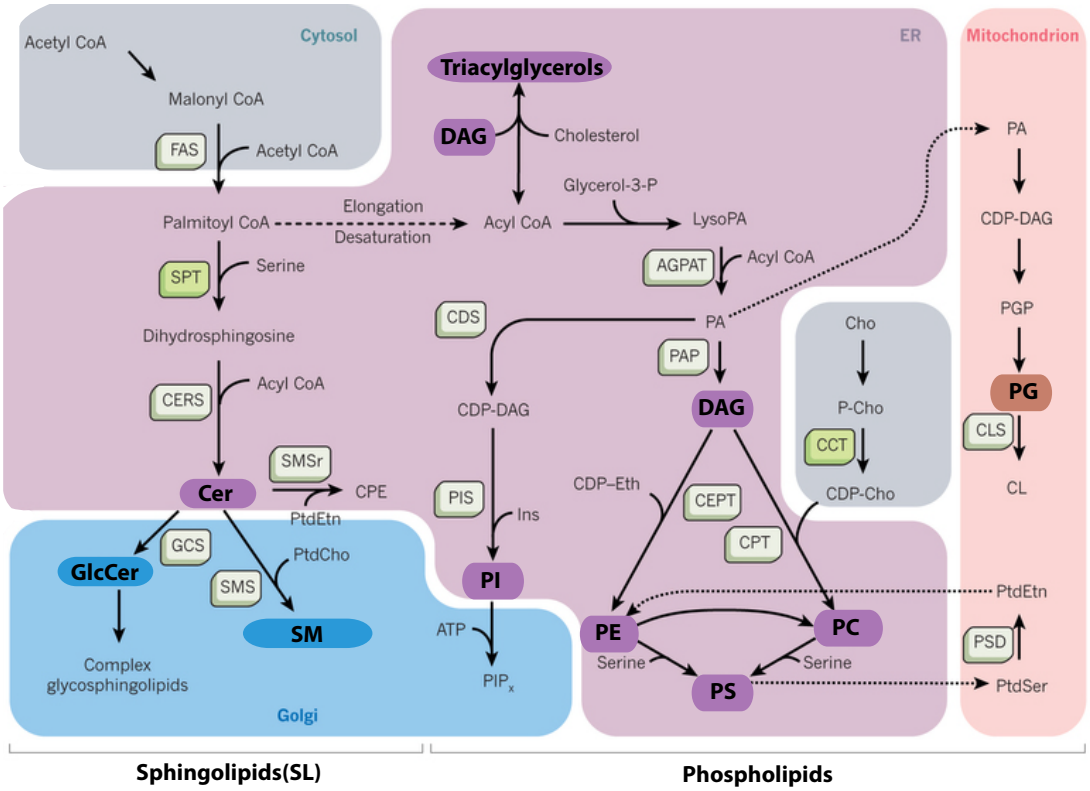

Figure 1.4: **Overview of the lipid biosynthesis processes.** Principal pathways for the production of: lipid storage (triacylglycerols) and the more complex membrane components sphingolipids (SL) and glycerophospholipids. The key lipid class members are highlighted (modified from [94]).

(PC), phosphatidylethanolamine (PE), phosphatidylserine (PS), phosphatidylinositol (PI) and phosphatidylglycerol (PG) [258] **(Figure 1.4)**. Glycerophospholipids are pathogenic indicators of many disorders, such as the neurodegenerative Alzheimers disease [247, 170] or cancer [58], suggesting their possible implication in ageing-related changes. Based on the diverse and widespread biological roles of lipids in terms of energy storage and intracellular signalling, complete quantitative lipid profiles will be important to understand how biological system are influenced by stress conditions.

1.5.2 Metabolic alterations as hallmark of stress and ageing

Lipids metabolism [251, 101, 112] is a biological modulator upon ageing [166, 97] or in response to stress [184, 96, 223].

Together with protein synthesis, and autophagy [200, 193] it acts in cellular processes

downstream of key pathways involved in growth, metabolism, stress responses, and cancer, such as the IIS pathway [70, 194, 53] and the target of rapamycin (TOR) pathway [261, 262, 99, 128, 251] **(Figure 1.5)**.

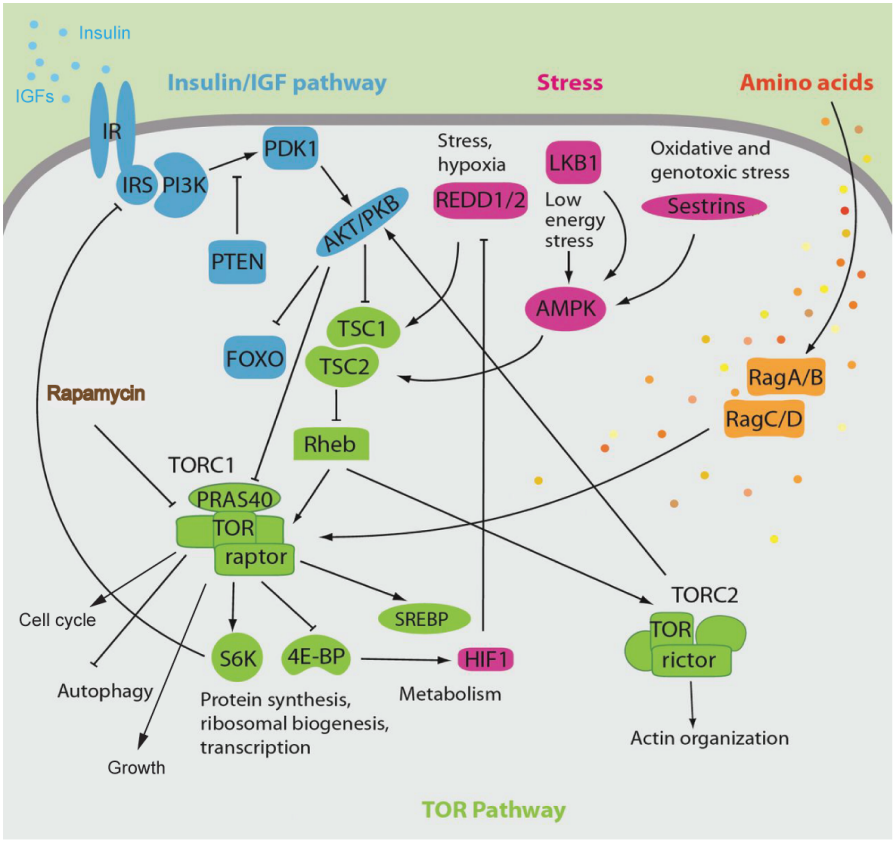

Figure 1.5: **IIS and TOR as sensor pathways for nutrients and stress.** TOR and IIS pathways incorporate endocrine (insulin and IGFs) and local signals (amino acids) in order to modulate growth and metabolism accordingly (modified from [18])

The TOR signalling network, in parallel to the phosphatidylinositol 3-kinase (PI3)/AKT pathway, controls fat metabolism by regulating the activation of the nuclear receptor PPAR, which is responsible for efficient lipid accumulation [112]. Parallel to this, TOR also regulates, through phosphorylation, two downstream effectors, the ribosomal protein S6 kinase beta-1 (S6K1, RSKS-1 in *C. elegans*) and the eukaryotic translation initiation factor 4E-binding protein 1 (4E-BP1), to positively regulate protein synthesis. Upon increased amino acid avail-

ability, TOR, via S6K1 phosphorylation, induces a negative feedback loop on the IIS pathway [230], an important regulator of glucose and lipid metabolism [205, 252, 70, 71]. In response to impaired proteostasis, a direct cause of ageing and genotoxic stress [189],TOR also activates autophagy pathways. Under unfavorable conditions (such as nutrient deprivation) the inhibition of TOR leads to autophagy, which through breakdown of lipid droplets (lipophagy), favours lipid mobilization for use as an energy source [216]. Autophagy, under the regulation of the IIS and TOR pathways, acts on lipid homeostasis upon germline loss *C. elegans* to positively modulate ageing and longevity [127]. The autophagy process starts with the recruitment, in a hierarchical order, of autophagy machinery components to sequester aberrant protein aggregates into autophagosomes, which subsequently will fuse to lysosomes for degradation [43, 259, 200] **(Figure 1.6)**.

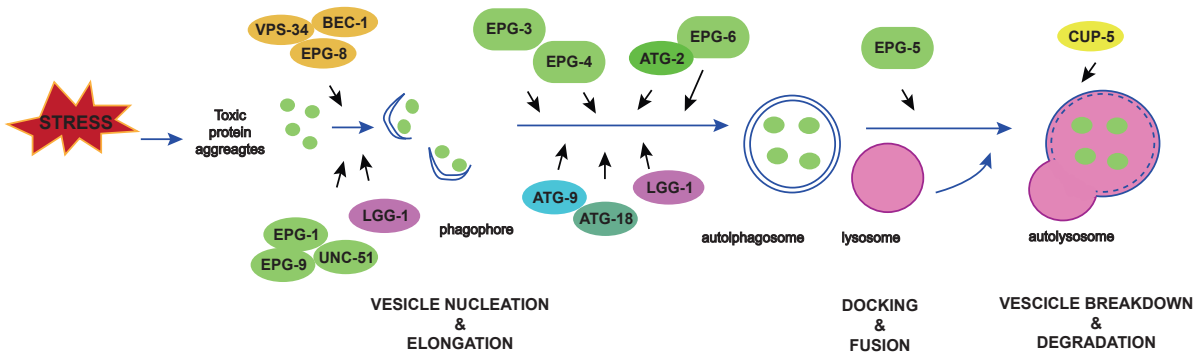

Figure 1.6: **Assembly of the *C. elegans* autophagy machinery.** Autophagy-related proteins and protein complexes are sequentially involved in the assembly of the autophagosome (macroautophagy) (modified from [259]).

1.5.3 Mass spectrometry approach and analysis

The liquid chromatography-tandem mass spectrometry (LC-MS/MS) is a very powerful and sensitive technique used to identify and quantify molecules, from simple to complex mixtures, based on their mass-to-charge (*m/z*) ratio. A MS experiment starts with protein extraction from the biological sample, followed by protein lysis, reduction of protein disulfide bonds, and cysteine alkylation. The proteins are then digested into small peptides, which are easily fractionated by LC to produce simpler spectra for protein identification. The purified sample is ionized and

placed in a mass detection system for analysis. The values on the x-axis in the mass spectra refer to mass-to-charge (*m/z*) ratios, whereas the values on the y-axis usually report the intensity or abundance of the peptides [82] **(Figure 1.7)**.

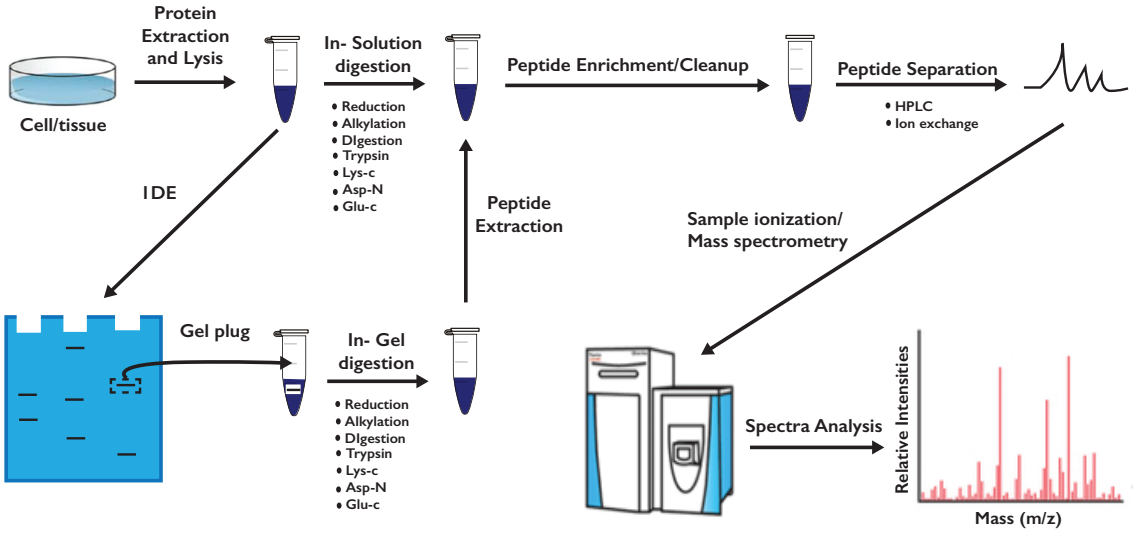

Figure 1.7: **Mass-spectrometry experimental procedure.** Sample preparation involves a first step of lysis, followed by protein or peptide enrichment, sample clean-up and protein digestion.

The identification of specific PTMs (e.g., phosphorylation, ubiquitination and glycosylation) is obtained by enrichment of specific target peptides and sample clean-up using PTM-specific antibodies or ligands. For example, global phosphorylation status can be assessed by immunoprecipitation (IP) using anti-phospho-specific antibodies or by a sample pull-down using titanium dioxide (TiO2) beads, which selectively binds phosphorylated serine (pS), threonine (pT) or tyrosine (pY). The raw files from the mass spectrometer are subjected to analysis using the MaxQuant software, implemented with the Andromeda search engine [42, 40]. Acquired MS/MS spectra are compared to reference proteome databases of the model organism used in the study (for example, Uniprot and Wormbase for *C. elegans* assays). Gene Ontologies (GO), KEGG and GSEA annotations (provided by the Uniprot database) are used as classification methods to gain more detailed information about the proteins changing in the tested sample. An improved knowledge about the protein signalling networks upon normal and altered conditions can be achieved by creating a protein-protein interaction map, with the help of bioinfor-

matics software platforms, such as Cytoscape [212]. In Cytoscape, protein abundance changes and PTMs alterations are integrated with interaction data available from database repositories, allowing to specifically highlighting regulated nodes and protein clusters.

1.6 Aim of study

The aim of this study is to use a MS technology-based approach to gain a comprehensive understanding of the response mechanisms to persistent DNA lesions on the *C. elegans* organismal level. We analysed proteome, phosphoproteome, and lipidome alterations in response to UV-B irradiation of *xpc-1;csb-1* mutant worms, that are completely defective in the NER-mediated removal of UV-induced DNA lesions [169]. This multiple omics approach on NER-deficient mutants will provide a unique and detailed vision of the organismal adaptations the response to persistent DNA damage. On the proteome level, we found similarities between the response to UV irradiation in NER-deficient animals and proteome alterations during ageing, as well as proteome alterations in response to starvation, both of which are regulated through the IIS pathway [174, 242, 141, 129, 188, 59, 53]. Moreover, at the metabolic level we observed a reduction in abundance of proteins functioning in carbohydrate, amino acid, and lipid metabolism that resemble metabolic changes observed upon starvation [129] and during ageing [174, 39]. We also observed a significant role of autophagy, under the regulation of TOR and IIS pathways, in the maintenance of tissue functioning amid persistent DNA damage. Next, we devised a comprehensive signalling response network to DNA damage by integrating proteome and phosphoproteome changes upon persistent DNA damage. Furthermore, by analysing lipidome changes, we identified metabolic alterations that indicate a shift to somatic preservation in response to DNA damage. With our analysis we provide new insights into the physiological adaptations of animal response to persistent DNA damage, and an interesting starting point for future investigations of protein candidates to develop signal transduction networks.

Chapter 2

Materials and Methods

2.1 *C. elegans* handling techniques

2.1.1 Growing conditions

In this study, *C. elegans* strains were cultured and maintained according to standard laboratory conditions (20°C) on nematode growth medium (NGM) plates seeded with OP50 *Escherichia coli* strain [22]. *E. coli* cultures were grown in lysogeny broth (LB) medium, overnight at 37 °C with constant shaking at 180 rpm. M9 buffer was used to collect and wash the worm samples. The strains and the specific solutions used in the study are listed in **Table 2.1** and **Table 2.2** .

Strain	Genotype
N2	Wildtype
BJS724	*atg-3(bp412)*
BJS725	*atg-9(bp564)*
BJS21	*xpc-1(tm3886)*;*csb-1(ok2335)*
BJS21	*xpc-1(tm3886)*;*csb-1(ok2335)*;*daf-16(mu86)*;zIs356[daf-16::GFP;rol-6]
RB796	*sta-1(ok587)*

Table 2.1: *C. elegans* strains used in this study provided by the CGC

M9 buffer	(for 1 liter)
KH_2PO_4	3 g
$NaHPO_4$	6 g
NaCl	5 g
reached 1 liter with distilled H_2O	
autoclaved at 121°C for 20 min	
cooled down to room temperature before adding:	
1 M $MgSO_4$	1 ml
NGM Agar	(for 1 liter)
Bacto Peptone	2.5 g
NaCl	3 g
Serva Agar	17 g
reached 1 liter with distilled H_2O	
autoclaved at 121°C for 20 min	
cooled down to room temperature before adding:	
1 M $CaCl_2$	1 ml
1 M $MgSO_4$	1 ml
5 mg/ml Cholesterol	1 ml
1 M KPO_4	25 ml
Nystatin	2.5 ml
EP Agar	(for 1 liter)
Bacto Peptone	20 g
NaCl	1.2 g
Serva Agar	25 g
reached 1 liter with distilled H_2O	
autoclaved at 121°C for 20 min	
cooled down to room temperature before adding:	
1 M $CaCl_2$	1 ml
1 M $MgSO_4$	1 ml
5 mg/ml Cholesterol	1 ml
1 M KPO_4	25 ml
Nystatin	2.5 ml
LB medium	(for 400 ml)
NaCl	4 g
Tryptone	4 g
Yeast extract	2 g
reached 400 ml with distilled H_2O	

Table 2.2: Common solutions used for *C. elegans* handling

2.1.2 Genotyping strains

The genotype of worm strains were confirmed using polymerase chain reaction (PCR) performed in the C1000 Thermal Cycler (BioRad) with the corresponding primer sets. The DNA was obtained by incubating the worms in worm lysis buffer, supplemented with proteinase K to allow protein digestion (see recipes below). After 1 h at 65 °C and 10 min at 95 °C in the Thermal Cycler, the lysate can be mixed with the PCR master mix to allow for the genotyping reaction to be run **(Table 2.3** and **Table 2.4)** .

Worm lysis buffer	(for 100 ml)
1 M KCl	5 ml
1 M Tris (pH 8.3)	1 ml
1 M $MgCl_2$	250 μl
Tween 20	450 μl
reached 100 ml with distilled H_2O	
autoclaved at 121°C for 20 min	
cooled down to room temperature before adding:	
Gelatine	0.01 g
Proteinase K (20 mg/ml) with 1:20 dilution right before use	

Table 2.3: *C. elegans* lysis buffer

PCR Master-mix	(for 20 μl)
Distilled H_2O	11.3 μl
5x reaction buffer(Bioline)	4 μl
50 mM $MgCl_2$	1 μl
10 mM dNTP	0.5 μl
10 mM primer forward	1 μl
10 mM primer reverse	1 μl
Mango Taq DNA polymerase	0.2 μl
Single-worm lysate	1 μl

Table 2.4: Reagents mix for PCR reaction

Running a gradient of the annealing temperatures allowed the optimization, for each mutation, of the final PCR programs (see the set up for a standard genotyping PCR in **Table 2.5**).

Standard Genotyping PCR		
95°C	4 minutes	*Initial denaturation*
95°C	30 seconds	*Denaturation*
55°C-60°C	30 seconds	*Annealing*
72°C	(1min/kb)	*Extension*
Go to step 2 for another 34 cycles	*Cycles of denaturation,annealing and extension*	
72°C	7 minutes	*Final extension*
10°C	forever	

Table 2.5: Standard PCR reaction for genotyping *C. elegans* strains

2.1.3 Hypochlorite treatment for worm synchronization

Adult worms growing on NGM plates were washed off with M9 buffer (see **Table 2.2**) adjusted to a volume of 4 ml and mixed with 1:1 volume of bleaching solution (see **Table 2.6**). The worms were lysed in this mixture by vortexing for 5 m to allow their rupture and the consequent release of the eggs. Eggs were collected by centrifugation for 1 m at 2000 rcf and washed three times with M9 buffer. Synchronized L1 larvae were obtained by leaving these eggs hatching in M9 buffer overnight at 20 °C with shaking.

Bleaching solution	(for 50 ml)
1 M KOH	12.5 ml
Sodium hypochloride	10 ml
reached 50 ml with distilled H_2O	

Table 2.6: Solution mix for hypochlorite treatment

2.2 Sample processing for mass spectrometry

2.2.1 Entire worm lysate (EWL) preparation for Mass Spectrometry

Aged-synchronized *xpc-1;csb-1* double mutants growing on EP-agar plates were treated with hypochlorite treatment to obtain a large population of synchronised L1 larvae. L1 larvae were filtered through a 11 m Nylon Net filter, then transferred to NGM OP50-seeded plates and fed for 3 h at 20°C before being UV-treated (310 nm) with 100mJ/cm^2, using a UV6 bulb (Phillips) in a Waldmann UV236B irradiation device or mock-treated. In parallel, worms for the starvation assay were kept rolling in M9 buffer. Around 2 million L1 larvae were used for

each replicate condition. Starved and UV-treated worms were kept at 20°C for 6 h before they were collected in M9 buffer. Worms were concentrated by centrifugation and washed using an Extraction buffer (see **Table 2.7**). The pellet was immediately flash frozen in liquid nitrogen.

Extraction solution	(for 25 ml)
1 M HEPES−KOH,pH 7.5	1.25 ml
5 M NaCl	1.5 ml
0.5 M EDTA,pH 8.0	50μl
10% Triton X	2.5 ml
10 % sodium deoxycholate	250μl
50 % glycerol	5 ml
reached 25 ml with distilled H_2O	
added 1 tablet of Protease inhibitor cocktail right before use	

Table 2.7: Protein extraction buffer

Worms pellets were resuspended in one volume of Extraction buffer (compatible with the Pierce 660nm Protein assay requirements) and homogenised in tubes with zirconia beads (4 cycles, 6000 x 2; 20 s) using the Precellys24 Homogenizer with the Cryolys Cooling Unit (Peqlab, Germany). The supernatant containing the proteins was collected after 15 m of centrifugation at 4°C. The total protein concentration was measured using the Pierce 660nm Protein assay (Thermo Scientific).

2.2.2 In solution digestion

Pellets were re-suspended in 6 M Urea, 2 M Thio-Urea in 10 mM Hepes buffer using a Bioruptor instrument. Clarification of lysate was done by centrifugation (14,000 rpm, 10 m). Supernatant was collected and proteins were reduced by Dithiothreitol (DTT, 10 mM, room temperature, 45 m) and alkylated by Iodacetamide (55 mM, room temperature in the dark, 45 m). Lys-C was added at a 1 to 100 (enzyme to substrate) ratio and pre-digestion was performed for at least 2h at room temperature. Urea concentration was diluted to 2M using 50 mM Ammonium bicarbonate and Trypsin was added at a 1 to 100 ratio. Digestion was performed overnight at room temperature and was stopped by acidification. Peptides were desalted by C18 Water Cartridges and 50 g peptides were used for proteome analysis while the remaining peptides were subjected for phosphopeptide enrichment.

2.2.3 Phosphopeptide enrichment

Eluted peptides were acidified to 6 % trifluoroacetic acid (TFA) and the final acetonitrile (ACN) concentration was 60 %. In total, 5 extraction steps were performed at a beads-to-peptide ratio of 3:1. In detail, beads were dissolved in 60 % ACN, 6 % TFA, added to peptide mixture, and incubated on a rotating wheel for 20 m at room temperature. This step was repeated five times and fractions were washed in 60 % ACN, 1 % TFA. Beads were transferred on C8 stage tips, pooling the last two fractions, and washed three times with 300 L of 60 % ACN, 1 % TFA. Then, beads were washed using 40 % ACN, 0.5 % CH3COOH. Phosphorylated peptides were eluted by 3 x 30 μL of 40 % ACN, 3.75 % NH4OH, dried in a speed vacuum and re-suspended in 2.5 % ACN, 5 % formic acid.

2.2.4 Peptide analysis by liquid chromatography and mass spectrometry

Peptides were eluted from C18 tips with 30 μL of 0.1 % formic acid in 60 %ACN, concentrated in a speed vacuum to complete dryness and re-suspended in 10 μL buffer A (0.1 % formic acid). The liquid chromatography tandem mass spectrometry (LC-MS/MS) equipment consisted out of an EASY nLC 1000 coupled with a nano-spray electroionization source to the quadrupole based QExactive Plus instrument (Thermo Scientific). Peptides were separated on an in-house packed 50 cm column (1.9 m C18 beads, Dr. Maisch) using a binary buffer system: A) 0.1 % formic acid, and B) 0.1 % formic acid in acetonitrile as described previously [120]. The content of buffer B was raised from 7 % to 23 % within 220 m and followed by an increase to 45 % within 10 m. Then, the column was washed with 85 % B for 5 m and re-equilibrated to 5 % B within. Total gradient time was 240 m. A similar gradient shape was applied for phosphor-proteome analysis but shortened to a total gradient time of 120 m. Eluting peptides were ionized by an applied voltage of approx. 2.2 kV. MS1 spectra were acquired using a resolution of 70,000 (at 200 *m/z*), an Automatic Gain Control (AGC) target of 3e6 and a maximum injection time of 20 ms in a scan range of 300-1750 Th. In a data-dependent mode, the 10 most intense peaks were selected for isolation and fragmentation in the higher-energy collisional dissociation (HCD) cell using a normalized collision energy of 25 % and an isolation window of 2.0 Th for proteome and 1.8 for phosphor-proteome analysis. Dynamic exclusion was enabled and set to 20 s. The MS/MS scan properties were: 17.500 resolution at 200 *m/z*,

an AGC target of 5e5 (for phosphor proteome analysis: 1e6) and a maximum injection time of 50 ms. Excellent reproducibility for the proteome dataset (r >0.95 for biological replicates) was determined by the Pearson correlation coefficient (r) **(Figure 2.1A)**. The correlation plot of the phosphoproteome dataset upon each treatment (untreated, UV-treated and starvation) shows how the biological replicates cluster together **(Figure 2.1B)**. The distributions of the individual phosphorylated residues (Ser/Thr/Tyr) **(Figure 2.1C)** and the number of phospho groups per peptide we detected, were similar to those obtained in previous studies [17, 147].

2.2.5 MaxQuant and bioinformatics

All raw files were subjected to MaxQuant 1.5.2.8 analysis using the implemented Andromeda search engine [42, 40]. Acquired MS/MS spectra were compared to the Uniprot reference proteome database of *C. elegans*. Using the implemented revert-algorithm, we used a false discovery rate (FDR) cutoff at the peptide-spectrum-match, protein and modif. site level of 1 %. For first and main MS/MS searches the peptide mass tolerance was set to 20 and 4.5 ppm, respectively. Phosphorylation (STY), acetylation at protein N-termini, and oxidation of methionine residues were defined as variable modification, while carbamidomethylation was set as a fixed modification. The minimal score for modified peptides was 40. Re-Quantify, label-free-quantification and match-between-runs options were enabled using default settings. BLAST searches were performed using desktop version 2.2.31 by comparing *C. elegans* and human reference proteomes of the Uniprot consortium (downloaded Jan. 2015). BLAST results were accompanied by E-values and Bitscores, as well as the alignment length. An e-value cutoff of 1E-4 was used. Note that the e-value is highly dependent on the search space and varies between different databases. Gene Ontology annotations for both species were imported based on Uniprot entries using Perseus. Heatmaps were done with the statistical programming software package Rstudio using the ggplots package. Network analysis was performed in Cytoscape [212, 37] using WormBase (www.wormbase.org) as the reference network. The color gradient of the nodes indicates the grades of up or down-regulation at the proteome level while the three different shapes indicate the phosphorylation status of these proteins. Proteomics light label free quantification data (not SILAC data) from [242] were imported based on the first Uniprot identifier and correlated to our dataset. Ratios were also calculated based on these values meaning that the calculated ratio might differ from the SILAC based ratio presented in the study. The

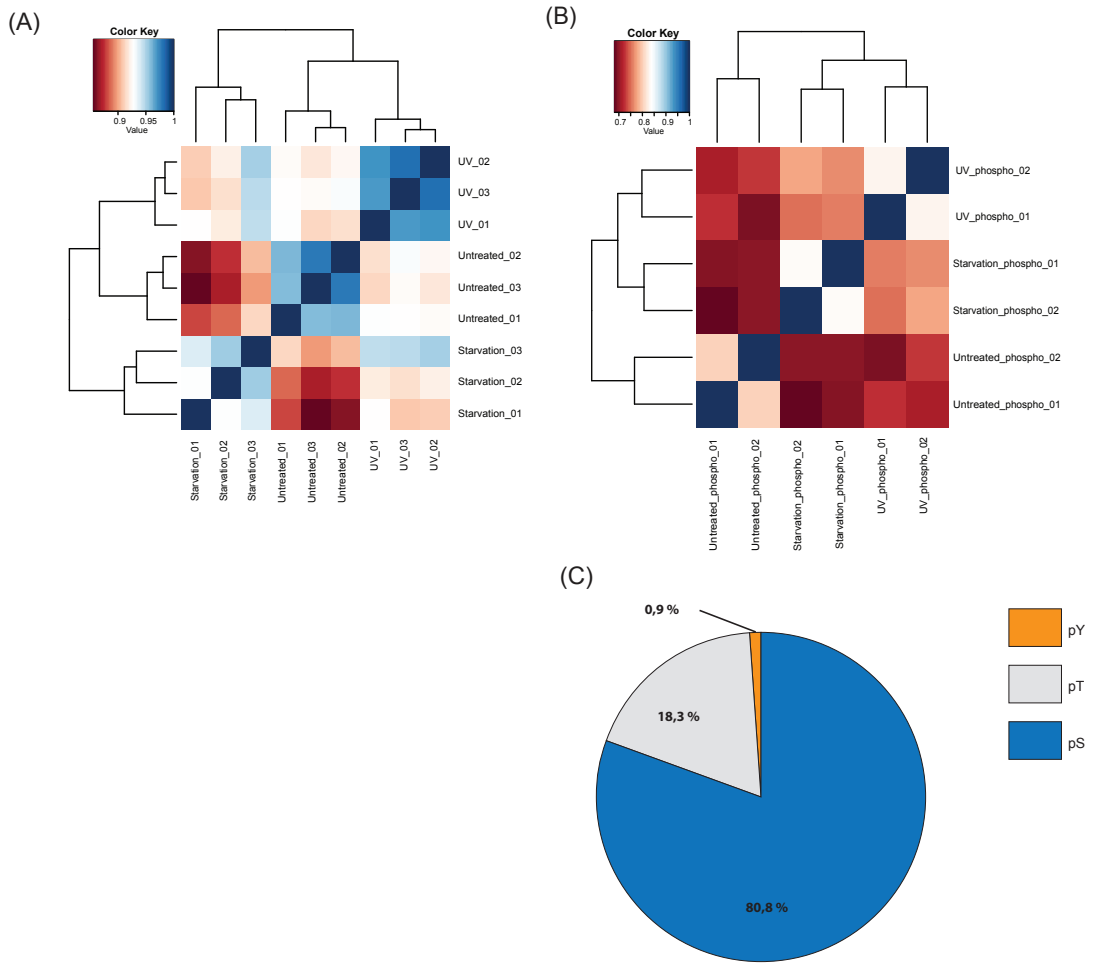

Figure 2.1: **Proteome and phosphoroteome datasets reproducibility from *xpc-1;csb-1* double mutants upon each treatment (untreated, UV-treated, and starvation).** (**A**) Almost a linear correlation was observed for biological replicates of the proteome dataset. (**B**) Biological replicates of the phosphoproteome dataset cluster together, within a range of correlation from 0,7 to 1 as reported in the colour key map on the top left of the panel. (**C**) Distribution of the individual phosphorylated residues (Ser/Thr/Tyr): serine phosphorylation was the most represented (shown in blue), while tyrosine phosphorylation occurred in less than 1 % of the phosphorylation sites (orange).

mass spectrometry proteomics data have been deposited to the ProteomeXchange Consortium via the PRIDE [239] partner repository with the dataset identifier *PXD005649*.

2.3 Lipid analysis

2.3.1 Thin layer chromatography

500,000 *C. elegans* L1 larvae, collected after starvation and UV treatment, were homogenized in 1 ml of Milli-Q water using the Precellys 24 Homogenisator (Peqlab, Erlangen, Germany) at 6,500 rpm for 30 s. The protein content of the homogenate was routinely determined using bicinchoninic acid. Lipids were extracted and purified as previously described [15]. Lipids were applied to 20 10 cm high performance thin layer chromatography (HPTLC) Silica Gel 60 plates (Merck, Darmstadt, Germany), which were pre-washed twice with chloroform/methanol 1:1 (v/v) and air-dried for 30 m. For the detection of triacylglycerols, each lane of the TLC plate was loaded with the equivalent of 40 g of protein. The TLC solvent system used was hexane/toluene 1:1 (v/v), followed by hexane/diethyl ether/glacial acetic acid 80:20:1 (v/v). Standard lipids (Sigma-Aldrich, Taufkirchen, Germany) applied to the TLC plates in addition to the lipid samples were used for lipid identification. For detection of lipid bands, the TLC plates were sprayed with a phosphoric acid/copper sulfate reagent 15.6 g of $CuSO_4$(H2O)5 and 9.4 ml of H3PO4 (85 %, w/v in 100 ml of water) and charred at 180 °C for 10 m [253].

2.3.2 Lipid analysis by mass spectrometry

Relative amounts of sphingolipids (ceramides, glucosylceramides, and sphingomyelins), were determined by liquid chromatography coupled to electrospray ionization tandem mass spectrometry (LC-ESI-MS/MS). Aliquots of the *C. elegans* L1 larvae homogenates (see above) being equivalent to 80 g of protein were diluted to 100 l with Milli-Q water. 750 μl of methanol/chloroform 2:1 (v/v) and internal standards (100 pmol ceramide 17:0, Matreya, Pleasant Gap, PA, USA; 123 pmol sphingomyelin 12:0, 122 pmol glucosylceramide 12:0, both Avanti Polar Lipids, Alabaster, AL, USA) were added. Lipid extraction and LC-ESI-MS/MS analysis were performed as previously described Schwamb:2012bi. Sphingolipid species were monitored in the positive ion mode with their specific multiple reaction monitoring (MRM) transitions. As characteristic product ions in Q3 the choline headgroup (*m/z* 184) was used for sphingomyelin species, and the C17 isosphingosine base after water loss (*m/z* 250) was used for endogenous ceramides and glucosylceramides [158]. Endogenous sphingolipids were quanti-

fied by normalizing their peak areas to those of the internal standards. Relative amounts of glycerophospholipids (PC, PE, PI, PS, PG) were determined by ESI-MS/MS with direct infusion of the lipid extract (Shotgun Lipidomics). Aliquots of the *C. elegans* L1 larvae homogenates (see above), equivalent to 100 g of protein were diluted to 500 l with Milli-Q water. 1.875 ml of methanol/chloroform 2:1 (v/v) and internal standards (135 pmol PC 17:0-14:1, 161 pmol PE 17:0-14:1, 127 pmol PI 17:0-14:1, 136 pmol PS 17:0-14:1, 155 pmol PG 17:0-14:1, Avanti Polar Lipids, Alabaster, AL, USA) were added. Lipid extraction and ESI-MS/MS analysis were performed as previously described [121].

2.4 Analysis of somatic arrest post UV-B-irradiation

An aged-synchronized population of adult worms was bleached, and the eggs were allowed to hatch overnight rolling at 20°C, in M9 buffer. Arrested L1 larvae were put onto empty NGM plates and irradiated with 310 nm UV-B light using Phillips UV6 bulbs in a Waldmann UV236B irradiation device, or were mock-treated. (Irradiation was measured using a UVX digital radiometer and a UVX-31 probe from UVP and was generally around 0.3 mW*cm-2). *E. coli* OP50 bacteria was to the plates, which were then incubated at 20 °C. After 48 h the larval stages were scored.

2.5 Statistical analysis

Statistical analyses were performed in Rstudio. Information about sample size and statistical methods isdescribed in figure legends. Volcano plots, scatter plots, and bar charts were created in Rstudio. The independent 2-group t-test was used for calculating statistical significance. A * single asterisk represents a p value < 0.05, **double asterisks < 0.01 and *** triple asterisks < 0.001.

2.6 Software and databases

Data analysis, processing and visualization were performed using the following software: MaxQuant and Perseus (MPI), Adobe Creative Suite CS4 (Adobe Systems Inc), Papers 3

(Mekentosj), Microsoft Office 2011 (Microsoft Corp.), GraphPad prism 5 (GraphPad Software), R (CRAN), R Studio (version 0.99.489, 2009-2015), TeXShop 3.36.1 (Richard Koch). Mining of scientific literature was done using National Center for Biotechnology Information database (NCBI,www.ncbi.nlm.nih.gov) was used to mining scientific literature. Interaction maps were built using the Cytoscape software 3.2.1 and the existing network of interaction provided by WormBase (www.wormbase.org). Gene Ontology Consortium (www.geneontology.org) was used to perform Gene ontology classification. Uniprot (EMBL-EBI) was used as a platform for protein information, such as protein sequence, classification and functional information. *C. elegans* handling techniques were obtained from WormBook (www.wormbase.org) and *C. elegans* specific gene and protein information were obtained from WormBase (www.wormbase.org).

2.7 Reagents and instruments

In this study standard laboratory techniques for molecular biology, biochemical and microbiological experiments have been used. Consumable plastic ware, reagents, chemicals and instruments were obtained from the following suppliers: Amersham Biosciences, Applied Biosystems, Bio-rad, Carl Roth, Clontech, Diagenode, Eppendorf, Fermentas, GE Healthcare, Invitrogen, Merck, Metabion, Millipore, New England Biolabs, Peqlab, Qiagen, Roche, Sarstedt, Serva, Sigma Aldrich, ThermoFisher Scientific, VWR, Union Biometrica.

Chapter 3

Results

In order to gain knowledge into the proteome response to unrepaired DNA damage at the organismal level, we employed a mass-spectrometry-based quantitative proteomics approach using *C. elegans* as a model. To achieve persistence of specific DNA lesions, we treated worms that were completely NER-deficient, due to mutations in the *xpc-1* and *csb-1* genes (*xpc-1(tm3886);csb-1(ok2335)*), with UV-B irradiation. We exposed worms synchronized at the first larvae stage (L1) and lysed them 6 h post UV or mock treatment. Proteins were digested in solution followed by peptide identification and quantification by liquid chromatography and tandem mass spectrometry (LC-MS/MS) as shown in **Figure 3.1**. To monitor the effectiveness of the DNA damage response, we followed in parallel the nuclear localization of DAF-16::GFP, that we previously showed to translocate into the nucleus in response to UV-induced DNA damage to mediate a gene expression program alleviating the UV-induced developmental arrest [169].

3.1 Proteome analysis upon UV treatment

3.1.1 Protein annotations based on Gene Ontologies classification method

In total more than 7500 proteins were quantified by our LC-MS/MS label-free-quantification based experimental strategy at a false discovery rate (FDR) of less than 1 % at the protein and peptide spectrum match level, of which more than 5000 proteins were quantified between UV and untreated conditions at least in two out of three biological replicates. Excellent reproducibility ($r > 0.95$ for biological replicates) was determined by the Pearson correlation coefficient (r)

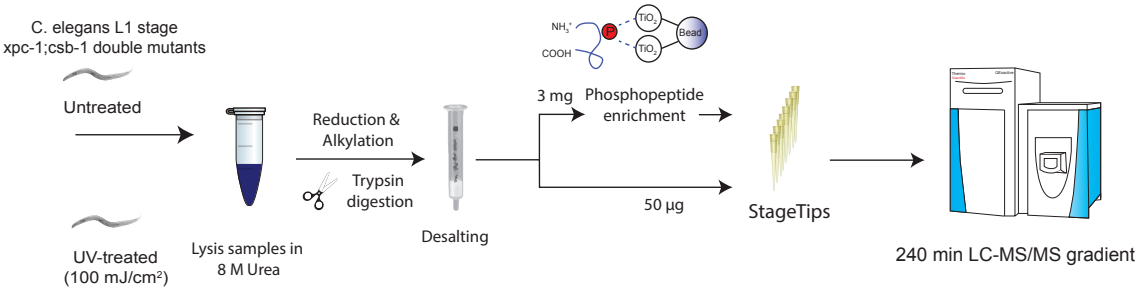

Figure 3.1: **Experimental workflow of the proteomic analysis upon UV-induced DNA damage in *C. elegans*.** Synchronized L1 worm population of *xpc-1;csb-1* double mutant was treated with UV light (100 mJ/cm^2). Worms were collected and concentrated by centrifugation 6 h post-treatment. The worm pellet was homogenized and the proteins were extracted. After digestion the peptides were analysed using the liquid chromatography-coupled mass spectrometry (LC-MS/MS) procedure.

(Figure 2.1A). To identify significantly regulated proteins, we performed a two-sided t-test and corrected for multiple testing by estimating the FDR to 5 % using a permutation based algorithm [229]. By this approach, we were able to identify about 1000 significantly differentially expressed proteins, of which more than 550 proteins were more than 2-fold altered between UV and untreated conditions, indicating comprehensive protein abundance changes in response to UV-induced stress. Gene Ontologies (GO) classification method was used to perform a more systematic analysis of protein changes in NER-deficient UV irradiated animals. GO annotations and associated data were obtained from Uniprot (release January 2016) and the online *C. elegans* portal WormBase (version WS246). As shown in **Figure 3.2A**, we observed abundance changes of significantly regulated proteins in most of the subcellular compartments. The volcano plot in **Figure 3.2B**, enables a quick visualization of the overall distribution of proteins identified in the screen. The $\log_2$ ratio of UV-treated vs. untreated for each protein group was plotted against the respective $\log_{10}$ p value. Between the 5126 detected proteins (highlighted in grey), we could display specific clusters of proteins with statistically significant (FDR $<$ 5 %) changes in abundance: the upregulated are highlighted in red, while the downregulated ones in blue.

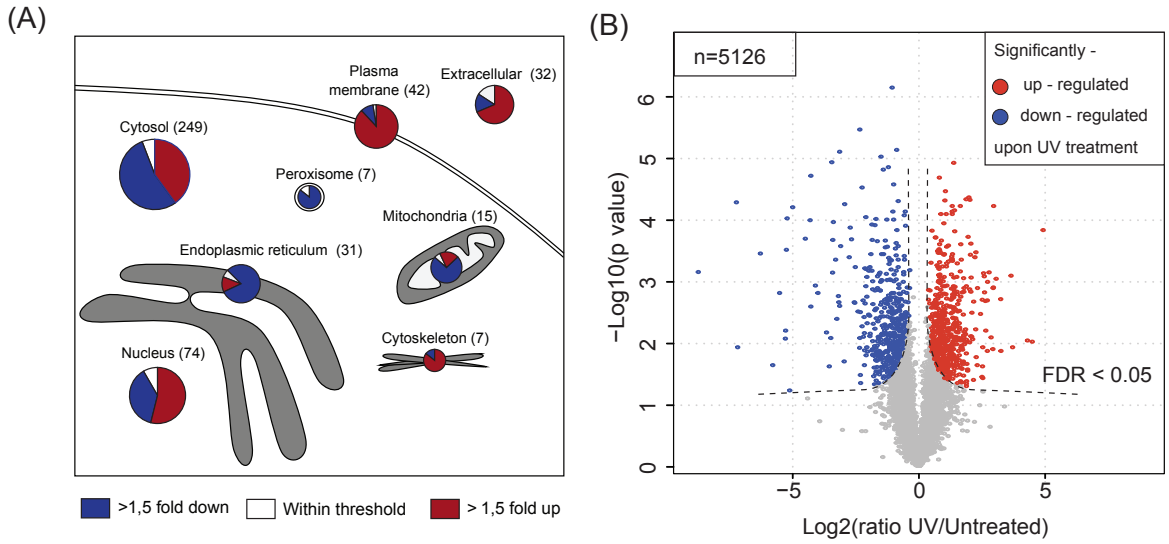

Figure 3.2: **Changes in abundance of proteins detected in *xpc-1;csb-1* double mutants upon UV treatment.** (**A**) Distribution of significantly regulated proteins (FDR <5 %) in the different subcellular compartments following GO classification. (**B**) Volcano plot of the proteins detected in *xpc-1;csb-1* double mutants upon UV treatment ($\log_2$ values of fold-changes are showed). The proteins found significantly (FDR <5 %) increased and decreased in abundance are highlighted in red and blue respectively.

Using the GO classification method, we recapitulated the most represented clusters of proteins which were found significantly (FDR <5 %) increased and decreased in abundance in UV-treated vs. not treated *xpc-1;csb-1* double mutants, respectively in **Figure 3.3** and **Figure 3.4**.

3.1.2 Implementation of *C. elegans* proteins annotations coverage

In order to improve the annotations of *C. elegans* proteins and obtain more insights into their potential functions, we used our data to perfotm a BLAST search results (e value $<10^{-4}$) of well annotated species, including human and mouse [180]. Using Gene Ontologies, KEGG and GSEA annotations provided by the Uniprot database for *C. elegans* protein entries and the corresponding human orthologues, we could observed an increased coverage of proteins annotation (the amount of annotated proteins raised from ca. 35 % in *C. elegans* to ca. 62 % in human) **(Figure 3.5)**. Based on the human annotations, we then implemented our data analysis by classifying into known GO clusters the proteins still missing any annotation in *C. elegans*.

Proteins significantly (FDR<5%) increased in abundance in UV-treated vs not treated *xpc-1;csb-1* double mutants

	UniProt accession	Gene name	Biological function	Fold change
Nucleus				
Histones	Q9XWP6	spr-5	Lysine-specific histone demethylase 1	1.7
	P34537	rfp-1	E3 ubiquitin-protein ligase mediating monoubiquitination of histone H2B	1.99
	Q27511	htz-1	Histone H2A	2.08
	G5ECH0	hda-3	Histone deacetylase	2.3
	Q9U757	hil-2	Histone H1.2	2.56
Chromatin organizers	G5EF53	swsn-4	SWI/SNF nucleosome remodeling complex component	1.61
	O61845	chd-7	Chromodomain and Helicase Domain protein	1.65
	Q19848	vrk-1	Ser/Thr kinase regulating the association of baf-1 with chromatin and nuclear membrane proteins	1.66
	Q21443	lmn-1	Lamin-1, Major component of the nuclear lamina	1.67
	O01971	emr-1	Emerin homolog, involved in chromosome segregation and cell division	1.85
	Q03565	baf-1	Barrier-to-autointegration factor, essential role in nuclear envelope formation	2.26
	Q9XTB5	lem-2	LEM protein, involved in chromosome segregation and cell division	2.5
	Q21831	snfc-5	SNF chromatin remodeling Complex component	2.53
Chromosome cohesion	Q9U2C1	smc-3	Structural maintenance of chromosomes protein 3	1.94
	Q21306	coh-1	Cohesin complex subunit	2.52
	Q19555	scc-3	Cohesin complex subunit	3.1
Regulators of transcription	O45624	math-33	Ubiquitin carboxyl-terminal hydrolase	1.62
from RNA polymerase II promoter	H2KYN6	smk-1	Suppressor of MEK null proteins; affects the transcription of DAF-16 target genes	1.64
	P34703	emb-5	Regulator of transcriptional elongation by RNA polymerase II	1.71
	B3GWA1	nono-1	Conserved nuclear protein, forms a complex with the mRNA export factor NXF-1	1.85
	Q197206	ceh-38	Homeobox protein,DNA-binding regulatory protein	1.92
	Q09390	hmg-1.2	Positive regulation of transcription from RNA polymerase II promoter	2.24
	Q9NAD6	sta-1	Signal transducer and activator of transcription 1	2.46
	G5EC23	hcf-1	Transcriptional regulator that associates with histone modification enzymes	2.5
	G5EBY0	rtfo-1	RNA polymerase-associated protein, component of the PAF1 complex	2.56
	Q9TZ93	spt-4	Transcription elongation factor	2.63
Synthetic multivulva class B	P90916	lin-53	Synthetic multivulva class B (synMuvB) protein, transcription factor member of the (DRM) complex	1.78
	Q23482	lin-37	Synthetic multivulva class B (synMuvB) protein, transcription factor member of the (DRM) complex	1.89
	G5EDT1	lin-35	Synthetic multivulva class B (synMuvB) protein, transcription factor member of the (DRM) complex	2.83
	Q22703	dpl-1	Synthetic multivulva class B (synMuvB) protein, transcription factor member of the (DRM) complex	3.02
mRNA processing	O44985	teg-4	Pre-mRNA splicing factor, tumorous enhancer of Glp-1	1.51
	Q9U2U0	uaf-2	Splicing factor	1.76
	Q9U2P3	pap-1	Poly (A) polymerase	1.83
	Q21832	rnp-4	Core component of the splicing-dependent multiprotein exon junction complex (EJC)	1.83
	Q9GRZ2	prp-65	Pre-mRNA processing factor 6	1.95
	Q09511	rsp-4	Splicing factor	2.33
	Q23543	lsm-7	mRNA splicing factor, via spliceosome	2.9
Ribonucleoproteins (RNP)	Q10013/Q9XTU6/Q9N4G9	snr- 3/-6/-7	Heptameric complex required for biogenesis and function of the snRNPs	1.88/2.62/2.91
	Q18265	fust-1	FUS/TLS RNA binding protein homolog	1.95
	Q21322	rnp-2	Small nuclear ribonucleoprotein (snRNP)-associated protein RNP-2/U1A	2.48
	Q27274	rop-1	Protein component of the Ro ribonucleoprotein (RNP) complex	4.06
	Q9BIB7/Q8MXR2	hrpf-1/-2	Orthologous to human hnRNP F and hnRNP H, act as pre-mRNA splicing factors	4.12/2.71
Transport	Q9TZQ3/G5EBV6	pgl-1/-3	P granule abnormality protein	1.52/3.72
	Q22078/G5EEH9/...	npp- 2/-4/-7/-9/-10/ -14/-16/-19	Nuclear Pore complex Proteins	1.57-4.04
	Q23089	xpo-1	Nuclear export receptor	1.61
	O17915/P34342	ran-1/2	GTP-binding nuclear protein	1.64/1.63
	Q18212	hel-1	Spliceosome RNA helicase DDX39B homolog	1.79
	P91867	thoc-3	THO Complex (Transcription factor/nuclear export) subunit	1.94
	G1K0V8	iff-1	Eukaryotic translation initiation factor 5A-1	2.01
	B5BM32	nxf-1	Nuclear RNA export factor 1	2.14
	Q9U757	nxt-1	NTF2-related export protein	2.15
	Q9BIB8	imb-1	Importin Beta family	2.15
	Q17561/Q21559	aly-1/-3	Ref/ALY RNA export adaptor family	3.45/1.58
Extracellular				
Transthyretins	Q03575/O17345/...	ttr-5/-6/-15/-17/-26/ -32/-51	Transthyretin-like protein	1.8-4.17
Fatty acid binding proteins/transporters	Q93796	nrf-5	Lipid-binding protein	1.9
	Q20223	lbp-1	Fatty acid-binding protein	2.5
Others	G5EFQ9	mec-5	Collagen unique in the number of Gly-X-Y repeats	1.58
	G5ECN9	egl-3	Prohormone convertase	1.92
	G5ECR5	sod-4	Extracellular superoxide dismutase [Cu-Zn]	8.32
Plasma membrane				
Transmembrane channel proteins	Q19746/Q9U3N4/...	inx-3/-6/-12/-16	Innexin	1.7-3.26
Heterotrimeric G proteins	P17343	gpb-1	Guanine nucleotide-binding protein subunit beta-1	1.65
	P51875	goa-1	Heterotrimeric G protein alpha subunit Go (Go/Gi class)	1.93
	G5EGU1	egl-30	Heterotrimeric G protein alpha subunit Gq (Gq/G11 class)	1.95
	O17589	eat-16	RGS protein ,interacts with the egl-30 and goa-1 signaling pathways	2.42
ATPases	P90735	eat-6	Alpha subunit of a sodium/potassium ATPase	1.7
	Q93235	nkb-1	Sodium/potassium-transporting ATPase subunit beta-1	1.79
	G5EEK9	vha-5	V-type proton ATPase subunit a	1.97
	Q95XP6	mca-3	Calcium-transporting ATPase	3.32
	Q8IA86	catp-3	Cation transporting ATPase	3.46
Amino acid, ion and ATP transporters	Q20943/Q9U2G5	mrp-2/7	ATP-binding cassette transporter, member of the ABCC subfamily	1.51/1.58
	G5EC65/Q8MQ15	abts-1/3	Sodium-driven chloride-bicarbonate transporter	1.77/1.75
	Q9XVU3/O45298	atgp-1/-2	Amino acid Transporter GlycoProtein subunit	2.16/1.51
	O02086/Q9U275	haf-2/-7	Transmembrane protein of the ATP-binding cassette transporter superfamily	2.75/2.16
Endocytosis/ Vesicles traffiking	O02626	aex-3	MAP kinase protein required for intracellular vesicle trafficking as well as synaptic vesicle release	1.83
	Q9U2S4	arf-6	ADP-Ribosylation Factor	1.83
	Q9U2T9	itsn-1	Endocytic adaptor protein to regulate cargo sorting through the endolysosomal system	1.84
	Q95QV3	rab-3	Involved in exocytosis by regulating a late step in synaptic vesicle fusion	1.9
	P83351	snap-29	SNARE, soluble essential protein for fusion of cellular membrane	2.12
	P39055	dyn-1	Dynamin GTPase, its activity is required for endocytosis, synaptic vesicle recycling	2.13
	G5EDC6	arl-8	Arf-like small GTPase, regulates transport of axonal presynaptic vesicle protein cargo	3.05
	Q22436	sqst-1	ATP-binding cassette transporter, member of the ABCC subfamily	30.27

Figure 3.3: **Most represented clusters of proteins which were found significantly (FDR <5 %) increased in abundance in *xpc-1;csb-1* double mutants upon UV irradiation.**

Proteins significantly (FDR<5%) decreased in abundance in UV- treated vs not treated *xpc-1;csb*-1 double mutants

	UniProt accession	Gene name	Biological function	Fold change
Ribosomes				
Large subunit	O02056/P49405/...	rpl-4/-5/-6/-7/10/ -11.2/-19/-20/-30	60Sribosomal proteins	0.42-0.70
Small subunit	P37165	ubl-1	Ubiquitin-like protein 1-40S ribosomal protein	0.4
	P48154/Q9N3X2/...	rps-1/-4/-6/-8/-12/ -13/-16/-22/-24	40S ribosomal proteins	0.44-0.69
Translation initiation factors	G5EGT7	iffb-1	Eukaryotic translation initiation factor eIF5B	0.56
	P30642	eif-3.D	Eukaryotic translation initiation factor 3 subunit D	0.62
	O61820	eif-3.E	Eukaryotic translation initiation factor 3 subunit E	0.65
	P34339	egl-45	Eukaryotic translation initiation factor 3 subunit A	0.66
Others	Q9XVT0	rrbs-1	Ribosome biogenesis regulatory protein homolog	0.31
	P48154/Q9N3X2/...	mrps-2/-5/-22/-30	Mitochondrial Ribosomal Protein, Small	0.46-0.69
	O02056/P49405/...	mrpl-15/-22/-35/ -38/-40/-50	Mitochondrial Ribosomal Protein, Large	0.49-0.69
UPS machinery and Chaperones				
	Q1ZXT4	sao-1	Suppressor of aph-1,regulates the Notch receptor signaling pathway	0.26
	Q86S73	ubc-26	UBiquitin Conjugating enzyme	0.31
	V6CJX7	hecd-1	E3 ubiquitin protein ligase 1 homolog, involved in ubiquitin-dependent protein catabolic process	0.50
	O17391	cul-3	RING-finger protein,form the catalytic core of SCF-type E3-ubiquitin ligase complex	0.58
	O17071	rpt-4	ATPase subunit of the 19S regulatory complex of the proteasome	0.68
Chaperones				
	Q17433/Q94216/...	dnj-2/-11/-13/-27/-29	Ribosome-associated molecular chaperones	0.09-0.69
	P90788	D2030.2	Orthologous to human ATP-dependent Clp protease, hsp100 family	0.48
	P47209/P46550	cct-5/-6	T-complex protein 1 subunit epsilon and zeta	0.67/0.67
Mitochondria				
	P54815	mspn-1	Mitochondrial sorting homolog	0.42
	Q9XVQ2	timm-23	Translocase, Inner Mitochondrial Membrane	0.47
	Q23125	W02B12.9	Mitochondrial iron transporter that mediates iron uptake enzymes	0.49
	P34519	K11H3.3	Putative tricarboxylate transport protein, mitochondrial	0.5
	H2KYN3	acdh-13	Acyl CoA DeHydrogenase involved in fatty acid beta-oxidation	0.53
	O01578	F53F10.3	Mitochondrial pyruvate carrier 2	0.58
Peroxisomes				
	O62140	acox-1	Acyl-coenzyme A oxidase	0.3
	P34355	C48B4.1	Peroxisomal acyl-coenzyme A oxidase 5	0.34
	Q09652	gstk-15	Glutathione S-transferase kappa 1	0.35
	G5EDP2	daf-22	Ortholog of human sterol carrier protein SCP2, catalyzes final step in peroxisomal fatty acid beta-oxidation	0.6
	Q27487	ctl-2	Peroxisomal catalase 1	0.7
Endoplasmic reticulum				
ER Chaperones	Q22235	enpl-1	Endoplasmin homolog	0.58
	P27420	hsp-3	Heat shock 70 kDa protein C	0.6
Others	Q20065	phy-2	Prolyl 4-hydroxylase subunit alpha-2	0.11
	Q10576	dpy-185	Prolyl 4-hydroxylase subunit alpha-1	0.11
	P34329	C14B9.2	Protein disulfide-isomerase A4	0.28
	O16309/Q23338/P91180	fkb-3/-4/-5	Peptidyl-prolyl cis-trans isomerase	0.35/0.32/0.20
	Q20822	srpa-68	Signal recognition particle subunit SRP68, has 7S RNA binding activity	0.45
	Q17770	pdi-2	Protein disulfide-isomerase 2	0.55
Fatty acid metabolism				
	Q9NEQ0/G5EGA5/...	fat-1/-2/-4/-6	Omega-3 fatty acid desaturases	0.02-0.24
	Q5TKA3/Q9XWD1/...	acs-1/-5/-7/-16/-22	Fatty Acid CoA Synthetase family	0.06-0.57
	P91871	fasn-1	Fatty Acid SyNthase	0.20
	Q9GZI3	pod-2	Acetyl-CoA carboxylase, catalyzes the first step in de novo fatty acid biosynthesis	0.30
	G5EEE5/Q9XVQ9/...	elo-1/-2/-5/-6	Elongation of very long chain fatty acids proteins	0.31-0.45
	P34559/Q9NEZ8	ech-6/-7	Enoyl-CoA hydratase	0.45/0.31
	P54688	bcat-1	Branched-chain-amino-acid aminotransferase	0.53
Glycerolipid/glycerophospholipid metabolism	O17680	sams-1	S-adenosylmethionine synthase 1	0.42
	G5EC53	mboa-3	Membrane Bound O-Acyl transferase	0.48
	Q22949/G5EFP8	acl-6/-7	Glycerol-3-phosphate acyltransferase, plays a role in triacylglycerol biosynthesis	0.51/0.32
	Q9GZF3	ckb-4	Choline/Ethanolamine kinase	0.51
	Q86MJ6	ckc-1	Choline/Ethanolamine kinase	0.55
Sphingolipid metabolism	Q20375/Q9XVI6	sptl-2/-3	Glycerol-3-phosphate acyltransferase, plays a role in triacylglycerol biosynthesis	0.28/0.25

Figure 3.4: **Most represented clusters of proteins which were found significantly (FDR <5 %) decreased in abundance in *xpc-1;csb-1* double mutants upon UV irradiation.**

Then, we used 1D enrichment analysis to identify groups of proteins that both in untreated and UV-treated conditions are involved in identical pathways, carry similar PFAM domains or localize in the same compartment (e.g. categorical annotations) between *C. elegans* and human [41]. Significantly regulated group of proteins (Benjamini-Hochberg FDR <0.02) were visual-

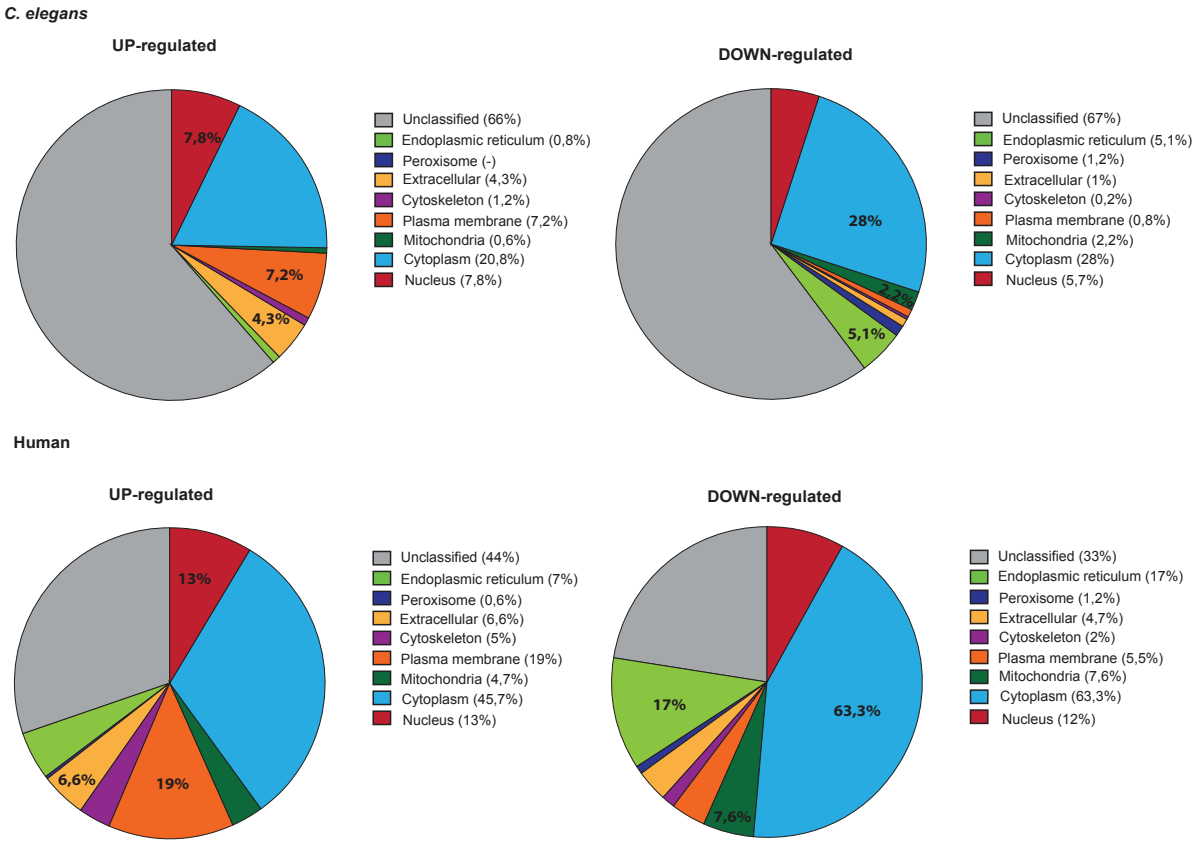

Figure 3.5: **Distribution of GO categories of significantly up and downregulated proteins in *xpc-1;csb-1* double mutants upon UV treatment.** The upper panel shows Gene Ontology annotations for *C. elegans* whereas the lower one the implemented GO annotation for human orthologues (e-value cut-off $<10^{-4}$).

ized by plotting the $\log_2$ of UV-treated to mock-treated mean of all proteins with the particular categorical annotation against the enrichment score **(Figure 3.6)**. Categories grouping proteins related to nuclear mechanisms and synaptic machinery showed a positive enrichment score, while categories related to protein synthesis and cellular metabolic processes were observed with a significant negative score. We also observed and overlap of the same categories between human and *C. elegans* organisms. Overall, this systematic analysis indicates widespread changes of protein levels during the UV-induced DNA damage in *C. elegans*.

3.1.3 Upregulated protein clusters upon genotoxic stress

Proteins belonging to the categories related to nuclear mechanisms such as chromatin remodelers, regulator of transcription, protein-DNA complex and structures of the nuclear pore,

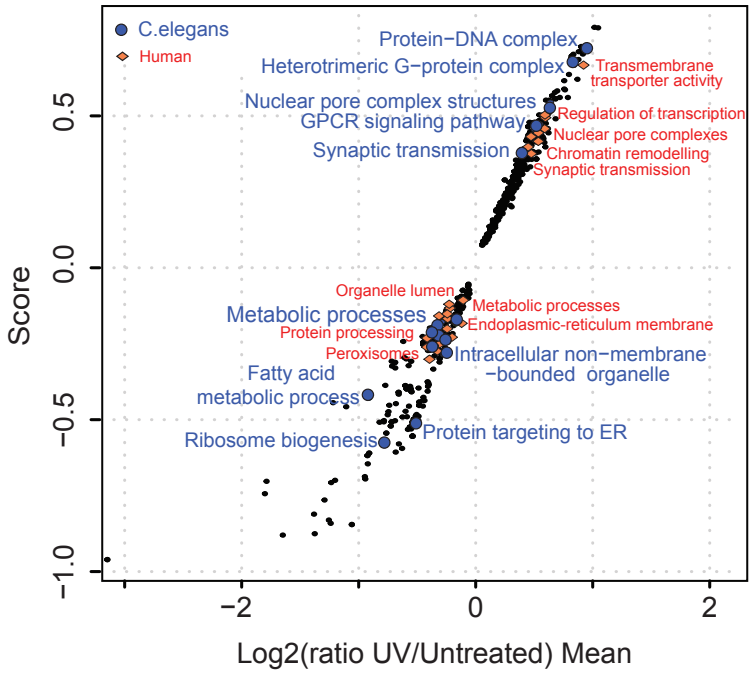

Figure 3.6: **1D enrichment plot highlights similarly regulated categories of proteins between *C. elegans* and Human.** Gene Ontology categories of Human (highlighted in orange) and *C. elegans* (highlighted in blue) of annotated proteins.

showed in our study a clear upregulation compared to the whole population of proteins. This upregulation is consistent with the chromatin remodelling, in response to DNA damage, important in modulating replication and transcription. In addition, the increased expression of members of the synaptic machinery and G-protein signalling partners, belonging to plasma membrane and extracellular space categories, suggests that signals are released from genotoxically-compromised cells that mediate the adaptation to the damage. The significantly enriched upregulated proteins belonging to the nuclear Gene Ontology category represented in **Figure 3.2A** and listed in **Figure 3.3**, includes some chromatin-remodelers, (CHD-7, BAF-1, SWSN-4, SNFC-5 and LMN-1), several transcription regulators (HMG-1.2, RTFO-1, STA-1, NONO-1, EMB-5, SPT-4, HCF-1, SMK-1) and some histone post-translational modifiers (SPR-5, HIL-2, HTZ-1, HDA-3) associated with the epigenetic control of gene expression. Some of the chromatin-associated proteins we found upregulated, as BAF-1, SWSN-4 and HCF-1, were

previously shown to interact with the IIS effector DAF-16 to remodel the local chromatin and in turn activate transcription [197, 139]. Other transcription factors specifically mediate the response to DNA damage and oxidative stress in *C. elegans* (SMK-1) [248], or play a role in the DNA-damage response to UV radiation in mammalian cells (NONO-1) [2]. Among the proteins upregulated upon UV-induced DNA damage we found also some transcription elongation, pre-mRNA processing proteins and some ribonucleoproteins (RNPs) **(Figure 3.3)**. This is consistent with the changes in spliceosome organization and the PTMs of splicing factors, found recently implicated in the cellular DNA-damage response [159, 171, 228, 136, 31, 187].

Nuclear import/export transport is enhanced upon DNA damage

Our data reveal that a number of factors involved in translation, spliceosome assembly, and nuclear-cytoplasmic transport were upregulated following UV treatment, suggesting an involvement of RNA biogenesis and translocation in the DNA damage response **(Figure 3.3)**. In line with this, changes in spliceosome organization and mobilization, as well as PTMs of slicing factors, have recently been implicated in the cellular DNA-damage response [159, 171, 228, 136]. We observed an UV-dependent induction of some ribonucleoprotein (RNPs) involved, together with their accessory proteins, in the assembly of the spliceosome on the pre-mRNA, and of many nuclear-cytoplasmic transport proteins **(Figure 3.3)**. The nuclear pore complex proteins (nucleoporins or NPPs), together with some Ran-GTPases are known factors playing an important role, not only in the nuclear import/export and the nuclear envelope (NE) assembly dynamics, but also in regulating the localization of MEL-28 [64, 49]. MEL-28 is a structural component of the nuclear envelope (NE) which, if depleted, leads to defects in distribution of the other integral nuclear-envelope proteins: EMR-1, LMN-1, LEM-2 and BAF-1 **(Figure 3.3)** [72]. These nuclear proteins provides an anchor by which chromosomes are attached to the nuclear membrane, and are required for proper chromosome segregation [10, 145]. They also promote the reorganization of damaged chromatin upon UV-C and ionizing radiation (IR)-induced DNA damage [57]. The protein BAF-1, in particular, is able to respond dynamically to stress: when immobilized at the nuclear lamina it stabilizes the chromatin structure and influences the gene expression via histone PTMs [164]. Exposure of human cells to UV treatment, instead, causes BAF-1 to dynamically interact with the histone H3/ H4 ubiquitin ligase complex (CUL4-DDB-ROC1), facilitating the recruitment of repair proteins to the damaged DNA [165].

BAF-1 expression is regulated by transcription factors that modulate lifespan, including SKN-1, PHA-4, DAF-16, and ELT-3 [9]. Similarly to what has been previously reported in aged IIS mutant worms [83] and in cells responding to DNA damage [17, 61, 155], proteins belonging to the nuclear category, but implicated in DNA replication and cell cycle progression (CDK-1, MCM-2,-7 and RFC-4), were decreased in abundance upon UV treatment.

Differences in ion transport and synaptic transmission in UV-treated worms

Apart from nuclear proteins, in our dataset we observed also a marked upregulation of proteins belonging to plasma membrane and extracellular space, suggesting a possible intra/extracellular trafficking of signals from genotoxically-compromised cells **(Figure 3.2A** and **Figure 3.6)**. Proteins belonging to the plasma membrane category are mostly transmembrane channel proteins, ATPases, amino acid, ion and ATP transporters and heterotrimeric G-proteins (key regulators of the GPCR signalling) **(Figure 3.3)**. The GPCR signalling has been implicated in different and fundamental aspects of development and behaviour, regulating in addition the synaptic transmission in the ventral cord motor neurons [161, 181]. ACh-dependent GPCR signalling was shown to inhibit the ubiquitin-proteasome system-mediated degradation of muscle proteins in *C. elegans* [224, 135]. The highest expression of the heterotrimeric G-proteins is found in excitable cells, together with components of the endocytic pathway involved in the initial vesicles assembly (ARF-6, ARL-8, DYN-1), vesicle fusion (SNAP-29 and AEX-3), and vesicles recycling through the endo-lysosomal system (ITSN-1 and SQST-1). All these proteins were upregulated in our dataset, suggesting a clear association of neuronal signalling and the regulation of DNA damage response **(Figure 3.3)**. The importance of the DNA damage response in the neuronal development has been highlighted in various human congenital progeroid syndromes including CS [116], and has been connected to ageing and age-related neurodegenerative disorders such as Alzheimers disease (AD) and amyotrophic lateral sclerosis (ALS) [98]. Consistent with neuronal developmental processes being affected by unrepaired DNA damage, we found also elevated levels of proteins implicated in axonal outgrowth (EAT-6, CAM-1, UNC-44, TBB-4) and neuronal positioning during development (SAX-7, WRK-1, UNC-33,-37). The extracellular proteins found increased in abundance following UV treatment were mainly hormone carrier transthyretin (TTR)-Related factors, reported already as elevated in aged *C. elegans* proteome studies [141, 242, 39], and associated to a mechanisms of neuro-

protection in a mouse model for AD [25]. The extracellular Cu^{2+}/Zn^{2+} superoxide dismutase SOD-4, and some lipid binding proteins/transporters NRF-5, LBP-1, EGL-3, which sequester respectively potential toxic peroxidation products and toxic FA, were also upregulated **(Figure 3.3)**.

3.1.4 Downregulated protein clusters upon genotoxic stress

The categories of downregulated proteins following UV treatments include instead a large number of ribosomal proteins, including components of the small (40S), large (60S) and mitochondrial ribosome subunits, together with components of the translation machinery **(Figure 3.4)**. Factors involved in protein homeostasis and lipid metabolism, localized between cytoplasm, mitochondria, endoplasmic reticulum (ER) and peroxisomes **(Figure 3.2A**, **Figure 3.4** and **Figure 3.6)**, showed a similar drop in abundance.
This general decline in protein synthesis and dampening of metabolic processes observed upon UV treatment is consistent with previous reports from proteomic studies in aged worms [16, 174, 141, 242, 39], supporting parallels between the DNA damage response and ageing [74].

Protein targeting for degradation

Impaired protein homeostasis has been suggested as a characteristic hallmark of ageing and some ageing-related diseases [189]. Specific mechanisms for protein fold stabilization restore the structure of misfolded polypeptides, or remove and degrade, via the proteasome or the lysosome, the aberrant proteins. In our dataset we found many components of the proteostasis network, as chaperones, ubiquitin ligases and members of the ubiquitin-proteasome system (UPS) machinery, together with ER proteins, peroxisomal enzymes and mitochondrial homeostasis related proteins generally downregulated **(Figure 3.4)**. A similar scenario has also been proposed in CSB ablated cells, which in global gene expression patterns showed endoplasmic reticulum stress and impaired unfolded proteins response mediating a pro-apoptotic effect [27]. Among the E3 ubiquitin ligases we have detected, Y54E10A.11 was the only ligase containing a RING-type-domain showing homology with the human E3 RING ubiquitin ligase TRAIP, found recently implicated in response to UV-induced DNA lesions in cells. Missense mutations

affecting the TRAIP RING-domain have also been identified in patients suffering of premature ageing syndromes [85]. The E3 ubiquitin ligase Y54E10A.11 in *C. elegans*, is a component of the ribosome quality control complex (RQC), which recognizes stalled ribosome and associates with the 60S subunit, allowing the ubiquitination and extraction of incompletely synthesized nascent polypeptides [52]. The translation stress specifically sensed by the RQC complex is communicated to the transcription factor HSF-1 [21], which in turn promotes lifespan extension [4, 111, 33, 167], suggesting a combined role in both longevity and stress responses. Misfolded proteins that cant be properly refolded or degraded due to chaperones and UPS machinery impairment, are targeted for autophagic degradation: they are imported into lysosomes during chaperone-mediated autophagy, or sequestered in autophagosomes during macroautophagy [157, 43] **(Figure 1.5)**. Compared to ageing, in which the autophagy is gradually impaired [146, 200], upon UV-induced DNA damage we found an upregulation of some members of the macroautophagy sub-pathway as ATG-3,-18 and SQST-1 (the homolog of the mammalian sequestosome p62 [143]). To assess whether the induction of autophagy was required for withstanding DNA damage we next tested the sensitivity of two autophagy mutants, *atg-3(bp412)* and *atg-9(bp564)* to UV treatment. We observed a significantly higher sensitivity in the autophagy mutants to UV treatment compared to wild type (WT) worms **(Figure 3.7)**, suggesting that proteins involved in the formation of autophagosomes are essential to endure DNA damage. Recent evidence have also demonstrated a role of autophagy, via the elimination of SQST-1, in the regulation of the DNA damage response via chromatin ubiquitination [245].

Translation and autophagy are both downstream targets of the IIS signalling and of the TOR pathway (CeTOR in *C. elegans*), key mechanisms regulating growth, metabolism and stress responses [251, 230] **(Figure 1.4)**. Under stress conditions as food deprivation, the inhibition of TOR leads to the activation of autophagy [148, 200]. Upon UV treatment instead, although we observed an increase in abundance of autophagy-related proteins, the main components of the CeTOR complex (LET-363 and DAF-15), as well as of the IIS and PI3/AKT pathways (DAF-2, -18, AKT-1, PPRT-1, SMK-1) were upregulated.

The increased autophagy can then be interpreted as a compensatory response to clear damaged proteins and recycle their component amino acids when both subpathways, the chaperone-mediates re-folding and the proteasomal degradation, are impaired. A proposed compensatory role of autophagy upon proteasome dysfunction indeed suggests that the two mechanisms are

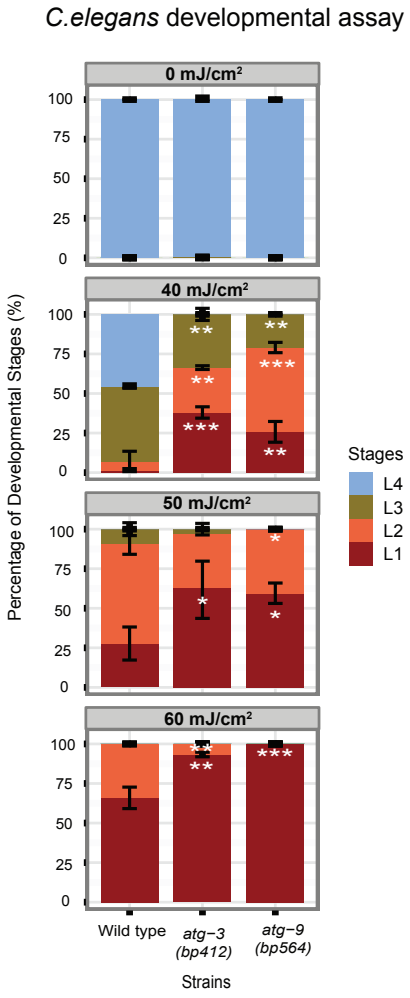

p-value	0 mJ/cm²	
	atg−3(bp412)	*atg−9(bp564)*
L1	--	--
L2	--	--
L3	0.374	--
L4	0.374	--

p-value	40 mJ/cm²	
	atg−3(bp412)	*atg−9(bp564)*
L1	**8.26E-05**	**0.00311**
L2	**0.00415**	**0.000346**
L3	**0.00406**	**0.00345**
L4	**0.000154**	**0.000154**

p-value	50 mJ/cm²	
	atg−3(bp412)	*atg−9(bp564)*
L1	**0.0497**	**0.0109**
L2	0.0526	**0.0134**
L3	0.1224	**0.0167**
L4	--	--

p-value	60 mJ/cm²	
	atg−3(bp412)	*atg−9(bp564)*
L1	**0.00239**	**0.00096**
L2	**0.00239**	**0.00096**
L3	--	--
L4	--	--

Figure 3.7: **Autophagy mutants are sensitive to UV-induced DNA damage.** Wild type (WT), *atg-3(bp412)* and *atg-9(bp564)* L1 larvae were irradiated or mock-treated and developmental stages were evaluated 48 h later. (average of n = 3 independent experiments per strain and dose is shown; >15 individuals analysed per experiment; error bars show the standard deviation (SD); *p <0.05, ** p <0.01 and ***p <0.001, two- tailed t-test compared with WT).

functionally coupled [56, 32]. At the same time, the activation of TOR upon persistent DNA damage can be explained as a way to control translation, through S6K1 (RSKS-1 in *C. elegans*) [230], to limit the production of abnormal proteins, and lipid metabolism, by regulating the activation of the nuclear receptor PPARγ [112], to preserve somatic functioning. In our study, we found that lipid metabolism was highly impaired due to a drop in abundance of key factors involved in fat biosynthesis and metabolism **(Figure 3.4)**. The regulation of these genes

involved in adipogenesis could be related to the activity of the nuclear receptor NHR-49, which in *C. elegans* has similar biological activity to the mammalian PPARγ in regulating the lipid biosynthesis and metabolism, by promoting for example FA desaturation and FA β-oxidation [235, 97]. Another *C. elegans* PPARγ hormone receptor, DAF-12, has been reported interacting with the IIS downstream effector DAF-16 in a reciprocal antagonistic manner [60].

In general all these observations suggest that amid persistent DNA damage worms reduce DNA transcription and translation, thus potentially avoiding the production of aberrant proteins. Meanwhile proteins refolding mechanisms are impaired while autophagy is promoted, suggesting protein recycling as part of metabolic shift in response to the DNA damage.

3.1.5 Analysis of proteome and transcriptome variations upon persistent DNA damage

In order to address whether the proteome alterations we observed might result from a transcriptional response to UV-induced DNA damage, we performed a Pearson correlation analysis with previously published transcriptomic data of worms that, due to a mutation in *xpa-1*, were similarly NER-deficient as the *xpc-1;csb-1* mutants employed here [169]. Since it exists a highly positive correlation between the gene expression changes in WT and NER-deficient *xpa-1* mutants in the UV response [169], our proteome analysis has been specifically focused on NER-deficient mutants. Indeed, we found a significant moderate positive correlation (r = 0.347) between the significantly changed transcripts and proteins upon UV **(Figure 3.8)**, suggesting that the expression levels of only a part of proteins can be explained by transcription, while a large fraction is subject to post-transcriptional regulation.

This aspect will be investigated in detail later, when we used a phosphopeptide enrichment approach to extend our MS analysis also to PTMs. The positive correlation between mRNA-level and protein-level changes we observed, is consistent with the observations described recently in nematodes during development [81] and during ageing [242]. Between the factors increased both at gene and protein expression level upon UV treatment (depicted in red in **Figure 3.8**) there were mainly members of the nucleus-cytoplasm molecular transport, some transmembrane channel proteins and extracellular TTR factors **(Figure 3.9)**. We observed the

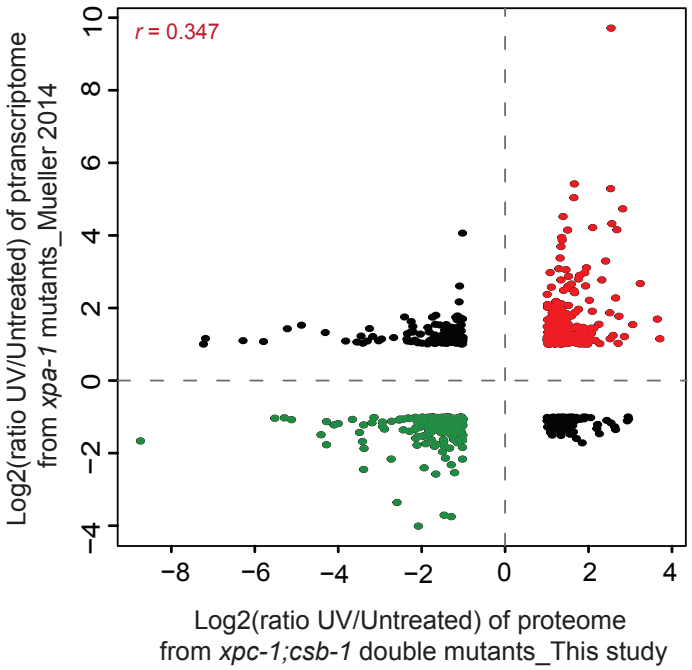

Figure 3.8: **Comparison between proteome of *xpc-1;csb-1* double mutants and transcriptome of similarly NER-deficient *xpa-1* mutants after UV treatment.** $\log_2$ values of fold-changes are shown in the dot-plot representation. The strength of the correlation is determined by the Pearson correlation coefficient (r), indicated in the figure. The proteins found commonly up- and down-regulated, both at the proteome and transcriptome level are highlighted in red and dark green.

same transcriptome/proteome trend also for stress response metabolism-related factors, such as the cytochrome P450 (CYP) and glutathione S-transferases family (GSTs) family members, together with many UDP-glucuronosyl transferases (UGTs) and some autophagy factors. The proteins we found UV-dependently elevated here, belonging to CYPs, GSTs and UGTs families for the detoxification response, were previously shown to be transcriptionally induced upon UV-C in WT, *xpa-1* and *glp-1* mutants [20]. Interestingly, key members of the IIS signalling reported an increase in abundance upon UV treatment, although at the transcript levels were significantly downregulated. An explanation for the DAF-2 increased protein abundance could be due to its accumulation at the cellular membrane in its inactive form: only upon insulin stimulus, in fact, the activated receptor gets internalized. The DAF-2 inactivation, together with the activation of the phosphatases PPTR-1 and DAF-18, promote the dephosphorylation of the serine/threonine-protein kinase AKT-1, which couldt act anymore act as repressor of the

DAF-16 nuclear translocation [123]. The active transcription factor DAF-16 can then regulate the expression of genes involved in stress resistance and longevity, possibly elevating in this way tolerance towards persistent DNA damage [169] (details about the phosphorylation status of the IIS members will be analysed later in the proteome/phosphoproteome interaction map). The categories showing instead a downregulation both at gene and protein expression level upon UV treatment (depicted in green in **Figure 3.8**), contain a family of dehydrogenases, key components of FA metabolism and protein kinases, many of which have been implicated in controlling larval development. Details on clusters of regulated proteins are reported in **Figure 3.9**.

3.2 Analysis of correlations between the UV-proteome and data from ageing and starvation studies

3.2.1 Correlation between proteome upon UV treatment and ageing

DNA damage is considered to be a driving force of ageing. In line with this concept, mutations in NER genes can accelerated ageing in mice and human patients [74]. We therefore wondered whether proteome changes in response to UV-induced DNA damage might bear similarities with those occurring during natural ageing. To this end we conducted a correlation analysis between proteomes of UV-treated *xpc-1;csb-1* double mutants, unable to repair the UV-induced DNA damage, and WT worms during ageing [242]. The Pearson correlation coefficient was increased between UV-treated *xpc-1;csb-1* double mutants and WT worms with age (from day 12 (r = 0.26) to day 27 (r = 0.34), **Figure 3.10**), suggesting that the regulation at the protein level upon persistent DNA damage recapitulates proteome alterations during the ageing process. The processes that were similarly regulated upon persistent DNA damage and during natural ageing revealed a general enrichment of factors involved in FA metabolism, oxidative-stress response, unfolded protein response (UPR) and belonging to IIS pathway [174, 242].

3.2.2 Correlation between proteomes from UV and starvation treatment

L1 larvae arrest for extended periods of time in the absence of food and only resume developmental growth when food becomes available. We have previously found similar and contrasting

Proteins significantly (FDR<5%) increased in abundance in *xpc-1;csb-1* double mutants upon UV treatment compared to the transcriptome of *xpa-1* mutants (Mueller et al.2014)

Gene family	Gene name	Fold change Proteome *xpc-1;csb-1*	Fold change Transcriptome *xpa-1*
Nuclear Pore complex Proteins (NPP)	npp-2, -4, -5, -7, -9, -10, -12, -14, -15, -16, -17,	↑	↑
Small Nuclear Ribonucleoprotein (SNR)	rnp-2	↑	↑
	rop-1	↑	↑
	snr-6, -7	↑	↑
Transmembrane transport proteins	inx-3, -6, -12, -13, -16	↑	↑
	xpo-1, -2	↑	↑
Extracellular Transthyretins (TTR)	ttr-5, -6, -7, -15, -17, -20, -26, -30, -32, -47, -51	↑	↑
Glutathione S- transferases (GST)	gst-12, -16, -20, -24	↑	↑
	gst-4	↑	↓
UDP-glucuronosyl transferases (UGTs)	ugt-26, -28, -29, -31	↑	↑
Cytochrome P450	cyp-14a5	↑	↑
	cyp-33c8	↑	↑
Autophagy (ATG)	atg-3, -18	↑	↑
C-type lectin (CLEC)	clec-17, -67	↑	↑
Insulin/IGF signalling	akt-1	↑	↓
	daf-2	↑	↓
	pptr-1	↑	↓

Proteins significantly (FDR<5%) decreased in abundance in *xpc-1;csb-1* double mutants upon UV treatment compared to the transcriptome of *xpa-1* mutants (Mueller et al.2014)

Gene family	Gene name	Fold change Proteome *xpc-1;csb-1*	Fold change Transcriptome *xpa-1*
Fatty Acid CoA Synthetase (ACS)	acs-1, -5, -7	↓	↓
	acs-16, -22	↓	↑
Fatty Acid - desaturase (FAT)	fat-1, -6	↓	↓
	fat-4	↓	↑
- 2-hydroxylase	C25A1.5	↓	↓
Fatty Acid Elongation (ELO)	elo-1, -2	↓	↓
	elo-6	↓	↑
DeHydrogenases	dhs-3, -18	↓	↓
	dhs-27	↓	↑
Peptidyl-prolyl cis-trans isomerase (FKB)	fkb-3, -5	↓	↓
	fkb-4	↓	↑
Peroxisomal Membrane Protein (PMP)	pmp-2, -4, -5	↓	↓
Mitochondrial ribosomal protein (MRPL/MRPS)	mrpl-15, -22, -35, -38, -50	↓	↓
	mrps-5, -22, -30	↓	↓
Kinases	air-1	↓	↓
	ckd-1, -12	↓	↓
	kin-20	↓	↓
	mtk-1	↓	↓
	nsy-1	↓	↓
	plk-1	↓	↓
	spk-1	↓	↓
	riok-1	↓	↓
Translation initiation factor	eif-3.D, -3.E	↓	↓
	egl-45	↓	↓

Figure 3.9: **Most represented clusters of proteins which were found up- and/or down-regulated at the proteome (*xpc-1;csb-1* double mutants) and at the transcriptome (*xpa-1* mutants) level after UV treatment.** Red arrows refer to upregulation while blue arrows refer to downregulation.

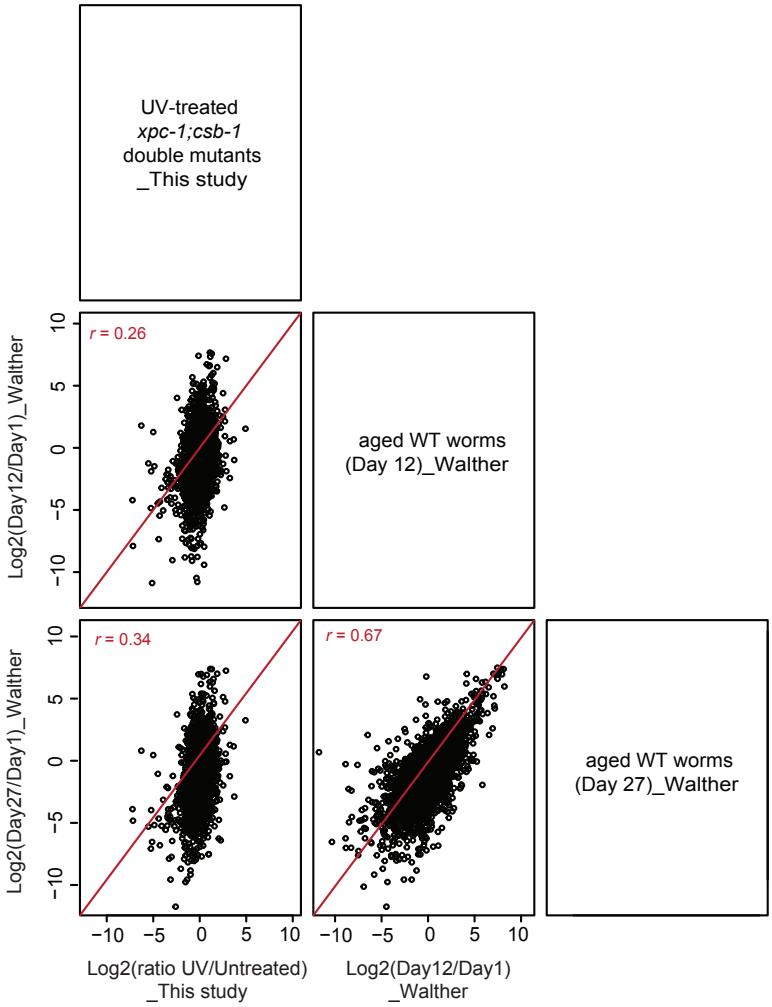

Figure 3.10: **Comparison between proteins detected in *xpc-1;csb-1* double mutants upon UV treatment vs. ageing in WT worms (Walther et al.,2015 [242]).** $\log_2$ values of fold-changes are shown in the dot-plot representation. The strength of the correlation is determined by the Pearson correlation coefficient (r), indicated in the figure.

transcription responses between starvation conditions and UV-induced DNA damage in NER-deficient mutants [169]. We performed, in parallel to UV treatment, also starvation experiment using *xpc-1;csb-1* double mutants: three independent biological replicates were analysed and an excellent reproducibility (r >0.95 for biological replicates) was reported **(Figure 2.1A)**. To determine whether proteome changes upon starvation and UV treatment were related, we compared the changes in protein abundance occurring in *xpc-1;csb-1* double mutants upon the two treatments. We obtained a positive Pearson correlation between the proteomes of UV-treated

and starved animals (r = 0.77) **(Figure 3.11)**.

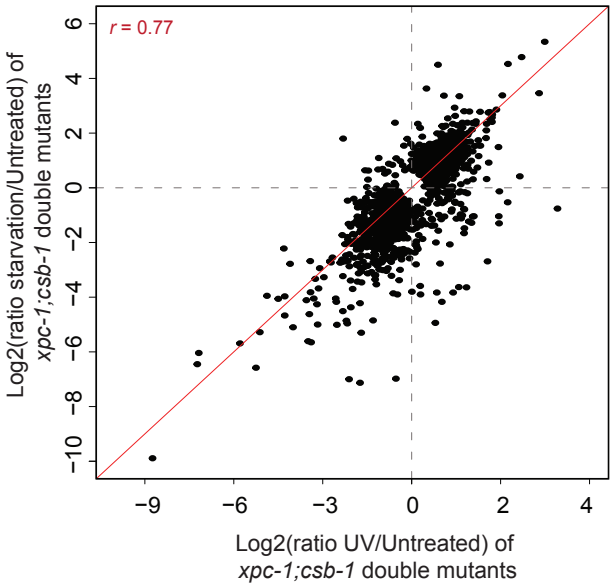

Figure 3.11: **A positively high correlation is registered for proteins that significantly change in abundance in *xpc-1;csb-1* double mutants upon UV treatment vs. starvation.** $\log_2$ values of fold-changes are shown in the dot-plot representation. The strength of the correlation is determined by the Pearson correlation coefficient (r), indicated in the figure.

In our study, upon UV treatment we detected mainly changes in abundance of chromatin-associated proteins and members involved in vesicles/neurotransmitters trafficking **(Figure 3.3** and **(Figure 3.6)**. A similar involvement of heterotrimeric G-proteins occurs in *C. elegans* pharynx for the starvation-induced activation of the Ras-MAP kinase pathway [254]. Upon UV treatment we observed also significant changes of metabolic pathways involved in the synthesis and use of carbohydrate, amino acid and lipids. In particular many enzymes involved in FA biosynthesis showed a significant drop in abundance **(Figure 3.4**,**Figure 3.6** and **Figure 3.9)**. Members of the same protein classes were found similarly changed in abundance also in our starvation study consistent with previous reports on starvation [129], in IIS deficient worms [70, 53] and upon ageing [141, 174, 39].

These results suggest that NER-deficient worms, when subjected to stress condition, such as UV treatment or starvation, activate a somatic preservation program to avoid energy expense, which resembles the metabolic shift occurring during ageing.

3.3 Lipidome analysis upon UV and starvation

3.3.1 Fatty acid biosynthetic pathways are affected by starvation and UV treatment

Based on these parallels indicating a dampening of metabolic processes following DNA damage and starvation, we decided to trace lipid profiles of *xpc-1;csb-1* double mutants upon the two treatments. Upon starvation and UV treatment, key enzymes involved in FA biosynthesis **(Figure 3.12)** and playing important roles in FA accumulation and consumption during lifespan [240, 95, 260] were downregulated both at the protein **(Figure 3.3)** and transcript level **(Figure 3.9)**. The expression of the same class of genes related to lipid metabolism has been found significantly decreased in the UV-irradiated and photoaged human skin, suggesting that inhibition of de novo lipid synthesis may have a detrimental effect, leading also to collagen destruction [110].

We used the Thin Layer Chromatography (TLC) and mass spectrometry (MS) to assess any evident changes in content of various lipid classes that could reflect the downregulation of enzymes of the FAs metabolism observed in the proteomics data. Upon UV treatment we observed a decrease in the amount of triacylglycerols, the storage form of FAs, with a consequent increase in free FAs content, that strikingly resembled the metabolic shift observed in aged nematodes [39]. This shift from triacylglycerols to free FAs was even more pronounced upon starvation **(Figure 3.13)**, consistently with the fact that worms derive energy from degradation of fat stored to survive the food deprivation [63, 216].

3.3.2 Change in sphingolipids abundance upon treatments

The downstream products of these FA biosynthetic pathways are normally used to synthesize more complex lipids: the SLs and the glycerophospholipids **(Figure 3.12)**. SL works as an intermediate for the production of Cer, a key product for the synthesis of glucosylceramide and sphingomyelin SM [236, 258] **(Figure 3.12)**. The ceramide signalling pathway downstream of SLs has reported having a role in stress responses: Cer is produced from SM in UV- and IR-treated mammalian cells [255, 256], whereas an increased synthesis of SM from Cer is

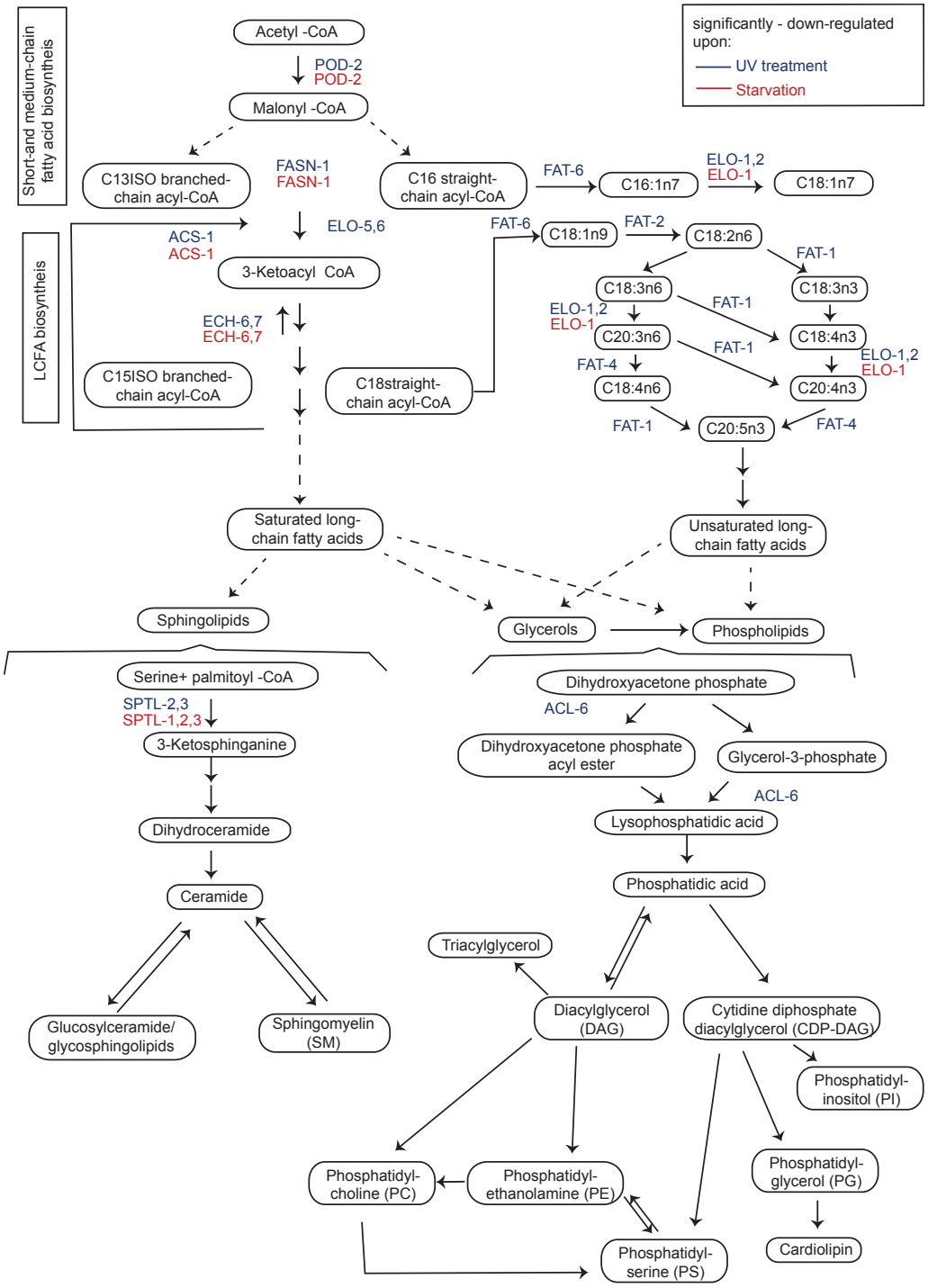

Figure 3.12: **Fatty acid biosynthetic pathways coupled with sphingolipid and phospholipid metabolic pathways.** Key members of these metabolic pathways were all significantly decreased in abundance in *xpc-1;csb-1* double mutants upon starvation and UV treatment. Regulated proteins upon starvation and UV treatment are highlighted in red and blue respectively.

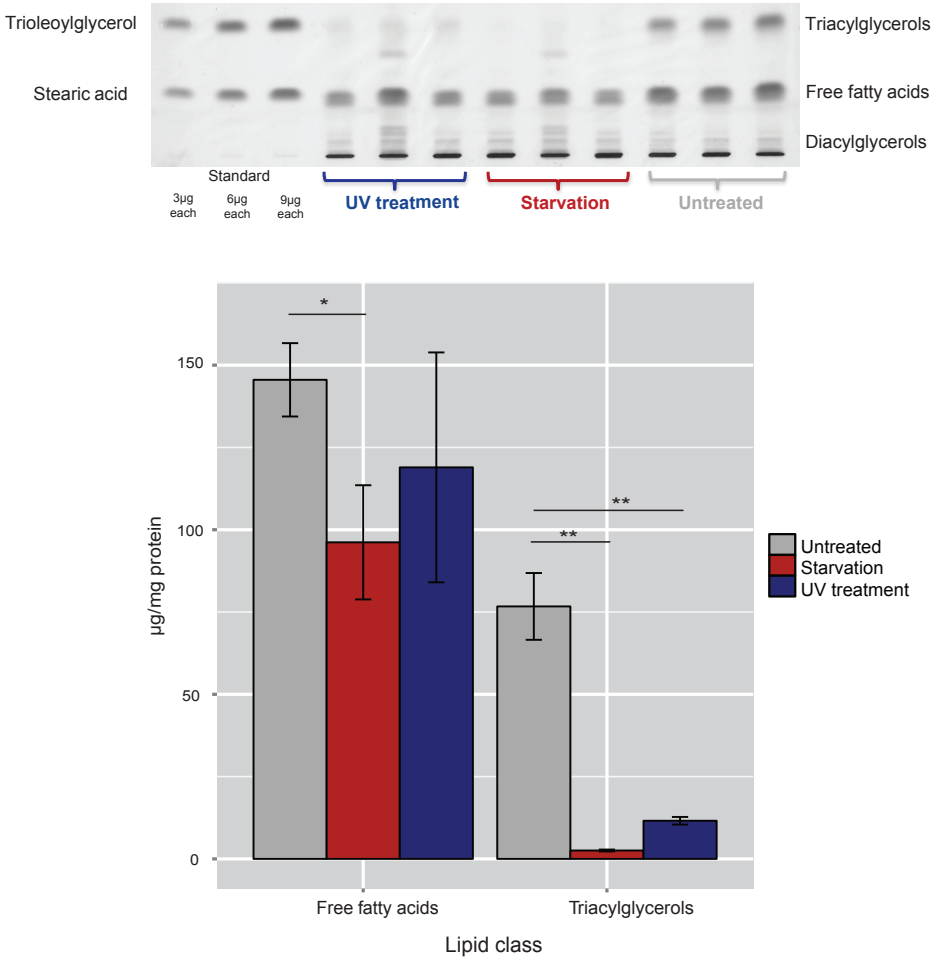

p-value	Starvation *vs* Untreated	UV *vs* Untreated
Free fatty acids	**0.01976**	0.31
Triacylglycerols	**0.006149**	**0.007389**

Figure 3.13: **A shift from triacylglycerols to free fatty acids was observed in *xpc-1;csb-1* double mutants larvae upon starvation and UV treatment.** Changes in fatty acid and triacylglycerol content upon each treatment were assessed using the TLC technique. Quantification of the TLC results is indicated by the histogram. Grey bars indicate untreated samples, while red and blue bars refer to starvation and UV treatment, respectively. Significant levels of pairwise comparisons are indicated by the p-value: *p <0.05, ** p <0.01 and ***p <0.001.

associated to accelerated development and ageing [46]. Similarly to the observations gained in ageing studies [46], our MS-based quantitative SLs profiling showed a general increase in SM and decrease in Cer amount upon both treatments **(Figure 3.14)**. This can be explained as a direct consequence of the impaired SFAs biosynthesis, which usually provides building blocks for the SLs synthesis **(Figure 3.12)**.

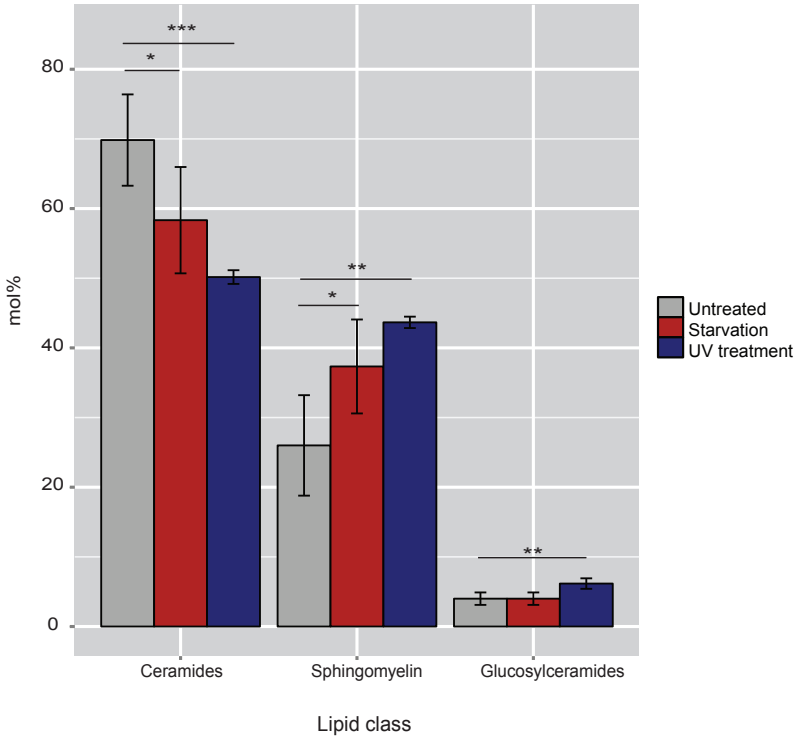

p-value	Starvation *vs* Untreated	UV *vs* Untreated
Ceramides	**0.01939**	**0.000642**
Sphingomyelin	**0.01507**	**0.001538**
Glucosylceramides	0.7858	**0.002402**

Figure 3.14: **Changes in the amount of three sphingolipids subclasses (ceramides, sphingomyelins and glucosylceramides) upon treatments in *xpc-1;csb-1* double mutants larvae.** Changes in the content of sphingolipids were assessed using Mass Spectrometry analysis. Grey bars indicate untreated samples, while red and blue bars refer to starvation and UV treatment, respectively. Significant levels of pairwise comparisons are indicated by the p-value: *p <0.05, ** p <0.01 and ***p <0.001.

Lowering SFA synthesis in cells, by impairing the function of critical factors involved in their biosynthesis, has a positive effect on the DNA damage response, reducing the risk of cancer development [257]. Previous studies on *C. elegans* mutants deficient for the monomethyl branched chain FAs (mmBCFAs) synthesis (elo-5 loss-of-function mutation), demonstrate an arrested development [261] similar to the starvation-induced L1 arrest [114]. This arrest could be rescued by specific SFAs-derived sphingolipids, the d17iso-glucosylceramides (d17iso-GlcCer), which act in the intestine, together with the downstream factors of the CeTOR pathway, to promote

postembryonic growth and development [261]. Our data on UV-treated animals suggest as well a link between lipids and CeTOR signalling in coordinating development since we observed both an increase in abundance of glucosylceramides (d17iso-GlcCer)and of members of the CeTOR pathway **(Figure 3.14)**. In line with previous study [114] reporting stable mmBCFAs levels in starved L1 larvae, we also observed stable levels of d17iso-GlcCer species upon starvation **(Figure 3.14)**. The previously described role of the GlcCer/TOR pathway in promoting development independently from the IIS and DAF-7/TGF-signalling [261, 114] might suggest its involvement in the UV-induced DNA damage response.

3.3.3 Glycerophospholipids profiling upon treatments

Another major component of cellular membranes is the lipid class of glycerophospholipids [236, 90, 258], synthesised from the intermediate phosphatidic acid, through a series of reduction and acylation reactions **(Figure 3.12)**. Phosphatidic acid is dephosphorylated to yield DAG, which successively is converted into PC and PE, both being intermediates for the formation of PS [137]. PS and PI are generally synthesized from the CDP-DAG precursor, which is also upstream of the synthesis of PG and cardiolipin (CL) [258]. Quantitative glycerophospholipids MS profiling, upon starvation and UV treatments, showed a change in abundance specifically of the DAG downstream products, indicating a preferential direction in the phospholipids synthesis **(Figure 3.15)**. Upon UV, the PC and the PC-derived PS were preferentially synthesized, whereas PE was significantly downregulated. In contrast, upon starvation the PE and the PE-derived PS were preferentially synthesized while PC was significantly downregulated. We did not observe changes of the other CDP-DAG derived phospholipids PI, while we observed a significant downregulation of PG in response to starvation **(Figure 3.15)**. This decrease upon starvation resembles the behaviour previously described in cells for the PG-derived downstream target CL, which drastically decreases in quantity when cells enter the cell cycle arrest [29]. Abnormalities in CL can impair mitochondrial bioenergetics [163], since this complex phospholipid is intimately involved in maintaining mitochondrial functionality and membrane integrity [186].

All together these observations suggest that the worms respond to persistent DNA damage by a metabolic shift reminiscent of adaptations during starvation [129] and ageing [141, 174].

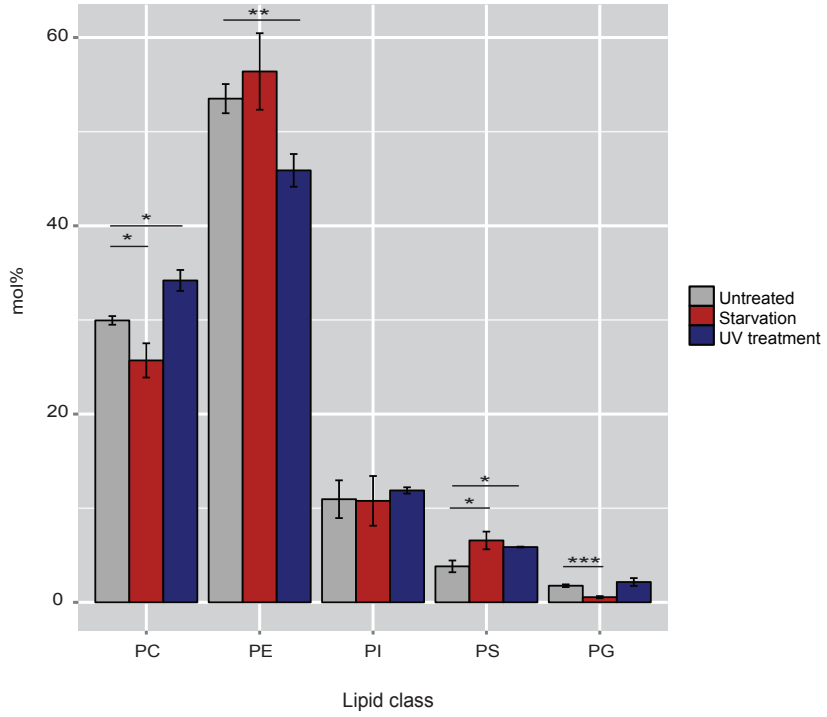

p-value	Starvation *vs* Untreated	UV *vs* Untreated
Phosphatidylcholine (PC)	**0.04848**	**0.01237**
Phosphatidylethanolamine (PE)	0.3456	**0.004986**
Phosphatidylinositol (PI)	0.931	0.5065
Phosphatidyserine (PS)	**0.018**	**0.02895**
Phosphatidylglycerol (PG)	**0.0003879**	0.2382

Figure 3.15: **Changes in the amount of the five glycerophospholipids subclasses (PC, PE, PI, PS and PG) upon treatments in *xpc-1;csb-1* double mutants larvae.** Changes in the content of sphingolipids were assessed using Mass Spectrometry analysis. Grey bars indicate untreated samples, while red and blue bars refer to starvation and UV treatment, respectively. Significant levels of pairwise comparisons are indicated by the p-value: *p <0.05, ** p <0.01 and ***p <0.001.

3.4 Proteome and phosphoproteome-coupled analysis to build a regulatory network in response to persistent DNA damage

To date, MS-coupled proteomics has developed as a very efficient technique [115] for detecting changes in protein abundance [129, 242] and the metabolic shifts induced by specific

treatments or particular genotypes [102, 39]. In order not only to detect protein expression changes but to also follow the dynamics of UV-induced PTMs, we extended our label-free quantitative MS analysis by performing phosphopeptide enrichment. Among the 7430 detected phosphosites, we identified 3276 of them that were significantly modulated in response to UV treatment: specifically 1571 were more than 1.5-fold downregulated and 1705 were more than 1.5-fold upregulated at the p-value <0.05. Different phosphorylation sites on the same protein may play specific roles in modulating the protein functions upon DNA damage. For example, in the phosphoproteome analysis, we detected phosphorylations on the TXY motif (Thr-xxx and Tyr-xxx), which are required for the activation of the ERK/MAP kinase (MPK-1). Previous studies showed that MPK-1 activity is primarily controlled by signalling-mediated cycles of phosphorylation and dephosphorylation, rather than its accumulation [132, 201]. To further understand signalling networks involving proteins that are changed upon DNA damage, we created a protein-protein interaction map (using the bioinformatics software platform Cytoscape [212]), based on the map of interactions available from the *C. elegans* data repository (WormBase, http://www.wormbase.org). For the network analysis we selected only significantly regulated proteins upon UV treatment and the significantly changed phosphosites normalized to the proteome. Network nodes are highlighted as up- or downregulated at the proteome level depending on the grades of the colour gradient and the different shapes indicate their phosphorylation status **(Figure 3.16)**.

The central node of the network is the DAF-2 protein, component of the IIS signalling, a pathway that has been implicated in the regulation of both the DNA damage response and longevity [156, 78, 169, 242]. The main clusters of upregulated proteins arising from the DAF-2 central node are: chromatin organizers, the synthetic multivulva class B family of proteins, the Ce-TOR and proteins involved in nucleus-cytoplasm transport **(Figure 3.16** and proteins listed in **Figure 3.3)**. Nuclear transport proteins as PGL-1 and PGL-3 are intermediary nodes between DAF-2 and some autophagy proteins, in particular with the highly upregulated SQST-1, which together with other upregulated components of the endocytic pathway is involved in the neuronal synaptic machinery **(Figure 3.16)**. The nodes that work in connection with the synaptic machinery for the hormones and neurotransmitters release, like heterotrimeric G-proteins, or for the mechanosensation, like the MEC proteins, were also found indirectly linked to DAF-2

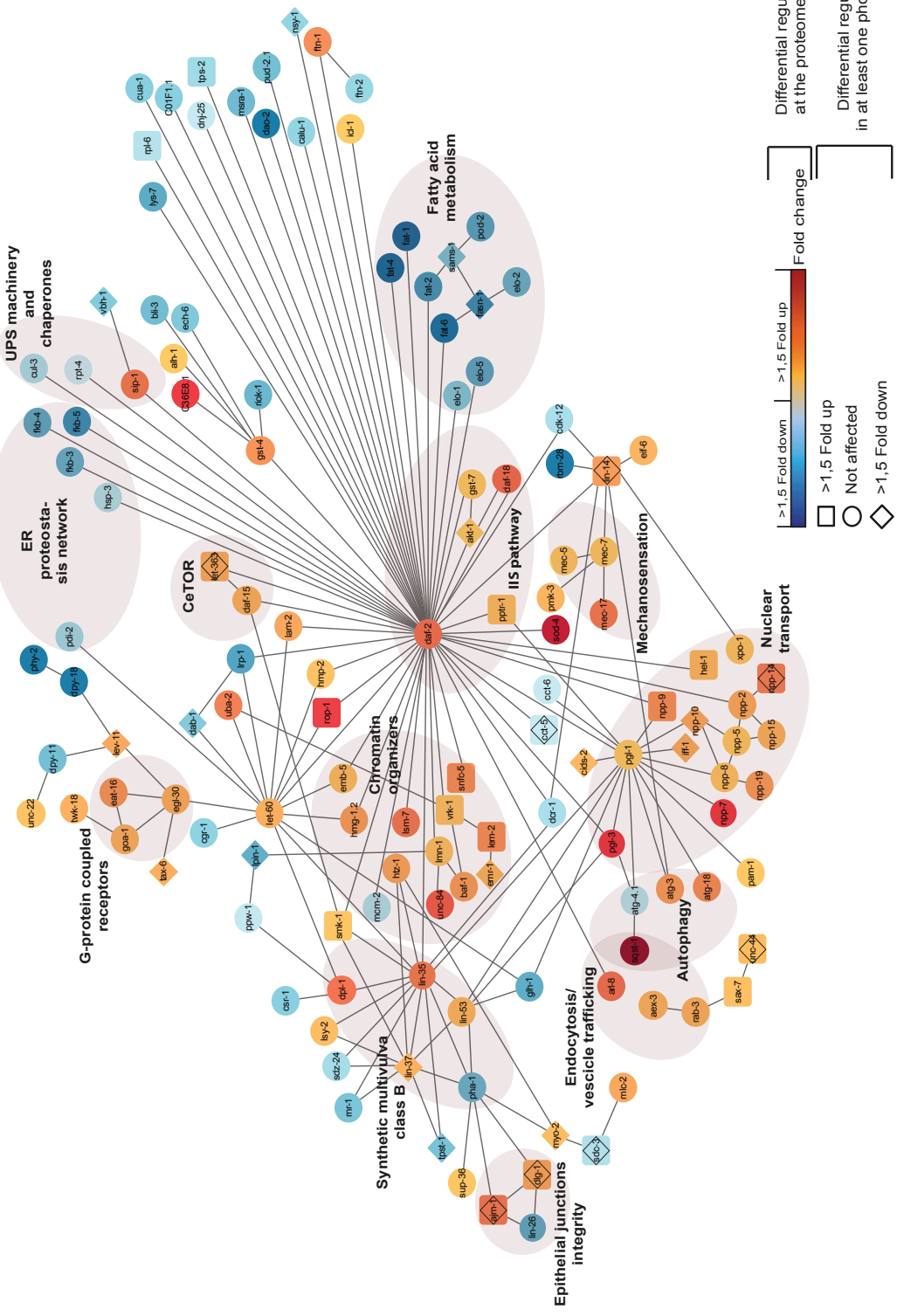

Figure 3.16: **Network of interactions between proteins that are significantly regulated in *xpc-1;csb-1* double mutants upon UV treatment.** The colour gradient bar indicates the different regulation at the proteome level: dark blue refers to proteins that are >1.5-fold downregulated, while dark red refers to proteins that are >1.5-fold upregulated. The different shapes indicate the significantly changed phosphosites normalized to the proteome.

and all upregulated. A member of the glutathione S-transferases family, GST-4, which plays a role in the detoxification from ROS, was also increased in abundance and under the regulation of DAF-2 **(Figure 3.16** and **Figure 3.9)**. As it happens upon ageing and in some age-related diseases, upon UV treatment we observed a general decrease in abundance of proteins related to protein homeostasis. Many factors belonging to the UPS machinery, as well as some chaperones, and members of the ER proteostasis network were downregulated and linked to the DAF-2 central node **(Figure 3.16** and **Figure 3.4)**. Members of FA metabolism, localized between the cytoplasm, ER, peroxisomes and mitochondria **(Figure 3.4)**, and proteins involved in amino-acid biosynthesis (SAMS-1), development (DAO-2, DNJ-25, CALU-1, CUA-1) and stress response (NSY-1 and LYS-7) were also decreased in abundance. This network of interactions suggests a general dampening of somatic functions in response to UV treatment, in favor of mechanisms involved in protein clearance, synaptic transmission and stress resistance, mainly targets of the IIS pathway [70, 194, 53]. Using the BiNGO tool from Cytoscape software [150, 37] we were able to determine which Gene Ontology biological processes were statistically overrepresented in our network of proteins. Within this interaction map **(Figure 3.17)** the main regulated metabolic processes upon UV-induced DNA damage were larval development, cellular biosynthetic processes, leading to modulation of translation, and organic acid biosynthetic processes, in particular the UFAs metabolism **(Figure 3.15)**.

Based on the combined proteome and phosphoproteome alterations previously observed, we next derived signalling pathways that respond to persistent DNA damage **(Figure 3.18)**. We included in the analysis also proteins that showed significant alterations at the phosphoproteome level without having quantitative values for the protein, getting in this way a comprehensive view of the PTM role in response to stress.

In the whole network of interactions, the epidermal growth factor (EGF) pathway appears as the central signalling platform. Intriguingly, EGF signalling has been linked to development, metabolism, and longevity in *C. elegans* [103]. The EGF pathway works through the activation of downstream signalling cascades, which include the phospholipase C (PLC)/PKC, the PI3/AKT and the Janus kinase/Signal transducer and activator of transcription (JAK/ STAT) pathways [104]. EGF also acts through the RAS/extracellular signal regulated kinase (ERK)

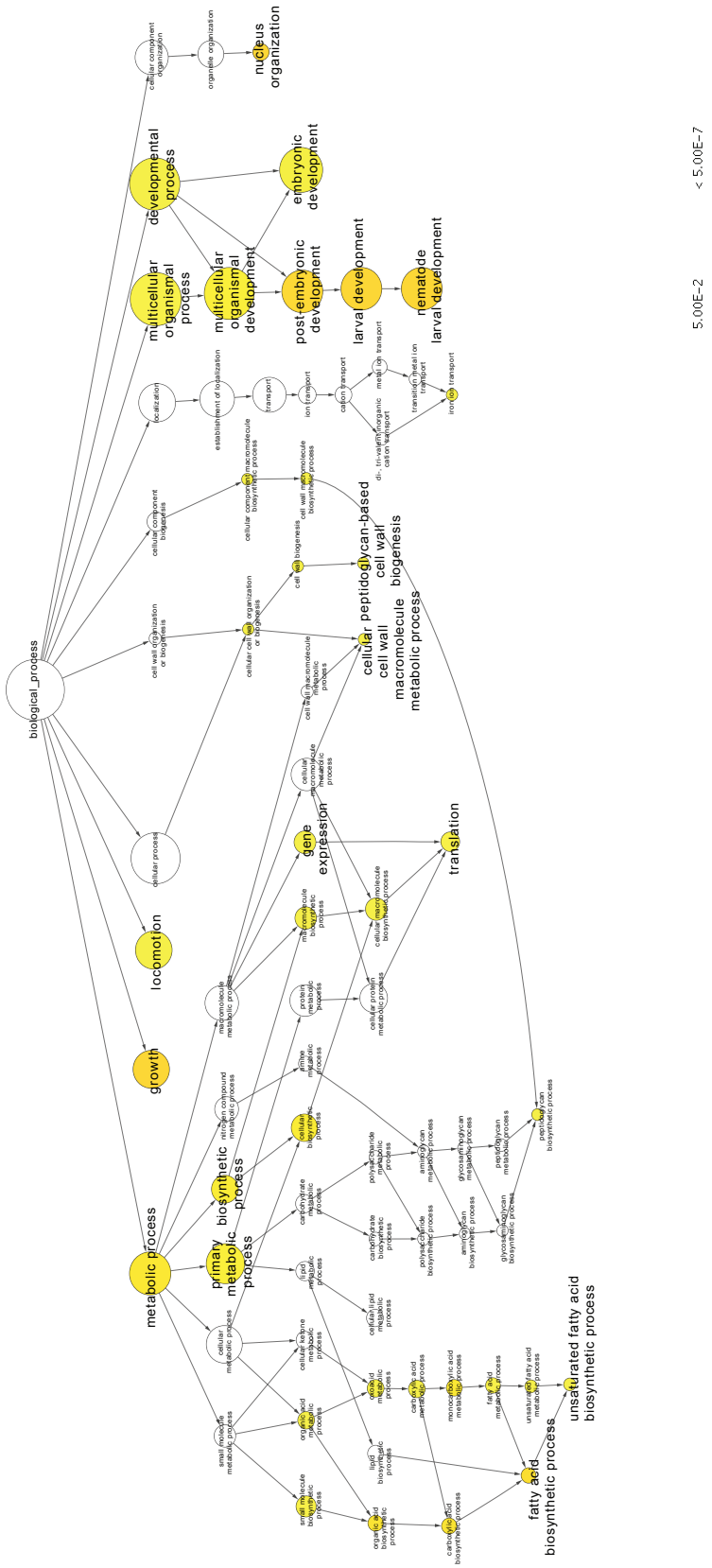

Figure 3.17: **Interaction map of Gene Ontologies biological processes that are statistically overrepresented in our network.** This map was created using the BiNGO tool in the Cytoscape software. The colour gradient indicates which biological processes might have a main role in the response towards UV.

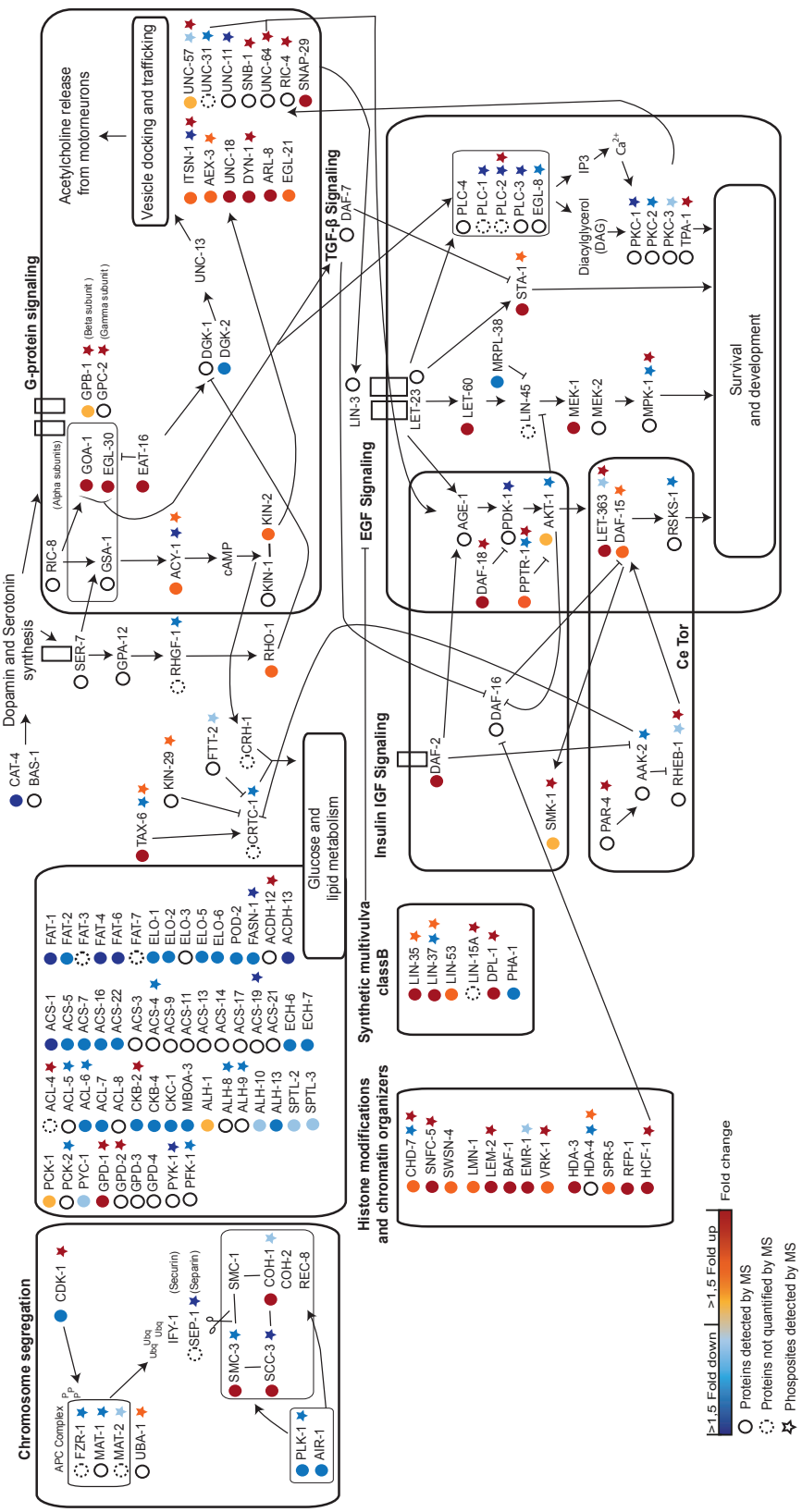

Figure 3.18: **Network of protein interactions in *xpc-1;csb-1* double mutants upon UV treatment.** The colour gradient bar indicates significant degrees of regulation at the proteome and phosphoproteome level: dark blue refers to >1.5-fold downregulation, while dark red refers >1.5-fold upregulation. Full circles show proteins that are detected by MS as downregulated (blue), or upregulated (red) or not significantly regulated (white). Dotted circles show proteins that are not quantified by MS. Stars show phosphosites detected by MS, at the p-value <0.05, as decreased (blue) or increased (red).

to regulate protein homeostasis via the expression of antioxidant genes and the stimulation of the UPS activity via the activation of SKR-5 protein [144]. Interestingly, we found two of the downstream effector of the EGF signalling, the transcription factor STA-1 and MPK-1, both significantly phosphorylated upon unrepaired DNA damage **(Figure 3.18)**, suggesting that these PTMs might have a role upon persistent DNA damage [109]. We tested threfore the sensitivity of the STAT mutant *sta-1(ok587)* upon UV treatment and indeed, it showed a significantly increased sensitivity compared to WT worms **(Figure 3.19)**, suggesting a possible role of this transcription factor in enduring DNA damage. The role of activated STAT transcription factors in repression of dauer formation [244] might suggests the possible involvement of STA-1, together with DAF-16, in alleviating the developmental arrest upon persistent DNA damage [169].

The EGF pathway, is also a biological target of the synthetic multivulva class A and B family of proteins **(Figure 3.3)**, which control the ectopic vulva development by tightly repressing the spatial expression of the EGF-like signalling molecule, encoded by the gene lin-3 [203]. EGF signalling also regulates cell growth and survival via the PI3/AKT kinase cascade, that impacts the activity of CeTOR and the IIS effector DAF-16 [87]. Between the signalling molecules commonly targeted by the EGF signalling [231] and the G-protein signalling [12], there are regulators of phospholipid metabolism such as PLC, which is involved in mediating the hydrolysis of phosphatidylinositol 4,5 bisphosphate (PIP2) into the second messengers DAG and inositol 1,4,5-triphosphate (IP3). DAG is a cofactor for the activation of PKC-dependent pathways, while the IP3 promotes the calcium release (Ca2+). DAG is an intermediate of the glycerophospholipids synthesis **(Figure 3.12)**, a mechanism that together with the lipid biosynthesis and metabolism we saw already being dampened **(Figure 3.13)**, due to a general decrease of the main factors involved in regulating it. Members of the DAG-downstream PKC pathway have been implicated in the regulation of *daf-2* IIS-dependent control of dauer formation [162] and also in the secretion of synaptic vesicles at the motor neurons [215]. Consistently, in our dataset we detected a high expression of the downstream components of G-protein signalling, involved in the neuronal synaptic machinery, and mediating the initial vesicles assembly **(Figure 3.6**, **Figure 3.16**, **Figure 3.18** and **Figure 3.3)**. The heterotrimeric G proteins α subunits, as EGL-30 and GOA-1, not only mediate serotonin signalling, promoting intracellular vesicle trafficking and synaptic transmission [181, 12, 30], but also regulate the expression of DAF-7, a

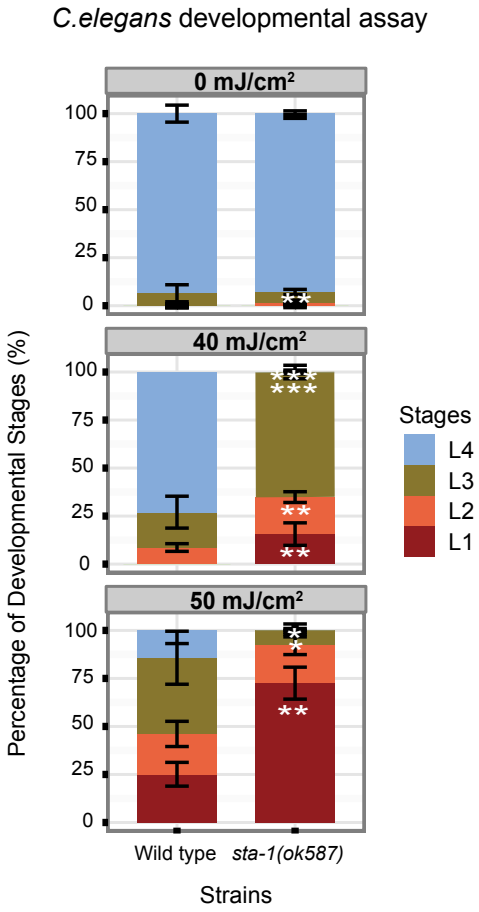

p-value	0 mJ/cm²
	sta-1(ok587)
L1	--
L2	**0.00146**
L3	0.754
L4	0.816

p-value	40 mJ/cm²
	sta-1(ok587)
L1	**0.0098**
L2	**0.0058**
L3	**0.00085**
L4	**6.67E-05**

p-value	50 mJ/cm²
	sta-1(ok587)
L1	**0.00137**
L2	0.859
L3	**0.0169**
L4	**0.0227**

Figure 3.19: **Animals lacking the transcription factor STA-1 are sensitive to persistent DNA damage caused by UV treatment.** Wild type (WT) and *sta-1(ok587)* L1 larvae were irradiated or mock-treated and developmental stages were evaluated 48 h later. (average of n = 3 independent experiments per strain and dose is shown; >20 individuals analysed per experiment; error bars show the standard deviation (SD); *p <0.05, ** p <0.01 and ***p <0.001, two- tailed t-test compared with WT)

member of the TGF-signalling pathway which during larval development is known to regulate DAF-16 and STA-1 nuclear localization [173, 213, 133, 244]. The activity of the two G-protein subunits EGL-30 and GOA-1 in regulating neurotransmitter secretion is itself regulated by the guanine nucleotide exchange factor RIC-8 [160]. RIC-8 is able to activate another subunit of the heterotrimeric G proteins pool, GSA-1, which through the activation of the adenylyl cyclase ACY-1 leads to the production of cyclic AMP (cAMP) [195].

This signalling cascade activates the regulatory subunits (KIN-1 and KIN-2) of cAMP dependent protein kinase A (PKA), to modulate growth and locomotion [207]. Once activated,

PKA acts on the cAMP- responsive element (CRE)-binding protein (CREB, CRH-1 in *C. elegans*), modifying its phosphorylation status and altering, in this way, its subcellular localization. This stimulates the association of CRH-1 with its cAMP-regulated transcriptional co-activator (CRTC, CRTC-1 in *C. elegans*). Together these two factors target the expression of genes, carrying CRE elements at the promoters site, which regulate the glucose and lipid metabolism [3]. CRH-1 and CRTC-1 are also targets of AMP-activated protein kinases (AMPK, AAK-2 in *C. elegans*) and calcineurin. In particular, AMPK and calcineurin antagonistically modulate the phosphorylation status of CRTC-1, controlling its activity and effect on ageing and longevity [151, 24]. Neuronal CRTC-1, in *C. elegans*, has been shown regulating metabolic genes in peripheral tissues antagonistically with the nuclear receptor NHR-49, previously mentioned as downstream target of TOR pathway in regulating lipid metabolism and fat accumulation [112, 235].

Apart from its involvement in the control of energy metabolism, AAK-2 also regulates longevity via interaction with the *daf-2*-mediated IIS pathway [45]. Previous tests performed in our laboratory on two independent alleles of *aak-2*, showed the involvement of AAK-2 also in response to DNA damage, due to their significantly increased sensitivity to UV treatment compared to wild type worms. Loss of AAK-2 in ASI neurons is also sufficient to promote fat reduction, slower movements, and the exit from dauer arrest, via an enhanced secretion of dense core vesicles, containing pro-growth regulators [44]. This enhanced secretions in *aak-2* mutants works through the activity of members from the dense core vesicle release machinery, as the protein UNC-31, which if mutated abrogate these effect [44]. UNC-31, together with another component of the synaptic vesicle fusion machinery, UNC-64, is known to be involved in the secretion of neurotransmitter inputs regulating lifespan and dauer formation through the IIS pathway [1]. Another factor involved in the determination of adult lifespan via regulation of the IIS downstream target DAF-16, is the enzyme HCF-1 [139]. This factor works also as transcriptional regulator of chromatin modification and histone phosphorylation [134]. Consistently, we also found a number of histone modifiers and chromatin organizers highly upregulated in response to UV treatment (**Figure 3.6**, **Figure 3.18** and **Figure 3.3**). Other proteins found increase in abundance upon UV belongs to the cohesion complexes, required for proper chromosome segregation and repair of double strand breaks [13, 177, 190]. The cohesion complex requires the activity of four proteins SMC-1, SMC-3, COH-1 and SCC-3, many of which were increased in

abundance upon UV treatment **(Figure 3.3)**. The dissociation of this cohesion complex by the action of AIR-1 and PLK-1 kinases [77] or the cleavage by separase (SEP-1), all found highly dampened upon UV treatment, is necessary for the segregation of sister chromatids during mitosis [86].

Taken together the network analysis reveal an intricate network of differentially regulated signalling nodes and centrally place IIS, EGF and AMPK signalling in the DNA damage response. The main findings lead us to propose a role of the intermediates of key pathways, such as IIS, CeTOR and the heterotrimeric G-proteins, on the EGF signalling cascade to affect stress response and regulate lipid metabolism. Moreover, the alterations in abundance of proteins involved in chromosome segregation and chromatin organization suggest that NER-deficient worms responds to persistent DNA damage by impairing DNA replication, meanwhile favouring transcription regulation and promoting a stress survival response.

Chapter 4

Discussion

Unrepaired DNA damage promotes cancer development and causally contributes to the ageing process. To better understand how metazoan organism respond to persistent DNA damage we have taken advantage of NER-deficient *C. elegans* mutants that are unable to remove UV-induced DNA lesions. The simple metazoan system is particularly useful to understand the physiological adaptations upon persistent DNA damage since, similarly to human NER-deficient patients, the worms show growth retardation, accelerated tissue dysfunction, and premature death. Previous experiments based primarily on transcriptome analyses of NER-deficient mice have suggested an adaptive survival response that is triggered in response to DNA damage to preserve tissue functionality by attenuated the somatic growth axis amid accumulating DNA damage during ageing [178, 234, 232, 73]. Although in *C. elegans*, detailed proteomic studies have been conducted to illustrate the scenario of the organismal response upon stress [129, 141] or during development [81] and ageing [242, 174, 141], still little is known about the physiological adaptations upon common genotoxic threats, such as UV radiation. In this study we used a proteomics and metabolomics approach to gain insights into the response to UV-induced DNA damage in NER-mutated worms, which mimics the scenario of NER-deficient patients. The alterations we observed at the proteomics, phosphproteomics and lipidomics levels in response to persistent DNA damage are highly consistent with a shift of the organisms resources to preservation of somatic function at the expense of growth signalling. Our analysis places the insulin-like growth factor receptor DAF-2 as a central hub, consistent with the role of the IIS effector transcription factor DAF-16 in counteracting the detrimental consequences of DNA damage [169] (**Figure 3.16** and **Figure 4.1**).

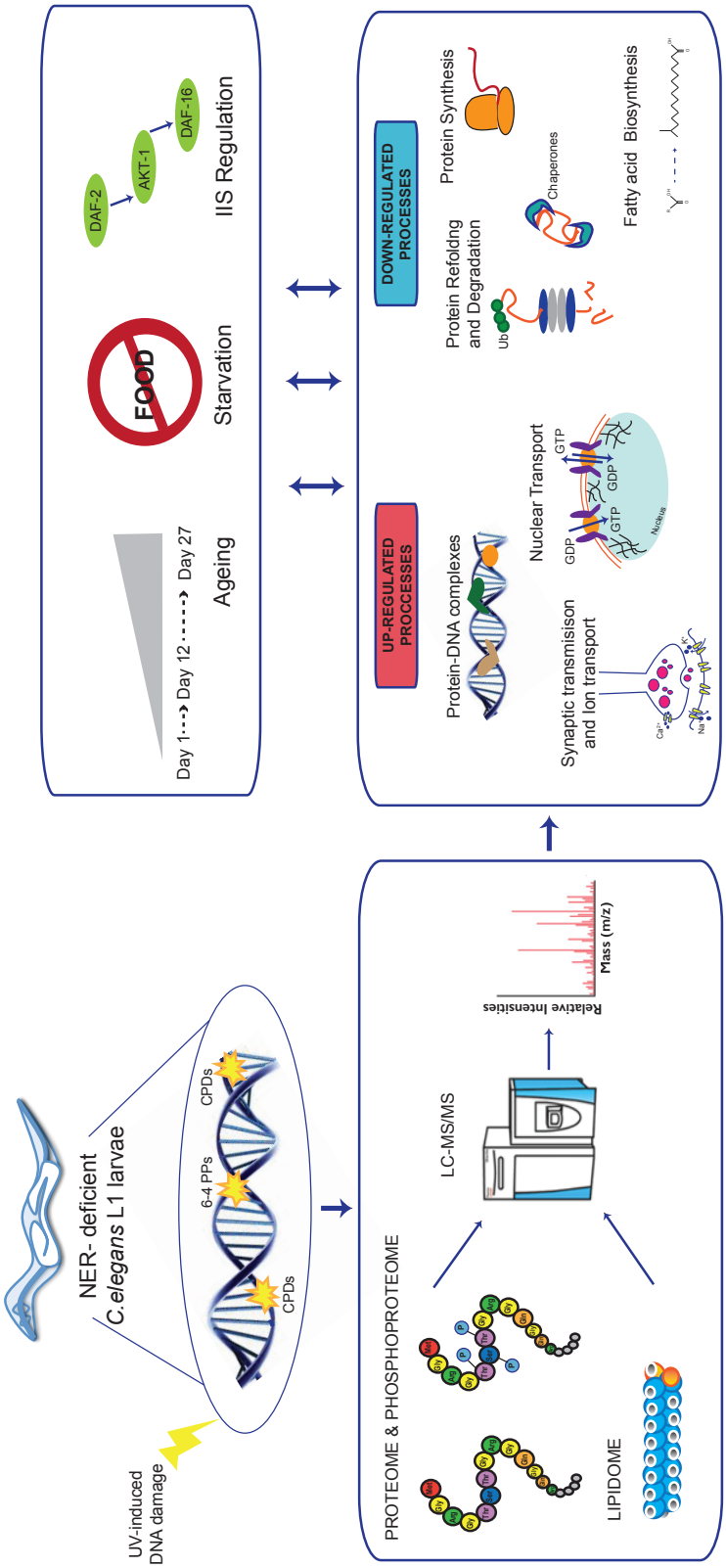

Figure 4.1: **Proteome, lipidome, and phosphoproteome analysis following UV treatment in NER-deficient *C. elegans*.** We detected similarities between the response to UV irradiation in NER-deficient animals and proteome alterations during ageing as well as in the response to starvation, both of which are regulated through the IIS pathway.

Modulation of protein-DNA complexes activity upon DNA damage

In line with previous studies of aged IIS mutant worms [83] and cells undergoing DNA damage [17, 61, 155], we also detected in our screen a reduction in transcription-associated processes upon DNA damage. This could be explained as a mechanisms adopted by the organism that is challenged by unrepaired DNA lesions, to avoid the synthesis of new aberrant proteins, which might be toxic for the cells. Consistent with function of chromatin remodelling in modulating repair, replication and transcription in response to DNA damage, we also observed a widespread induction of proteins involved in nuclear functions (**Figure 3.2A**, **Figure 3.3** and **Figure 3.6**). The mostly represented nuclear categories recollect some histone proteins, chromatin organizers and many regulator of transcription. Among the chromatin-associated proteins that we found increased in abundance upon UV treatment, BAF-1, SWSN-4 and HCF-1 **(Figure 3.3)** are known to interact with the transcription factor DAF-16 to remodel the local chromatin and in turn to activate transcription [197, 139, 9].

Cells frequently employ PTMs to regulate the activity of transcription factors and chromatin-associated proteins in response to alterations in the extracellular environment [100, 66]. Some of the transcription regulators we found increased in abundance in our study (RTFO-1, STA-1, HCF-1, SMK-1) were also significantly regulated at the phopshoproteome level **(Figure 3.3**, **Figure 3.16** and **Figure 3.18)**, suggesting a phosphorylation-dependent modulation of their activities. Changes in spliceosome organization and PTMs of splicing factors have been found recently implicated in the cellular DNA-damage response [159, 171, 228, 136, 31, 187]. In line with these observations we also observed changes in abundance of factors involved in transcription elongation and mRNA processing upon persistent DNA damage. The concomitant upregulation of factors playing important roles in mRNA nuclear import/export trafficking suggests an involvement of the RNA synthesis and translocation in the DNA damage response (**Figure 3.3**, **Figure 3.9** and **Figure 3.16**). Transport across the nuclear envelope has been described as an essential cellular function, since it regulates nuclear availability of proteins, which can directly affect gene expression and cell growth and proliferation [176, 105]. The trafficking of proteins between the cytoplasmic and the nuclear compartments is also finely regulated by PTMs; in particular, phosphorylation can stimulate or inhibit the passage of cargos through the nuclear pore complex structures [105]. Examples of proteins whose nuclear import is promoted upon phosphorylation are the members of Signal Transducers and

Activators of Transcription (STAT) family and the kinases downstream of the ERK pathway [176, 132, 201, 185]. Interestingly, in our study we found two downstream effectors of EGF signalling, the transcription factor STA-1 and MPK-1, both significantly phosphorylated upon unrepaired DNA damage **(Figure 3.18)**, suggesting that their nuclear translocation might have a role upon persistent DNA damage [109]. The STAT mutant *sta-1(ok587)* indeed showed a significantly increased sensitivity to UV treatment compared to WT worms **(Figure 3.19)**.

The nuclear import/export transport was not the only trafficking activity found improved upon UV treatment. The increased expression of members of the synaptic machinery downstream of the EGF and GPCR pathways **(Figure 3.3**, **Figure 3.6**, **Figure 3.16** and **Figure 3.18)**, suggests the implication of neuronal signalling in the release of possible intra/extracellular signals, mediating the organismal adaptation to persistent DNA damage. The EGF and the G-protein signalling pathway have also as common target some regulators of the lipid metabolism [104, 231, 118] **(Figure 3.18)**. Given the role of complex lipid classes not only as structural membrane components, but also as signal transduction molecules [153, 65], we hypothesized as well their active involvement in mediating the organismal response to persistent DNA damage. In line with the idea of an involvement of lipids in controlling intracellular signalling network, we detected an increased abundance of some extracellular lipid binding proteins/transporters **(Figure 3.3)**.The lipid intermediate DAG, generated upon activation of PLC downstream of the EGF signalling, has been previously identified as a second messenger in the activation of PKC [227, 179], a known regulator of the DAF-2 IIS-dependent control of dauer formation [162] **(Figure 3.18)**.

Protein homeostasis is impaired upon persistent DNA damage

The loss of protein homeostasis is a common trait found in organisms upon stress, ageing, and in age-associated diseases [107, 189]. In line with proteomic studies of aged animals [16, 174, 141, 242, 39], in our dataset we observed a drop in abundance of a large number of ribosomal proteins and components of the translation machinery **(Figure 3.4** and **Figure 3.6)**. This result can be interpreted as a response to avoid the production and accumulation of aberrant proteins, which if not cleared, can be deleterious for the organism. Indeed, the pro-

teostasis network, important for the refolding or degradation of unfolded proteins, was in fact dampened in animals carrying persistent DNA damage. Many chaperones, ubiquitin ligases, members of the UPS machinery, together with various peroxisomal enzymes and mitochondrial homeostasis related proteins, were all decreased in abundance upon UV treatment **(Figure 3.4** and **Figure 3.9)**. Although this drop in protein homeostasis (**Figure.3.4**), we observed a consistently elevated autophagy activity following DNA damage **(Figure 3.16)**. This elevated autophagy activity can be interpreted as a compensatory response to clear damaged proteins and recycle their amino acids when protein homeostasis is impaired [56, 32, 107]. Autophagy-defective mutants showed indeed a significantly increased sensitivity to UV treatment compared to WT worms a upon UV treatment **(Figure 3.7)**, suggesting that a mechanism of degradation of aberrant proteins is required to stand the persistent DNA damage. Consistent with a shift from UPS-mediated to autophagic degradation, oncogenically transformed human cells treated with proteasome inhibitors, also showed an enhanced ability to trigger autophagy, suggesting a strong dependence of transformed cells on this mechanism of protein degradation for survival [55]. Interestingly, the member of macroautophagy SQST-1 (mammalian p62), highly upregulated in our study **(Figure 3.3)**, selectively targets unfolded proteins for degradation via macroautophagy and shuttles between the nucleus and the cytoplasm, creating a link between autophagy, UPS and DNA repair [88, 117]. Moreover, SQST-1 participates in the neuronal pathway, suggesting its possible involvement in coupling autophagy and synaptic mechanisms to regulate *C. elegans* growth and development. A role of autophagy in receptor degradative trafficking at the presynaptic terminals to control neuronal excitation and inhibition has been previously described in *C. elegans* [199]. The increased abundance of autophagy proteins upon UPR impairment, together with the upregulation of members of the endocytosis/vesicle trafficking observed upon UV treatment, might suggest the necessity of the NER mutant worms of alleviating stress, when recycling pathways are compromised, by releasing unwanted or damaged material, for example in the form of exosomes. Since exosomes are small vesicles released in the extracellular environment [8], they might have a role as signal transferred from one cell to another, to mediate the whole organismal adaptation to persistent DNA damage.

Metabolic adaptations upon unrepaired DNA damage

Similarly to the proteome alterations occurring during ageing [174, 242, 141] **(Figure 3.10)** and in response to starvation [129] **(Figure 3.11)**, upon persistent DNA damage we detected significant changes of metabolic pathways involved in the synthesis and use of carbohydrate, amino acid and lipids **(Figure 3.4**, **(Figure 3.6** and **Figure 3.18)**. Lipid and carbohydrate metabolism, together with protein synthesis and autophagy, are important mechanisms regulated through the IIS and the TOR pathways [70, 53, 251, 128, 99, 193] **(Figure 3.15)**. As in proteomic studies of IIS-deficient worms [70, 53], or upon starvation [129], and during ageing [141, 174, 39], many enzymes involved in fatty acid biosynthesis also showed significant decreases in abundance in our study **(Figure 3.4**, **Figure 3.9**, **(Figure 3.16** and **Figure 3.18)**. The consequence of this decreased FA biosynthesis **(Figure 3.13)** is an imbalance in the downstream complex lipid classes, the sphingolipids and the glycerophospholipids **(Figure 3.14** and **Figure 3.15)**. As in ageing studies [46, 79], we observed an increase in SM synthesis from the sphingolipids intermediate Cer, and in parallel an upregulation of the d17iso-GlcCer, which together with the CeTOR signalling is involved in bypassing the developmental arrest caused by the decreased FA synthesis [261] **(Figure 3.14)**. The MS profiling of the other lipid class, the glycerophospholipids, revealed a preferential direction in the phospholipids synthesis downstream of the DAG upon UV treatment and starvation **(Figure 3.15)**. In particular, the two major phospholipids subclasses, PC and PE, showed a striking opposite change in abundance upon the two treatments. Previously, it was demonstrated that the PC/PE ratio is a critical modulator of membrane composition/integrity [140]: the positive PC/PE ratio we observed upon UV treatment suggests retention of membrane structure, in contrast to starvation where the increase of PE will suggest a loss of membrane integrity with an increase of solutes permeability. Upon starvation we also observed a significant decrease of PG **(Figure 3.15)**, the upstream regulator of CL, suggesting a link of this lipid subclass with mitochondria dysfunctions **(Figure 3.4** and **Figure 3.9)** as observed in starvation studies [6] and in neurodegenerative disorders as AD [163]. Recent findings in human centenarians suggested glycerophospholipids and sphingolipids classes as putative markers and modulators of healthy ageing, which is usually characterized by established membrane lipid remodelling process and a better antioxidant capacity [166, 38, 79, 163]. In agreement with ageing studies, together with changes in phospholipid composition we also observed an increase in cellular detoxification mechanisms upon persistent DNA damage, through

enhanced CYPs, GSTs and UGTs enzymes activity **(Figure 3.7** and **Figure 3.9)**. A similarly altered phospholipid composition was observed also in synaptic brain mitochondria, which if dysfunctional lead to neurodegenerative disorders as AD. Despite the increase in amount of choline-containing phospholipids (PC and SM), the amount of CL content was found significantly decreased, suggesting reduced function and oxidative capacity of synaptic mitochondria [163]. Taken together, our observations suggest that the worms respond to persistent DNA damage by a metabolic shift reminiscent of adaptations during starvation **(Figure 3.11)** and ageing **(Figure 3.10)**.

In general, all of these findings reflect the necessity of worms to cope with persistent DNA damage by saving energy, through decreased lipid metabolism and protein synthesis, meanwhile trying to avoid accumulation of aberrant proteins, which can be toxic for organisms. The increased autophagy activity, coupled with an extracellular trafficking, suggests the requirement of a signal transduction throughout the whole organisms to modulate its adaptation to the damage.

Networks of proteins involved in response to persistent DNA damage

We next combined proteome and phosphoproteome datasets in a protein-protein interaction map to extend our analysis to the identification of regulators that are linked to IIS and modulate a range of cellular processes. The network analysis revealed an intricate connection of differentially regulated signalling nodes, and assigned central roles for the IIS **(Figure 3.16)**, and the EGF- and AMPK-like signalling pathways in response to DNA damage **(Figure 3.18)**. Mutations affecting the AMP-activated protein kinases AAK-2, playing a central role in controlling energy metabolism and regulating longevity through the CeTOR and the *daf-2*-mediated IIS pathways [175, 45], have been reported, in previous tests performed in our laboratory, increasing the *C. elegans* sensitivity to UV-induced DNA damage. Upon UV treatment, upregulation of members both of the CeTOR and IIS pathway, reminiscent of recent *C. elegans* studies during ageing [174], reinforces the concept of response to accumulating DNA damage during the natural ageing process. Moreover, the dampening of lipid biosynthesis **(Figure 3.13)** suggests that at least in *C. elegans*, physiological adaptations occur in favor of a tissue maintenance program, allowing survival upon unrepaired DNA damage. This survival program is also promoted by an increase in autophagy **(Figure 3.16)**, which favors proteostasis [32, 157, 43] and stress

resistance [56, 122].

In conclusion, our analysis of proteome, lipidome, and phosphoproteome in NER-deficient *C. elegans* provides a comprehensive picture of the response processes involved to persistent DNA damage in a metazoan animal model. The future prospective for this proteomic and metabolomic investigation will be to further experimentally assess the protein and signalling mechanisms we found significantly regulated to establish a more complete model of how animals respond to persistent DNA damage. The final aim of such a general analysis is to translate the findings about signal transduction networks we found involved in the *C. elegans* response to UV treatment to other model organisms and ultimately to humans, to help deciphering outcomes of syndromes related to NER deficiencies.

Chapter 5

References

[1] M. Ailion, T. Inoue, C. I. Weaver, R. W. Holdcraft, and J. H. Thomas. Neurosecretory control of aging in Caenorhabditis elegans. *Proceedings of the National Academy of Sciences*, 96(13):7394–7397, June 1999.

[2] L. Alfano, C. Costa, A. Caporaso, A. Altieri, P. Indovina, M. Macaluso, A. Giordano, and F. Pentimalli. NONO regulates the intra-S-phase checkpoint in response to UV radiation. *Oncogene*, 35(5):567–576, Feb. 2016.

[3] J. Y. Altarejos and M. Montminy. CREB and the CRTC co-activators: sensors for hormonal and metabolic signals. *Nature Reviews Molecular Cell Biology*, 12(3):141–151, Mar. 2011.

[4] J. Anckar and L. Sistonen. Regulation of H SF1 Function in the Heat Stress Response: Implications in Aging and Disease. *Annual review of biochemistry*, 80(1):1089–1115, July 2011.

[5] J. O. Andressoo and J. H. J. Hoeijmakers. Transcription-coupled repair and premature ageing. *Mutation Research/Fundamental and Molecular Mechanisms of Mutagenesis*, 577(1-2):179–194, Sept. 2005.

[6] S. Awad, D. Constantin-Teodosiu, I. A. Macdonald, and D. N. Lobo. Short-term starvation and mitochondrial dysfunction - a possible mechanism leading to postoperative insulin resistance. *Clinical nutrition (Edinburgh, Scotland)*, 28(5):497–509, Oct. 2009.

[7] V. Babu, K. Hofmann, and B. Schumacher. A C. elegans homolog of the Cockayne syndrome complementation group A gene. *DNA Repair*, 24:57–62, Dec. 2014.

[8] F. Baixauli, C. López-Otín, and M. Mittelbrunn. Exosomes and autophagy: coordinated mechanisms for the maintenance of cellular fitness. *Frontiers in immunology*, 5(4):403, 2014.

[9] D. Z. Bar, M. Davidovich, A. T. Lamm, H. Zer, K. L. Wilson, and Y. Gruenbaum. BAF-1 mobility is regulated by environmental stresses. *Molecular biology of the cell*, 25(7):1127–1136, Apr. 2014.

[10] R. Barkan, R. Barkan, A. J. Zahand, A. J. Zahand, K. Sharabi, K. Sharabi, A. T. Lamm, A. T. Lamm, N. Feinstein, N. Feinstein, E. Haithcock, E. Haithcock, K. L. Wilson, K. L. Wilson, J. Liu, J. Liu, Y. Gruenbaum, and Y. Gruenbaum. Ce-emerin and LEM-2: essential roles in Caenorhabditis elegans development, muscle function, and mitosis. *Molecular biology of the cell*, 23(4):543–552, Feb. 2012.

[11] D. Barneda and M. Christian. Lipid droplet growth: regulation of a dynamic organelle. *Current Opinion in Cell Biology*, 47:9–15, Feb. 2017.

[12] C. A. Bastiani, S. Gharib, M. I. Simon, and P. W. Sternberg. Caenorhabditis elegans Galphaq regulates egg-laying behavior via a PLCbeta-independent and serotonin-dependent signaling pathway and likely functions both in the nervous system and in muscle. *Genetics*, 165(4):1805–1822, Dec. 2003.

[13] A. Baudrimont, A. Penkner, A. Woglar, Y. M. Mamnun, M. Hulek, C. Struck, R. Schnabel, J. Loidl, and V. Jantsch. A new thermosensitive smc-3 allele reveals involvement of cohesin in homologous recombination in C. elegans. *PLoS ONE*, 6(9):e24799, 2011.

[14] L. R. Baugh. To grow or not to grow: nutritional control of development during Caenorhabditis elegans L1 arrest. *Genetics*, 194(3):539–555, July 2013.

[15] B. F. Belgardt, J. Mauer, F. T. Wunderlich, M. B. Ernst, M. Pal, G. Spohn, H. S. Brönneke, S. Brodesser, B. Hampel, A. C. Schauss, and J. C. Brüning. Hypothalamic and pituitary

c-Jun N-terminal kinase 1 signaling coordinately regulates glucose metabolism. *Proceedings of the National Academy of Sciences of the United States of America*, 107(13):6028–6033, Mar. 2010.

[16] A. Ben-Zvi, E. A. Miller, and R. I. Morimoto. Collapse of proteostasis represents an early molecular event in Caenorhabditis elegans aging. *Proceedings of the National Academy of Sciences of the United States of America*, 106(35):14914–14919, Sept. 2009.

[17] A. Bensimon, A. Schmidt, Y. Ziv, R. Elkon, S. Y. Wang, D. J. Chen, R. Aebersold, and Y. Shiloh. ATM-Dependent and -Independent Dynamics of the Nuclear Phosphoproteome After DNA Damage. *Science Signaling*, 3(151):rs3–rs3, Dec. 2010.

[18] I. Bjedov and L. Partridge. A longer and healthier life with TOR down-regulation: genetics and drugs. *Biochemical Society Transactions*, 39(2):460–465, Apr. 2011.

[19] S. J. Boulton, A. Gartner, J. Reboul, P. Vaglio, N. Dyson, D. E. Hill, and M. Vidal. Combined functional genomic maps of the C. elegans DNA damage response. *Science*, 295(5552):127–131, Jan. 2002.

[20] W. A. Boyd, T. L. Crocker, A. M. Rodriguez, M. C. K. Leung, D. Wade Lehmann, J. H. Freedman, B. Van Houten, and J. N. Meyer. Nucleotide excision repair genes are expressed at low levels and are not detectably inducible in Caenorhabditis elegans somatic tissues, but their function is required for normal adult life after UVC exposure. *Mutation Research/Fundamental and Molecular Mechanisms of Mutagenesis*, 683(1-2):57–67, Jan. 2010.

[21] O. Brandman, J. Stewart-Ornstein, D. Wong, A. Larson, C. C. Williams, G.-W. Li, S. Zhou, D. King, P. S. Shen, J. Weibezahn, J. G. Dunn, S. Rouskin, T. Inada, A. Frost, and J. S. Weissman. A ribosome-bound quality control complex triggers degradation of nascent peptides and signals translation stress. *CELL*, 151(5):1042–1054, Nov. 2012.

[22] S. Brenner. The genetics of Caenorhabditis elegans. *Genetics*, 77(1):71–94, May 1974.

[23] A. B. Britt. Repair of DNA Damage Induced by Solar UV. *Photosynthesis Research*, 81(2):105–112, July 2004.

[24] K. Burkewitz, I. Morantte, H. J. M. Weir, R. Yeo, Y. Zhang, F. K. Huynh, O. R. Ilkayeva, M. D. Hirschey, A. R. Grant, and W. B. Mair. Neuronal CRTC-1 Governs Systemic Mitochondrial Metabolism and Lifespan via a Catecholamine Signal. *CELL*, 160(5):842–855, Feb. 2015.

[25] J. N. Buxbaum, Z. Ye, N. Reixach, L. Friske, C. Levy, P. Das, T. Golde, E. Masliah, A. R. Roberts, and T. Bartfai. Transthyretin protects Alzheimer's mice from the behavioral and biochemical effects of Abeta toxicity. *Proceedings of the National Academy of Sciences of the United States of America*, 105(7):2681–2686, Feb. 2008.

[26] L. Byerly, S. Scherer, and R. L. Russell. The life cycle of the nematode Caenorhabditis elegans. II. A simplified method for mutant characterization. *Developmental Biology*, 51(1):34–48, July 1976.

[27] M. Caputo, A. Balzerano, I. Arisi, M. D'Onofrio, R. Brandi, S. Bongiorni, S. Brancorsini, M. Frontini, and L. Proietti-De-Santis. CSB ablation induced apoptosis is mediated by increased endoplasmic reticulum stress response. *PLoS ONE*, 12(3):e0172399, 2017.

[28] L. Castells-Roca, M. M. Mueller, and B. Schumacher. Longevity through DNA damage tolerance. *Cell cycle (Georgetown, Tex.)*, 14(4):467–468, 2015.

[29] Y.-J. Chao, W.-H. Chang, H.-C. Ting, W.-T. Chao, and Y.-H. H. Hsu. Cell Cycle Arrest and Cell Survival Induce Reverse Trends of Cardiolipin Remodeling. *PLoS ONE*, 9(11):e113680–19, Nov. 2014.

[30] N. K. Charlie, M. A. Schade, A. M. Thomure, and K. G. Miller. Presynaptic UNC-31 (CAPS) is required to activate the G alpha(s) pathway of the Caenorhabditis elegans synaptic signaling network. *Genetics*, 172(2):943–961, Feb. 2006.

[31] X. Chen, J. D. Smith, H. Shi, D. D. Yang, R. A. Flavell, and S. L. Wolin. The Ro autoantigen binds misfolded U2 small nuclear RNAs and assists mammalian cell survival after UV irradiation. *Current Biology*, 13(24):2206–2211, Dec. 2003.

[32] X. Chen and X. M. Yin. Coordination of autophagy and the proteasome in resolving endoplasmic reticulum stress. *Veterinary Pathology*, 48(1):245–253, Jan. 2011.

[33] N. Chondrogianni, K. Georgila, N. Kourtis, N. Tavernarakis, and E. S. Gonos. 20S proteasome activation promotes life span extension and resistance to proteotoxicity in Caenorhabditis elegans. *FASEB journal : official publication of the Federation of American Societies for Experimental Biology*, 29(2):611–622, Feb. 2015.

[34] E. Chorell, T. Moritz, S. Branth, H. Antti, and M. B. Svensson. Predictive metabolomics evaluation of nutrition-modulated metabolic stress responses in human blood serum during the early recovery phase of strenuous physical exercise. *Journal of Proteome Research*, 8(6):2966–2977, June 2009.

[35] E. Citterio, V. Van Den Boom, G. Schnitzler, R. Kanaar, E. Bonte, R. E. Kingston, J. H. Hoeijmakers, and W. Vermeulen. ATP-dependent chromatin remodeling by the Cockayne syndrome B DNA repair-transcription-coupling factor. *Molecular and Cellular Biology*, 20(20):7643–7653, Oct. 2000.

[36] J. E. Cleaver, E. T. Lam, and I. Revet. Disorders of nucleotide excision repair: the genetic and molecular basis of heterogeneity. *Nature reviews. Genetics*, 10(11):756–768, Oct. 2009.

[37] M. S. Cline, M. Smoot, E. Cerami, A. Kuchinsky, N. Landys, C. Workman, R. Christmas, I. Avila-Campilo, M. Creech, B. Gross, K. Hanspers, R. Isserlin, R. Kelley, S. Killcoyne, S. Lotia, S. Maere, J. Morris, K. Ono, V. Pavlovic, A. R. Pico, A. Vailaya, P.-L. Wang, A. Adler, B. R. Conklin, L. Hood, M. Kuiper, C. Sander, I. Schmulevich, B. Schwikowski, G. J. Warner, T. Ideker, and G. D. Bader. Integration of biological networks and gene expression data using Cytoscape. *Nature Protocols*, 2(10):2366–2382, 2007.

[38] S. Collino, I. Montoliu, F.-P. J. Martin, M. Scherer, D. Mari, S. Salvioli, L. Bucci, R. Ostan, D. Monti, E. Biagi, P. Brigidi, C. Franceschi, and S. Rezzi. Metabolic signatures of extreme longevity in northern Italian centenarians reveal a complex remodeling of lipids, amino acids, and gut microbiota metabolism. *PLoS ONE*, 8(3):e56564, 2013.

[39] N. Copes, C. Edwards, D. Chaput, M. Saifee, I. Barjuca, D. Nelson, A. Paraggio, P. Saad, D. Lipps, S. M. Stevens, and P. C. Bradshaw. Metabolome and proteome changes with aging in Caenorhabditis elegans. *Experimental Gerontology*, 72:67–84, Dec. 2015.

[40] J. Cox and M. Mann. MaxQuant enables high peptide identification rates, individualized p.p.b.-range mass accuracies and proteome-wide protein quantification. *Nature biotechnology*, 26(12):1367–1372, Dec. 2008.

[41] J. Cox and M. Mann. 1D and 2D annotation enrichment: a statistical method integrating quantitative proteomics with complementary high-throughput data. *BMC bioinformatics*, 13 Suppl 16(Suppl 16):S12, 2012.

[42] J. Cox, N. Neuhauser, A. Michalski, R. A. Scheltema, J. V. Olsen, and M. Mann. Andromeda: a peptide search engine integrated into the MaxQuant environment. *Journal of Proteome Research*, 10(4):1794–1805, Apr. 2011.

[43] A. M. Cuervo, E. Bergamini, U. T. Brunk, W. Dröge, M. Ffrench, and A. Terman. Autophagy and Aging: The Importance of Maintaining "Clean" Cells. *Autophagy*, 1(3):131–140, Oct. 2014.

[44] K. A. Cunningham, A. D. Bouagnon, A. G. Barros, L. Lin, L. Malard, M. A. Romano-Silva, and K. Ashrafi. Loss of a neural AMP-activated kinase mimics the effects of elevated serotonin on fat, movement, and hormonal secretions. *PLoS Genetics*, 10(6):e1004394, June 2014.

[45] R. Curtis, G. O'Connor, and P. S. DiStefano. Aging networks in Caenorhabditis elegans: AMP-activated protein kinase (aak-2) links multiple aging and metabolism pathways. *Aging Cell*, 5(2):119–126, Apr. 2006.

[46] R. G. Cutler, K. W. Thompson, S. Camandola, K. T. Mack, and M. P. Mattson. Sphingolipid metabolism regulates development and lifespan in Caenorhabditis elegans. *Mechanisms of ageing and development*, 143-144:9–18, Dec. 2014.

[47] J. de Boer, J. O. Andressoo, J. de Wit, J. Huijmans, R. B. Beems, H. van Steeg, G. Weeda, G. T. J. van der Horst, W. van Leeuwen, A. P. N. Themmen, M. Meradji, and J. H. J. Hoeijmakers. Premature aging in mice deficient in DNA repair and transcription. *Science*, 296(5571):1276–1279, May 2002.

[48] J. de Boer and J. H. Hoeijmakers. Cancer from the outside, aging from the inside: mouse models to study the consequences of defective nucleotide excision repair. *Biochimie*, 81(1-2):127–137, Jan. 1999.

[49] S. de Boor, P. Knyphausen, N. Kuhlmann, S. Wroblowski, J. Brenig, L. Scislowski, L. Baldus, H. Nolte, M. Krüger, and M. Lammers. Small GTP-binding protein Ran is regulated by posttranslational lysine acetylation. *Proceedings of the National Academy of Sciences of the United States of America*, 112(28):E3679–88, July 2015.

[50] W. L. de Laat, E. Appeldoorn, K. Sugasawa, E. Weterings, N. G. Jaspers, and J. H. Hoeijmakers. DNA-binding polarity of human replication protein A positions nucleases in nucleotide excision repair. *Genes & Development*, 12(16):2598–2609, Aug. 1998.

[51] A. de Vries, C. T. van Oostrom, F. M. Hofhuis, P. M. Dortant, R. J. Berg, F. R. de Gruijl, P. W. Wester, C. F. van Kreijl, P. J. Capel, H. van Steeg, and S. J. Verbeek. Increased susceptibility to ultraviolet-B and carcinogens of mice lacking the DNA excision repair gene XPA. *Nature*, 377(6545):169–173, Sept. 1995.

[52] Q. Defenouillère, Y. Yao, J. Mouaikel, A. Namane, A. Galopier, L. Decourty, A. Doyen, C. Malabat, C. Saveanu, A. Jacquier, and M. Fromont-Racine. Cdc48-associated complex bound to 60S particles is required for the clearance of aberrant translation products. *Proceedings of the National Academy of Sciences of the United States of America*, 110(13):5046–5051, Mar. 2013.

[53] G. Depuydt, F. Xie, V. A. Petyuk, A. Smolders, H. M. Brewer, D. G. Camp, R. D. Smith, and B. P. Braeckman. LC-MS proteomics analysis of the insulin/IGF-1-deficient Caenorhabditis elegans daf-2(e1370) mutant reveals extensive restructuring of intermediary metabolism. *Journal of Proteome Research*, 13(4):1938–1956, Apr. 2014.

[54] J. J. DiGiovanna and K. H. Kraemer. Shining a light on xeroderma pigmentosum. *The Journal of investigative dermatology*, 132(3 Pt 2):785–796, Mar. 2012.

[55] W.-X. Ding, H.-M. Ni, W. Gao, X. Chen, J. H. Kang, D. B. Stolz, J. Liu, and X.-M. Yin. Oncogenic transformation confers a selective susceptibility to the combined suppression

of the proteasome and autophagy. *Molecular cancer therapeutics*, 8(7):2036–2045, July 2009.

[56] W.-X. Ding, H.-M. Ni, W. Gao, T. Yoshimori, D. B. Stolz, D. Ron, and X.-M. Yin. Linking of autophagy to ubiquitin-proteasome system is important for the regulation of endoplasmic reticulum stress and cell viability. *The American journal of pathology*, 171(2):513–524, Aug. 2007.

[57] C. M. Dittrich, K. Kratz, A. Sendoel, Y. Gruenbaum, J. Jiricny, and M. O. Hengartner. LEM-3 - A LEM domain containing nuclease involved in the DNA damage response in C. elegans. *PLoS ONE*, 7(2):e24555, 2012.

[58] V. Dolce, A. R. Cappello, R. Lappano, and M. Maggiolini. Glycerophospholipid synthesis as a novel drug target against cancer. *Current molecular pharmacology*, 4(3):167–175, Nov. 2011.

[59] M.-Q. Dong, J. D. Venable, N. Au, T. Xu, S. K. Park, D. Cociorva, J. R. Johnson, A. Dillin, and J. R. Yates. Quantitative mass spectrometry identifies insulin signaling targets in C. elegans. *Science*, 317(5838):660–663, Aug. 2007.

[60] P. Dowell, T. C. Otto, S. Adi, and M. D. Lane. Convergence of peroxisome proliferator-activated receptor gamma and Foxo1 signaling pathways. *Journal of Biological Chemistry*, 278(46):45485–45491, Nov. 2003.

[61] R. Drissi, M.-L. Dubois, M. Douziech, and F.-M. Boisvert. Quantitative Proteomics Reveals Dynamic Interactions of the Minichromosome Maintenance Complex (MCM) in the Cellular Response to Etoposide Induced DNA Damage. *Molecular & Cellular Proteomics*, 14(7):2002–2013, July 2015.

[62] D. Edifizi and B. Schumacher. Genome Instability in Development and Aging: Insights from Nucleotide Excision Repair in Humans, Mice, and Worms. *Biomolecules*, 5(3):1855–1869, 2015.

[63] I. C. Elle, S. V. Rødkær, J. Fredens, and N. J. Færgeman. A method for measuring fatty acid oxidation in C. elegans. *Worm*, 1(1):26–30, Jan. 2012.

[64] A. G. Fernandez and F. Piano. MEL-28 Is Downstream of the Ran Cycle and Is Required for Nuclear-Envelope Function and Chromatin Maintenance. *Current Biology*, 16(17):1757–1763, Sept. 2006.

[65] A. Z. Fernandis and M. R. Wenk. Membrane lipids as signaling molecules. *Current opinion in lipidology*, 18(2):121–128, Apr. 2007.

[66] T. M. Filtz, W. K. Vogel, and M. Leid. Regulation of transcription factor activity by interconnected post-translational modifications. *Trends in pharmacological sciences*, 35(2):76–85, Feb. 2014.

[67] M. E. Fitch, S. Nakajima, A. Yasui, and J. M. Ford. In vivo recruitment of XPC to UV-induced cyclobutane pyrimidine dimers by the DDB2 gene product. *Journal of Biological Chemistry*, 278(47):46906–46910, Nov. 2003.

[68] P. Fortini, B. Pascucci, E. Parlanti, M. D'Errico, V. Simonelli, and E. Dogliotti. The base excision repair: mechanisms and its relevance for cancer susceptibility. *Biochimie*, 85(11):1053–1071, Nov. 2003.

[69] M. Fousteri and L. H. Mullenders. Transcription-coupled nucleotide excision repair in mammalian cells: molecular mechanisms and biological effects. *Cell Research*, 18(1):73–84, Jan. 2008.

[70] S. Fuchs, J. G. Bundy, S. K. Davies, J. M. Viney, J. S. Swire, and A. M. Leroi. A metabolic signature of long life in Caenorhabditis elegans. *BMC biology*, 8:14, 2010.

[71] M. Gallo and D. L. Riddle. Regulation of metabolism in Caenorhabditis elegans longevity. *Journal of biology*, 9(1):7, 2010.

[72] V. Galy, P. Askjaer, C. Franz, C. López-Iglesias, and I. W. Mattaj. MEL-28, a novel nuclear-envelope and kinetochore protein essential for zygotic nuclear-envelope assembly in C. elegans. *Current Biology*, 16(17):1748–1756, Sept. 2006.

[73] G. A. Garinis, L. M. Uittenboogaard, H. Stachelscheid, M. Fousteri, W. van IJcken, T. M. Breit, H. van Steeg, L. H. F. Mullenders, G. T. J. van der Horst, J. C. Brüning, C. M. Niessen, J. H. J. Hoeijmakers, and B. Schumacher. Persistent transcription-blocking

DNA lesions trigger somatic growth attenuation associated with longevity. *Nature Cell Biology*, 11(5):604–615, Apr. 2009.

[74] G. A. Garinis, G. T. J. van der Horst, J. Vijg, and J. H. J. Hoeijmakers. DNA damage and ageing: new-age ideas for an age-old problem. *Nature Cell Biology*, 10(11):1241–1247, Nov. 2008.

[75] A. Ghazalpour, B. Bennett, V. A. Petyuk, L. Orozco, R. Hagopian, I. N. Mungrue, C. R. Farber, J. Sinsheimer, H. M. Kang, N. Furlotte, C. C. Park, P.-Z. Wen, H. Brewer, K. Weitz, D. G. Camp, C. Pan, R. Yordanova, I. Neuhaus, C. Tilford, N. Siemers, P. Gargalovic, E. Eskin, T. Kirchgessner, D. J. Smith, R. D. Smith, and A. J. Lusis. Comparative analysis of proteome and transcriptome variation in mouse. *PLoS Genetics*, 7(6):e1001393, June 2011.

[76] M. A. Gillette and S. A. Carr. Quantitative analysis of peptides and proteins in biomedicine by targeted mass spectrometry. *Nature methods*, 10(1):28–34, Jan. 2013.

[77] J. F. Giménez-Abián, I. Sumara, T. Hirota, S. Hauf, D. Gerlich, C. de la Torre, J. Ellenberg, and J.-M. Peters. Regulation of sister chromatid cohesion between chromosome arms. *Current Biology*, 14(13):1187–1193, July 2004.

[78] T. R. Golden and S. Melov. Microarray analysis of gene expression with age in individual nematodes. *Aging Cell*, 3(3):111–124, June 2004.

[79] V. Gonzalez-Covarrubias, M. Beekman, H.-W. Uh, A. Dane, J. Troost, I. Paliukhovich, F. M. van der Kloet, J. Houwing-Duistermaat, R. J. Vreeken, T. Hankemeier, and E. P. Slagboom. Lipidomics of familial longevity. *Aging Cell*, 12(3):426–434, June 2013.

[80] R. Groisman, J. Polanowska, I. Kuraoka, J.-i. Sawada, M. Saijo, R. Drapkin, A. F. Kisselev, K. Tanaka, and Y. Nakatani. The ubiquitin ligase activity in the DDB2 and CSA complexes is differentially regulated by the COP9 signalosome in response to DNA damage. *CELL*, 113(3):357–367, May 2003.

[81] D. Grün, M. Kirchner, N. Thierfelder, M. Stoeckius, M. Selbach, and N. Rajewsky. Conservation of mRNA and Protein Expression during Development of C. elegans. *CellReports*, 6(3):565–577, Feb. 2014.

[82] R. L. Gundry, M. Y. White, C. I. Murray, L. A. Kane, Q. Fu, B. A. Stanley, and J. E. Van Eyk. Preparation of proteins and peptides for mass spectrometry analysis in a bottom-up proteomics workflow. *Current protocols in molecular biology*, Chapter 10:Unit10.25–10.25.23, Oct. 2009.

[83] J. Halaschek-Wiener, J. S. Khattra, S. McKay, A. Pouzyrev, J. M. Stott, G. S. Yang, R. A. Holt, S. J. M. Jones, M. A. Marra, A. R. Brooks-Wilson, and D. L. Riddle. Analysis of long-lived C. elegans daf-2 mutants using serial analysis of gene expression. *Genome Research*, 15(5):603–615, May 2005.

[84] Y. A. Hannun and L. M. Obeid. Principles of bioactive lipid signalling: lessons from sphingolipids. *Nature Reviews Molecular Cell Biology*, 9(2):139–150, Feb. 2008.

[85] M. E. Harley, O. Murina, A. Leitch, M. R. Higgs, L. S. Bicknell, G. Yigit, A. N. Blackford, A. Zlatanou, K. J. Mackenzie, K. Reddy, M. Halachev, S. McGlasson, M. A. M. Reijns, A. Fluteau, C.-A. Martin, S. Sabbioneda, N. H. Elcioglu, J. Altmüller, H. Thiele, L. Greenhalgh, L. Chessa, M. Maghnie, M. Salim, M. B. Bober, P. Nürnberg, S. P. Jackson, M. E. Hurles, B. Wollnik, G. S. Stewart, and A. P. Jackson. TRAIP promotes DNA damage response during genome replication and is mutated in primordial dwarfism. *Nature Genetics*, 48(1):36–43, Jan. 2016.

[86] S. Hauf, I. C. Waizenegger, and J. M. Peters. Cohesin cleavage by separase required for anaphase and cytokinesis in human cells. *Science*, 293(5533):1320–1323, Aug. 2001.

[87] N. Hay. Interplay between FOXO, TOR, and Akt. *Biochimica et biophysica acta*, 1813(11):1965–1970, Nov. 2011.

[88] G. Hewitt, B. Carroll, R. Sarallah, C. Correia-Melo, M. Ogrodnik, G. Nelson, E. G. Otten, D. Manni, R. Antrobus, B. A. Morgan, T. von Zglinicki, D. Jurk, A. Seluanov, V. Gorbunova, T. Johansen, J. F. Passos, and V. I. Korolchuk. SQSTM1/p62 mediates crosstalk between autophagy and the UPS in DNA repair. *Autophagy*, 12(10):1917–1930, Oct. 2016.

[89] M. Y. Hirai, M. Yano, D. B. Goodenowe, S. Kanaya, T. Kimura, M. Awazuhara, M. Arita, T. Fujiwara, and K. Saito. Integration of transcriptomics and metabolomics for under-

standing of global responses to nutritional stresses in Arabidopsis thaliana. *Proceedings of the National Academy of Sciences*, 101(27):10205–10210, July 2004.

[90] D. Hishikawa, T. Hashidate, T. Shimizu, and H. Shindou. Diversity and function of membrane glycerophospholipids generated by the remodeling pathway in mammalian cells. *Journal of lipid research*, 55(5):799–807, May 2014.

[91] J. H. Hoeijmakers. Genome maintenance mechanisms for preventing cancer. *Nature*, 411(6835):366–374, May 2001.

[92] J. H. J. Hoeijmakers. DNA damage, aging, and cancer. *The New England journal of medicine*, 361(15):1475–1485, Oct. 2009.

[93] S. Hölper, H. Nolte, E. Bober, T. Braun, and M. Krüger. Dissection of metabolic pathways in the Db/Db mouse model by integrative proteome and acetylome analysis. *Molecular bioSystems*, 11(3):908–922, Mar. 2015.

[94] J. C. M. Holthuis and A. K. Menon. Lipid landscapes and pipelines in membrane homeostasis. *Nature*, 510(7503):48–57, June 2014.

[95] M. Horikawa, T. Nomura, T. Hashimoto, and K. Sakamoto. Elongation and desaturation of fatty acids are critical in growth, lipid metabolism and ontogeny of Caenorhabditis elegans. *Journal of biochemistry*, 144(2):149–158, Aug. 2008.

[96] M. Horikawa and K. Sakamoto. Fatty-acid metabolism is involved in stress-resistance mechanisms of Caenorhabditis elegans. *Biochemical and biophysical research communications*, 390(4):1402–1407, Dec. 2009.

[97] N. S. Hou and S. Taubert. Function and Regulation of Lipid Biology in Caenorhabditis elegans Aging. *Frontiers in physiology*, 3:143, 2012.

[98] Y. Hou, H. Song, D. L. Croteau, M. Akbari, and V. A. Bohr. Genome instability in Alzheimer disease. *Mechanisms of ageing and development*, Apr. 2016.

[99] J. J. Howell and B. D. Manning. mTOR couples cellular nutrient sensing to organismal metabolic homeostasis. *Trends in endocrinology and metabolism: TEM*, 22(3):94–102, Mar. 2011.

[100] T. Hunter and M. Karin. The regulation of transcription by phosphorylation. *CELL*, 70(3):375–387, Aug. 1992.

[101] S. Imamura, Y. Kawase, I. Kobayashi, M. Shimojima, H. Ohta, and K. Tanaka. TOR (target of rapamycin) is a key regulator of triacylglycerol accumulation in microalgae. *Plant signaling & behavior*, 11(3):e1149285, 2016.

[102] D. L. Ippolito, J. A. Lewis, C. Yu, L. R. Leon, and J. D. Stallings. Alteration in circulating metabolites during and after heat stress in the conscious rat: potential biomarkers of exposure and organ-specific injury. *BMC physiology*, 14(1):14, Dec. 2014.

[103] H. Iwasa, S. Yu, J. Xue, and M. Driscoll. Novel EGF pathway regulators modulate C. elegans healthspan and lifespan via EGF receptor, PLC-gamma, and IP3R activation. *Aging Cell*, 9(4):490–505, Aug. 2010.

[104] R. N. Jorissen, F. Walker, N. Pouliot, T. P. J. Garrett, C. W. Ward, and A. W. Burgess. Epidermal growth factor receptor: mechanisms of activation and signalling. *Experimental Cell Research*, 284(1):31–53, Mar. 2003.

[105] A. Kaffman and E. K. O'Shea. Regulation of nuclear localization: a key to a door. *Annual review of cell and developmental biology*, 15(1):291–339, 1999.

[106] I. Kamileri, I. Karakasilioti, A. Sideri, T. Kosteas, A. Tatarakis, I. Talianidis, and G. A. Garinis. Defective transcription initiation causes postnatal growth failure in a mouse model of nucleotide excision repair (NER) progeria. *Proceedings of the National Academy of Sciences of the United States of America*, 109(8):2995–3000, Feb. 2012.

[107] S. Kaushik and A. M. Cuervo. Proteostasis and aging. *Nature medicine*, 21(12):1406–1415, Dec. 2015.

[108] M. G. Kemp, J. T. Reardon, L. A. Lindsey-Boltz, and A. Sancar. Mechanism of release and fate of excised oligonucleotides during nucleotide excision repair. *The Journal of biological chemistry*, 287(27):22889–22899, June 2012.

[109] N. N. Khodarev, A. J. Minn, E. V. Efimova, T. E. Darga, E. Labay, M. Beckett, H. J. Mauceri, B. Roizman, and R. R. Weichselbaum. Signal transducer and activator of tran-

scription 1 regulates both cytotoxic and prosurvival functions in tumor cells. *Cancer Research*, 67(19):9214–9220, Oct. 2007.

[110] E. J. Kim, X.-J. Jin, Y. K. Kim, I. K. Oh, J. E. Kim, C.-H. Park, and J. H. Chung. UV decreases the synthesis of free fatty acids and triglycerides in the epidermis of human skin in vivo, contributing to development of skin photoaging. *Journal of dermatological science*, 57(1):19–26, Jan. 2010.

[111] G. Kim, A. B. Meriin, V. L. Gabai, E. Christians, I. Benjamin, A. Wilson, B. Wolozin, and M. Y. Sherman. The heat shock transcription factor Hsf1 is downregulated in DNA damage-associated senescence, contributing to the maintenance of senescence phenotype. *Aging Cell*, 11(4):617–627, Aug. 2012.

[112] J. E. Kim and J. Chen. regulation of peroxisome proliferator-activated receptor-gamma activity by mammalian target of rapamycin and amino acids in adipogenesis. *Diabetes*, 53(11):2748–2756, Nov. 2004.

[113] J. K. Kim, D. Patel, and B. S. Choi. Contrasting structural impacts induced by cis-syn cyclobutane dimer and (6-4) adduct in DNA duplex decamers: implication in mutagenesis and repair activity. *Photochemistry and photobiology*, 62(1):44–50, July 1995.

[114] M. Kniazeva, T. Euler, and M. Han. A branched-chain fatty acid is involved in postembryonic growth control in parallel to the insulin receptor pathway and its biosynthesis is feedback-regulated in C. elegans. *Genes & Development*, 22(15):2102–2110, Aug. 2008.

[115] H. C. Köfeler, A. Fauland, G. N. Rechberger, and M. Trötzmüller. Mass spectrometry based lipidomics: an overview of technological platforms. *Metabolites*, 2(1):19–38, Jan. 2012.

[116] M. Koob, V. Laugel, M. Durand, H. Fothergill, C. Dalloz, F. Sauvanaud, H. Dollfus, I. J. Namer, and J.-L. Dietemann. Neuroimaging in Cockayne syndrome. *AJNR. American journal of neuroradiology*, 31(9):1623–1630, Oct. 2010.

[117] V. I. Korolchuk, F. M. Menzies, and D. C. Rubinsztein. A novel link between autophagy and the ubiquitin-proteasome system. *Autophagy*, 5(6):862–863, Aug. 2009.

[118] E. Kostenis. A glance at G-protein-coupled receptors for lipid mediators: a growing receptor family with remarkably diverse ligands. *Pharmacology & therapeutics*, 102(3):243–257, June 2004.

[119] K. H. Kraemer, N. J. Patronas, R. Schiffmann, B. P. Brooks, D. Tamura, and J. J. DiGiovanna. Xeroderma pigmentosum, trichothiodystrophy and Cockayne syndrome: A complex genotype–phenotype relationship. *Neuroscience*, 145(4):1388–1396, Apr. 2007.

[120] R. K. Krishnan, H. Nolte, T. Sun, H. Kaur, K. Sreenivasan, M. Looso, S. Offermanns, M. Krüger, and J. M. Swiercz. Quantitative analysis of the TNF-α-induced phosphoproteome reveals AEG-1/MTDH/LYRIC as an IKKβ substrate. *Nature Communications*, 6:6658, Apr. 2015.

[121] V. Kumar, J.-E. Bouameur, J. Bär, R. H. Rice, H.-T. Hornig-Do, D. R. Roop, N. Schwarz, S. Brodesser, S. Thiering, R. E. Leube, R. J. Wiesner, P. Vijayaraj, C. B. Brazel, S. Heller, H. Binder, H. Löffler-Wirth, P. Seibel, and T. M. Magin. A keratin scaffold regulates epidermal barrier formation, mitochondrial lipid composition, and activity. *The Journal of cell biology*, 211(5):1057–1075, Dec. 2015.

[122] C. Kumsta, J. T. Chang, J. Schmalz, and M. Hansen. Hormetic heat stress and HSF-1 induce autophagy to improve survival and proteostasis in C. elegans. *Nature Communications*, 8:1–12, Feb. 2017.

[123] J. N. Landis and C. T. Murphy. Integration of diverse inputs in the regulation of Caenorhabditis elegans DAF-16/FOXO. *Developmental Dynamics*, 239(5):1405–1412, May 2010.

[124] H. Lans, J. A. Marteijn, B. Schumacher, J. H. J. Hoeijmakers, G. Jansen, and W. Vermeulen. Involvement of Global Genome Repair, Transcription Coupled Repair, and Chromatin Remodeling in UV DNA Damage Response Changes during Development. *PLoS Genetics*, 6(5):e1000941–15, May 2010.

[125] H. Lans and W. Vermeulen. Nucleotide Excision Repair in Caenorhabditis elegans. *Molecular Biology International*, 2011(4):1–12, 2011.

[126] H. Lans and W. Vermeulen. Tissue specific response to DNA damage: C. elegans as role model. *DNA Repair*, pages 1–8, May 2015.

[127] L. R. Lapierre, A. Meléndez, and M. Hansen. Autophagy links lipid metabolism to longevity in C. elegans. *Autophagy*, 8(1):144–146, Jan. 2012.

[128] M. Laplante and D. M. Sabatini. mTOR signaling in growth control and disease. *CELL*, 149(2):274–293, Apr. 2012.

[129] M. Larance, E. Pourkarimi, B. Wang, A. Brenes Murillo, R. Kent, A. I. Lamond, and A. Gartner. Global Proteomics Analysis of the Response to Starvation in C. elegans. *Molecular & Cellular Proteomics*, 14(7):1989–2001, July 2015.

[130] A. Lass, R. Zimmermann, M. Oberer, and R. Zechner. Lipolysis - a highly regulated multi-enzyme complex mediates the catabolism of cellular fat stores. *Progress in lipid research*, 50(1):14–27, Jan. 2011.

[131] V. Laugel, C. Dalloz, M. Durand, F. Sauvanaud, U. Kristensen, M. C. Vincent, L. Pasquier, S. Odent, V. Cormier-Daire, B. Gener, E. S. Tobias, J. L. Tolmie, D. Martin-Coignard, V. Drouin-Garraud, D. Heron, H. Journel, E. Raffo, J. Vigneron, S. Lyonnet, V. Murday, D. Gubser-Mercati, B. Funalot, L. Brueton, J. Sanchez Del Pozo, E. Muñoz, A. R. Gennery, M. Salih, M. Noruzinia, K. Prescott, L. Ramos, Z. Stark, K. Fieggen, B. Chabrol, P. Sarda, P. Edery, A. Bloch-Zupan, H. Fawcett, D. Pham, J. M. Egly, A. R. Lehmann, A. Sarasin, and H. Dollfus. Mutation update for the CSB/ ERCC6and CSA/ ERCC8genes involved in Cockayne syndrome. *Human mutation*, 31(2):113–126, Feb. 2010.

[132] M.-H. Lee, M. Ohmachi, S. Arur, S. Nayak, R. Francis, D. Church, E. Lambie, and T. Schedl. Multiple functions and dynamic activation of MPK-1 extracellular signal-regulated kinase signaling in Caenorhabditis elegans germline development. *Genetics*, 177(4):2039–2062, Dec. 2007.

[133] R. Y. Lee, J. Hench, and G. Ruvkun. Regulation of C. elegans DAF-16 and its human ortholog FKHRL1 by the daf-2 insulin-like signaling pathway. *Current Biology*, 11(24):1950–1957, Dec. 2001.

[134] S. Lee, V. Horn, E. Julien, Y. Liu, J. Wysocka, B. Bowerman, M. O. Hengartner, and W. Herr. Epigenetic regulation of histone H3 serine 10 phosphorylation status by HCF-1 proteins in C. elegans and mammalian cells. *PLoS ONE*, 2(11):e1213, 2007.

[135] S. Lehmann, F. Shephard, L. A. Jacobson, and N. J. Szewczyk. Integrated control of protein degradation in C. elegans muscle. *Worm*, 1(3):141–150, July 2012.

[136] S. C. Lenzken, A. Loffreda, and S. M. L. Barabino. RNA splicing: a new player in the DNA damage response. *International Journal of Cell Biology*, 2013(9):153634–12, 2013.

[137] P. A. Leventis and S. Grinstein. The distribution and function of phosphatidylserine in cellular membranes. *Annual review of biophysics*, 39(1):407–427, 2010.

[138] G.-M. Li. Mechanisms and functions of DNA mismatch repair. *Cell Research*, 18(1):85–98, Jan. 2008.

[139] J. Li, A. Ebata, Y. Dong, G. Rizki, T. Iwata, and S. S. Lee. Caenorhabditis elegans HCF-1 functions in longevity maintenance as a DAF-16 regulator. *PLoS Biology*, 6(9):e233, Sept. 2008.

[140] Z. Li, L. B. Agellon, T. M. Allen, M. Umeda, L. Jewell, A. Mason, and D. E. Vance. The ratio of phosphatidylcholine to phosphatidylethanolamine influences membrane integrity and steatohepatitis. *Cell Metabolism*, 3(5):321–331, May 2006.

[141] V. Liang, M. Ullrich, H. Lam, Y. L. Chew, S. Banister, X. Song, T. Zaw, M. Kassiou, J. Götz, and H. R. Nicholas. Altered proteostasis in aging and heat shock response in C. elegans revealed by analysis of the global and de novo synthesized proteome. *Cellular and Molecular Life Sciences*, 71(17):3339–3361, Sept. 2014.

[142] M. R. Lieber. The mechanism of double-strand DNA break repair by the nonhomologous DNA end-joining pathway. *Annual review of biochemistry*, 79(1):181–211, 2010.

[143] A. Lilienbaum. Relationship between the proteasomal system and autophagy. *International journal of biochemistry and molecular biology*, 4(1):1–26, 2013.

[144] G. Liu, J. Rogers, C. T. Murphy, and C. Rongo. EGF signalling activates the ubiquitin proteasome system to modulate C. elegans lifespan. *The EMBO journal*, 30(15):2990–3003, Aug. 2011.

[145] J. Liu, K. K. Lee, M. Segura-Totten, E. Neufeld, K. L. Wilson, and Y. Gruenbaum. MAN1 and emerin have overlapping function(s) essential for chromosome segregation and cell division in Caenorhabditis elegans. *Proceedings of the National Academy of Sciences*, 100(8):4598–4603, Apr. 2003.

[146] C. López-Otín, M. A. Blasco, L. Partridge, M. Serrano, and G. Kroemer. The hallmarks of aging. *CELL*, 153(6):1194–1217, June 2013.

[147] A. Lundby, A. Secher, K. Lage, N. B. Nordsborg, A. Dmytriyev, C. Lundby, and J. V. Olsen. Quantitative maps of protein phosphorylation sites across 14 different rat organs and tissues. *Nature Communications*, 3:876, June 2012.

[148] F. Madeo, N. Tavernarakis, and G. Kroemer. Can autophagy promote longevity? *Nature Cell Biology*, 12(9):842–846, Sept. 2010.

[149] S. Madronich, R. L. McKenzie, L. O. Björn, and M. M. Caldwell. Changes in biologically active ultraviolet radiation reaching the Earth's surface. *Journal of photochemistry and photobiology. B, Biology*, 46(1-3):5–19, Oct. 1998.

[150] S. Maere, K. Heymans, and M. Kuiper. BiNGO: a Cytoscape plugin to assess overrepresentation of gene ontology categories in biological networks. *Bioinformatics (Oxford, England)*, 21(16):3448–3449, Aug. 2005.

[151] W. Mair, I. Morantte, Ana P. C. Rodrigues, G. Manning, M. Montminy, R. J. Shaw, and A. Dillin. Lifespan extension induced by AMPK and calcineurin is mediated by CRTC-1 and CREB. *Nature*, 470(7334):404–408, Apr. 2012.

[152] J. A. Marteijn, H. Lans, W. Vermeulen, and J. H. J. Hoeijmakers. Understanding nucleotide excision repair and its roles in cancer and ageing. *Nature Publishing Group*, 15(7):465–481, July 2014.

[153] T. F. Martin. Phosphoinositide lipids as signaling molecules: common themes for signal transduction, cytoskeletal regulation, and membrane trafficking. *Annual review of cell and developmental biology*, 14(1):231–264, 1998.

[154] T. Matsunaga, K. Hieda, and O. Nikaido. Wavelength dependent formation of thymine dimers and (6-4) photoproducts in DNA by monochromatic ultraviolet light ranging from 150 to 365 nm. *Photochemistry and photobiology*, 54(3):403–410, Sept. 1991.

[155] S. Matsuoka, B. A. Ballif, A. Smogorzewska, E. R. McDonald, K. E. Hurov, J. Luo, C. E. Bakalarski, Z. Zhao, N. Solimini, Y. Lerenthal, Y. Shiloh, S. P. Gygi, and S. J. Elledge. ATM and ATR Substrate Analysis Reveals Extensive Protein Networks Responsive to DNA Damage. *Science*, 316(5828):1160–1166, May 2007.

[156] J. J. McElwee, E. Schuster, E. Blanc, J. H. Thomas, and D. Gems. Shared transcriptional signature in Caenorhabditis elegans Dauer larvae and long-lived daf-2 mutants implicates detoxification system in longevity assurance. *Journal of Biological Chemistry*, 279(43):44533–44543, Oct. 2004.

[157] E. V. Megalou and N. Tavernarakis. Autophagy in Caenorhabditis elegans. *BBA - Molecular Cell Research*, 1793(9):1444–1451, Sept. 2009.

[158] V. Menuz, K. S. Howell, S. Gentina, S. Epstein, I. Riezman, M. Fornallaz-Mulhauser, M. O. Hengartner, M. Gomez, H. Riezman, and J.-C. Martinou. Protection of C. elegans from anoxia by HYL-2 ceramide synthase. *Science*, 324(5925):381–384, Apr. 2009.

[159] G. Merdzhanova, V. Edmond, S. De Seranno, A. Van den Broeck, L. Corcos, C. Brambilla, E. Brambilla, S. Gazzeri, and B. Eymin. E2F1 controls alternative splicing pattern of genes involved in apoptosis through upregulation of the splicing factor SC35. *Cell Death and Differentiation*, 15(12):1815–1823, Dec. 2008.

[160] K. G. Miller, M. D. Emerson, J. R. McManus, and J. B. Rand. RIC-8 (Synembryn): a novel conserved protein that is required for G(q)alpha signaling in the C. elegans nervous system. *Neuron*, 27(2):289–299, Aug. 2000.

[161] K. G. Miller, M. D. Emerson, and J. B. Rand. Goalpha and diacylglycerol kinase negatively regulate the Gqalpha pathway in C. elegans. *Neuron*, 24(2):323–333, Oct. 1999.

[162] J. M. Monje, A. M. Brokate-Llanos, M. M. Pérez-Jiménez, M. A. Fidalgo, and M. J. Muñoz. pkc-1 regulates daf-2 insulin/IGF signalling-dependent control of dauer formation in Caenorhabditis elegans. *Aging Cell*, 10(6):1021–1031, Dec. 2011.

[163] V. F. Monteiro-Cardoso, M. M. Oliveira, T. Melo, M. R. M. Domingues, P. I. Moreira, E. Ferreiro, F. Peixoto, and R. A. Videira. Cardiolipin profile changes are associated to the early synaptic mitochondrial dysfunction in Alzheimer's disease. *Journal of Alzheimer's disease : JAD*, 43(4):1375–1392, 2015.

[164] R. Montes de Oca, P. R. Andreassen, and K. L. Wilson. Barrier-to-Autointegration Factor influences specific histone modifications. *Nucleus (Austin, Tex.)*, 2(6):580–590, Nov. 2011.

[165] R. Montes de Oca, C. J. Shoemaker, M. Gucek, R. N. Cole, and K. L. Wilson. Barrier-to-autointegration factor proteome reveals chromatin-regulatory partners. *PLoS ONE*, 4(9):e7050, 2009.

[166] I. Montoliu, M. Scherer, F. Beguelin, L. DaSilva, D. Mari, S. Salvioli, F.-P. J. Martin, M. Capri, L. Bucci, R. Ostan, P. Garagnani, D. Monti, E. Biagi, P. Brigidi, M. Kussmann, S. Rezzi, C. Franceschi, and S. Collino. Serum profiling of healthy aging identifies phospho- and sphingolipid species as markers of human longevity. *Aging*, 6(1):9–25, Jan. 2014.

[167] J. F. Morley and R. I. Morimoto. Regulation of longevity in Caenorhabditis elegans by heat shock factor and molecular chaperones. *Molecular biology of the cell*, 15(2):657–664, Feb. 2004.

[168] J. Moser, H. Kool, I. Giakzidis, K. Caldecott, L. H. F. Mullenders, and M. I. Fousteri. Sealing of chromosomal DNA nicks during nucleotide excision repair requires XRCC1 and DNA ligase III alpha in a cell-cycle-specific manner. *Molecular Cell*, 27(2):311–323, July 2007.

[169] M. M. Mueller, L. Castells-Roca, V. Babu, M. A. Ermolaeva, R.-U. Muller, P. Frommolt, A. B. Williams, S. Greiss, J. I. Schneider, T. Benzing, B. Schermer, and B. Schumacher.

DAF-16/FOXO and EGL-27/GATA promote developmental growth in response to persistent somatic DNA damage. *Nature Cell Biology*, 16(12):1168–1179, Nov. 2014.

[170] C. Mulder, L.-O. Wahlund, T. Teerlink, M. Blomberg, R. Veerhuis, G. J. van Kamp, P. Scheltens, and P. G. Scheffer. Decreased lysophosphatidylcholine/phosphatidylcholine ratio in cerebrospinal fluid in Alzheimer's disease. *Journal of neural transmission (Vienna, Austria : 1996)*, 110(8):949–955, Aug. 2003.

[171] M. J. Muñoz, M. S. Pérez Santangelo, M. P. Paronetto, M. de la Mata, F. Pelisch, S. Boireau, K. Glover-Cutter, C. Ben-Dov, M. Blaustein, J. J. Lozano, G. Bird, D. Bentley, E. Bertrand, and A. R. Kornblihtt. DNA damage regulates alternative splicing through inhibition of RNA polymerase II elongation. *CELL*, 137(4):708–720, May 2009.

[172] C. T. Murphy, S. A. McCarroll, C. I. Bargmann, A. Fraser, R. S. Kamath, J. Ahringer, H. Li, and C. Kenyon. Genes that act downstream of DAF-16 to influence the lifespan of Caenorhabditis elegans. *Nature*, 424(6946):277–283, July 2003.

[173] E. M. Myers. Gαo and Gαq regulate the expression of daf-7, a TGFβ-like gene, in Caenorhabditis elegans. *PLoS ONE*, 7(7):e40368, 2012.

[174] V. Narayan, T. Ly, E. Pourkarimi, A. B. Murillo, A. Gartner, A. I. Lamond, and C. Kenyon. Deep Proteome Analysis Identifies Age-Related Processes in C. elegans. *Cell Systems*, pages 1–17, July 2016.

[175] P. Narbonne and R. Roy. Caenorhabditis elegans dauers need LKB1/AMPK to ration lipid reserves and ensure long-term survival. *Nature*, 457(7226):210–214, Jan. 2009.

[176] J. D. Nardozzi, K. Lott, and G. Cingolani. Phosphorylation meets nuclear import: a review. *Cell communication and signaling : CCS*, 8(1):32, Dec. 2010.

[177] K. Nasmyth. How might cohesin hold sister chromatids together? *Philosophical Transactions of the Royal Society B: Biological Sciences*, 360(1455):483–496, Mar. 2005.

[178] L. J. Niedernhofer, G. A. Garinis, A. Raams, A. S. Lalai, A. R. Robinson, E. Appeldoorn, H. Odijk, R. Oostendorp, A. Ahmad, W. van Leeuwen, A. F. Theil, W. Vermeulen, G. T. J.

van der Horst, P. Meinecke, W. J. Kleijer, J. Vijg, N. G. J. Jaspers, and J. H. J. Hoeijmakers. A new progeroid syndrome reveals that genotoxic stress suppresses the somatotroph axis. *Nature*, 444(7122):1038–1043, Dec. 2006.

[179] Y. Nishizuka. Protein kinase C and lipid signaling for sustained cellular responses. *The FASEB Journal*, 9(7):484–496, Apr. 1995.

[180] H. Nolte, A. Konzer, A. Ruhs, B. Jungblut, T. Braun, and M. Krüger. Global protein expression profiling of zebrafish organs based on in vivo incorporation of stable isotopes. *Journal of Proteome Research*, 13(4):2162–2174, Apr. 2014.

[181] S. Nurrish, L. Ségalat, and J. M. Kaplan. Serotonin inhibition of synaptic transmission: Galpha(0) decreases the abundance of UNC-13 at release sites. *Neuron*, 24(1):231–242, Sept. 1999.

[182] S. Ogg, S. Paradis, S. Gottlieb, G. I. Patterson, L. Lee, H. A. Tissenbaum, and G. Ruvkun. The Fork head transcription factor DAF-16 transduces insulin-like metabolic and longevity signals in C. elegans. *Nature*, 389(6654):994–999, Oct. 1997.

[183] T. Ogi, S. Limsirichaikul, R. M. Overmeer, M. Volker, K. Takenaka, R. Cloney, Y. Nakazawa, A. Niimi, Y. Miki, N. G. Jaspers, L. H. F. Mullenders, S. Yamashita, M. I. Fousteri, and A. R. Lehmann. Three DNA polymerases, recruited by different mechanisms, carry out NER repair synthesis in human cells. *Molecular Cell*, 37(5):714–727, Mar. 2010.

[184] T. G. Oliveira, R. B. Chan, F. V. Bravo, A. Miranda, R. R. Silva, B. Zhou, F. Marques, V. Pinto, J. J. Cerqueira, G. Di Paolo, and N. Sousa. The impact of chronic stress on the rat brain lipidome. *Molecular Psychiatry*, 21(1):80–88, Mar. 2015.

[185] P. Pandey, J. Raingeaud, M. Kaneki, R. Weichselbaum, R. J. Davis, D. Kufe, and S. Kharbanda. Activation of p38 mitogen-activated protein kinase by c-Abl-dependent and -independent mechanisms. *Journal of Biological Chemistry*, 271(39):23775–23779, Sept. 1996.

[186] G. Paradies, V. Paradies, V. De Benedictis, F. M. Ruggiero, and G. Petrosillo. Functional role of cardiolipin in mitochondrial bioenergetics. *Biochimica et biophysica acta*, 1837(4):408–417, Apr. 2014.

[187] M. P. Paronetto, B. Miñana, and J. Valcárcel. The Ewing sarcoma protein regulates DNA damage-induced alternative splicing. *Molecular Cell*, 43(3):353–368, Aug. 2011.

[188] C. Pontoizeau, L. Mouchiroud, L. Molin, A. Mergoud-dit Lamarche, N. Dallière, P. Toulhoat, B. Elena-Herrmann, and F. Solari. Metabolomics Analysis Uncovers That Dietary Restriction Buffers Metabolic Changes Associated with Aging in Caenorhabditis elegans. *Journal of Proteome Research*, 13(6):2910–2919, June 2014.

[189] E. T. Powers, R. I. Morimoto, A. Dillin, J. W. Kelly, and W. E. Balch. Biological and Chemical Approaches to Diseases of Proteostasis Deficiency. *Annual review of biochemistry*, 78(1):959–991, June 2009.

[190] M. Räschle, G. Smeenk, R. K. Hansen, T. Temu, Y. Oka, M. Y. Hein, N. Nagaraj, D. T. Long, J. C. Walter, K. Hofmann, Z. Storchova, J. Cox, S. Bekker-Jensen, N. Mailand, and M. Mann. DNA repair. Proteomics reveals dynamic assembly of repair complexes during bypass of DNA cross-links. *Science*, 348(6234):1253671, May 2015.

[191] R. P. Rastogi, Richa, A. Kumar, M. B. Tyagi, and R. P. Sinha. Molecular mechanisms of ultraviolet radiation-induced DNA damage and repair. *Journal of nucleic acids*, 2010(6551):592980–32, 2010.

[192] J. L. Ravanat, T. Douki, and J. Cadet. Direct and indirect effects of UV radiation on DNA and its components. *Journal of photochemistry and photobiology. B, Biology*, 63(1-3):88–102, Oct. 2001.

[193] B. Ravikumar, S. Sarkar, J. E. Davies, M. Futter, M. Garcia-Arencibia, Z. W. Green-Thompson, M. Jimenez-Sanchez, V. I. Korolchuk, M. Lichtenberg, S. Luo, D. C. O. Massey, F. M. Menzies, K. Moreau, U. Narayanan, M. Renna, F. H. Siddiqi, B. R. Underwood, A. R. Winslow, and D. C. Rubinsztein. Regulation of mammalian autophagy in physiology and pathophysiology. *Physiological reviews*, 90(4):1383–1435, Oct. 2010.

[194] B. Reynolds, R. Laynes, M. H. Ogmundsdóttir, C. A. R. Boyd, and D. C. I. Goberdhan. Amino acid transporters and nutrient-sensing mechanisms: new targets for treating insulin-linked disorders? *Biochemical Society Transactions*, 35(Pt 5):1215–1217, Nov. 2007.

[195] N. K. Reynolds, M. A. Schade, and K. G. Miller. Convergent, RIC-8-dependent Galpha signaling pathways in the Caenorhabditis elegans synaptic signaling network. *Genetics*, 169(2):651–670, Feb. 2005.

[196] F. Ribezzo, Y. Shiloh, and B. Schumacher. Systemic DNA damage responses in aging and diseases. *Seminars in Cancer Biology*, pages 1–10, Jan. 2016.

[197] C. G. Riedel, R. H. Dowen, G. F. Lourenco, N. V. Kirienko, T. Heimbucher, J. A. West, S. K. Bowman, R. E. Kingston, A. Dillin, J. M. Asara, and G. Ruvkun. DAF-16 employs the chromatin remodeller SWI/SNF to promote stress resistance and longevity. *Nature Cell Biology*, 15(5):491–501, Apr. 2013.

[198] T. Riedl, F. Hanaoka, and J.-M. Egly. The comings and goings of nucleotide excision repair factors on damaged DNA. *The EMBO journal*, 22(19):5293–5303, Oct. 2003.

[199] A. M. Rowland, J. E. Richmond, J. G. Olsen, D. H. Hall, and B. A. Bamber. Presynaptic terminals independently regulate synaptic clustering and autophagy of GABAA receptors in Caenorhabditis elegans. *The Journal of neuroscience : the official journal of the Society for Neuroscience*, 26(6):1711–1720, Feb. 2006.

[200] D. C. Rubinsztein, G. Mariño, and G. Kroemer. Autophagy and Aging. *CELL*, 146(5):682–695, Sept. 2011.

[201] R. Rutkowski, R. Dickinson, G. Stewart, A. Craig, M. Schimpl, S. M. Keyse, and A. Gartner. Regulation of Caenorhabditis elegans p53/CEP-1–Dependent Germ Cell Apoptosis by Ras/MAPK Signaling. *PLoS Genetics*, 7(8):e1002238–21, Aug. 2011.

[202] P. Ruzanov and D. L. Riddle. Deep SAGE analysis of the Caenorhabditis elegans transcriptome. *Nucleic Acids Research*, 38(10):3252–3262, June 2010.

[203] A. M. Saffer, D. H. Kim, A. van Oudenaarden, and H. R. Horvitz. The Caenorhabditis elegans synthetic multivulva genes prevent ras pathway activation by tightly repressing global ectopic expression of lin-3 EGF. *PLoS Genetics*, 7(12):e1002418, Dec. 2011.

[204] M. Saijo. The role of Cockayne syndrome group A (CSA) protein in transcription-coupled nucleotide excision repair. *Mechanisms of ageing and development*, 134(5-6):196–201, May 2013.

[205] A. R. Saltiel and C. R. Kahn. Insulin signalling and the regulation of glucose and lipid metabolism. *Nature*, 414(6865):799–806, Dec. 2001.

[206] A. T. Sands, A. Abuin, A. Sanchez, C. J. Conti, and A. Bradley. High susceptibility to ultraviolet-induced carcinogenesis in mice lacking XPC. *Nature*, 377(6545):162–165, Sept. 1995.

[207] M. A. Schade, N. K. Reynolds, C. M. Dollins, and K. G. Miller. Mutations that rescue the paralysis of Caenorhabditis elegans ric-8 (synembryn) mutants activate the G alpha(s) pathway and define a third major branch of the synaptic signaling network. *Genetics*, 169(2):631–649, Feb. 2005.

[208] P. Schultz, S. Fribourg, A. Poterszman, V. Mallouh, D. Moras, and J. M. Egly. Molecular structure of human TFIIH. *CELL*, 102(5):599–607, Sept. 2000.

[209] B. Schumacher, G. A. Garinis, and J. H. J. Hoeijmakers. Age to survive: DNA damage and aging. *Trends in Genetics*, 24(2):77–85, Feb. 2008.

[210] C. P. Selby and A. Sancar. Cockayne syndrome group B protein enhances elongation by RNA polymerase II. *Proceedings of the National Academy of Sciences*, 94(21):11205–11209, Oct. 1997.

[211] R. B. Setlow and W. L. Carrier. Pyrimidine dimers in ultraviolet-irradiated DNA's. *Journal of molecular biology*, 17(1):237–254, May 1966.

[212] P. Shannon, A. Markiel, O. Ozier, N. S. Baliga, J. T. Wang, D. Ramage, N. Amin, B. Schwikowski, and T. Ideker. Cytoscape: a software environment for integrated models of biomolecular interaction networks. *Genome Research*, 13(11):2498–2504, Nov. 2003.

[213] W. M. Shaw, S. Luo, J. Landis, J. Ashraf, and C. T. Murphy. The C. elegans TGF-beta Dauer pathway regulates longevity via insulin signaling. *Current Biology*, 17(19):1635–1645, Oct. 2007.

[214] M. K. Shivji, V. N. Podust, U. Hübscher, and R. D. Wood. Nucleotide excision repair DNA synthesis by DNA polymerase epsilon in the presence of PCNA, RFC, and RPA. *Biochemistry*, 34(15):5011–5017, Apr. 1995.

[215] D. Sieburth, J. M. Madison, and J. M. Kaplan. PKC-1 regulates secretion of neuropeptides. *Nature neuroscience*, 10(1):49–57, Jan. 2007.

[216] R. Singh, S. Kaushik, Y. Wang, Y. Xiang, I. Novak, M. Komatsu, K. Tanaka, A. M. Cuervo, and M. J. Czaja. Autophagy regulates lipid metabolism. *Nature*, 458(7242):1131–1135, Apr. 2009.

[217] H. Slaper, G. J. Velders, J. S. Daniel, F. R. de Gruijl, and J. C. van der Leun. Estimates of ozone depletion and skin cancer incidence to examine the Vienna Convention achievements. *Nature*, 384(6606):256–258, Nov. 1996.

[218] L. Staresincic, A. F. Fagbemi, J. H. Enzlin, A. M. Gourdin, N. Wijgers, I. Dunand-Sauthier, G. Giglia-Mari, S. G. Clarkson, W. Vermeulen, and O. D. Schärer. Coordination of dual incision and repair synthesis in human nucleotide excision repair. *The EMBO journal*, 28(8):1111–1120, Apr. 2009.

[219] L. Stergiou, K. Doukoumetzidis, A. Sendoel, and M. O. Hengartner. The nucleotide excision repair pathway is required for UV-C-induced apoptosis in Caenorhabditis elegans. *Cell Death and Differentiation*, 14(6):1129–1138, Mar. 2007.

[220] K. Sugasawa, J. M. Ng, C. Masutani, S. Iwai, P. J. van der Spek, A. P. Eker, F. Hanaoka, D. Bootsma, and J. H. Hoeijmakers. Xeroderma pigmentosum group C protein complex is the initiator of global genome nucleotide excision repair. *Molecular Cell*, 2(2):223–232, Aug. 1998.

[221] K. Sugasawa, Y. Okuda, M. Saijo, R. Nishi, N. Matsuda, G. Chu, T. Mori, S. Iwai, K. Tanaka, K. Tanaka, and F. Hanaoka. UV-induced ubiquitylation of XPC protein mediated by UV-DDB-ubiquitin ligase complex. *CELL*, 121(3):387–400, May 2005.

[222] P. Sung and H. Klein. Mechanism of homologous recombination: mediators and helicases take on regulatory functions. *Nature Reviews Molecular Cell Biology*, 7(10):739–750, Oct. 2006.

[223] J. Swierczynski, A. Hebanowska, and T. Sledzinski. Role of abnormal lipid metabolism in development, progression, diagnosis and therapy of pancreatic cancer. *World journal of gastroenterology*, 20(9):2279–2303, Mar. 2014.

[224] N. J. Szewczyk, J. J. Hartman, S. J. Barmada, and L. A. Jacobson. Genetic defects in acetylcholine signalling promote protein degradation in muscle cells of Caenorhabditis elegans. *Journal of Cell Science*, 113 (Pt 11):2003–2010, June 2000.

[225] J. S. Taylor, H. F. Lu, and J. J. Kotyk. Quantitative conversion of the (6-4) photoproduct of TpdC to its Dewar valence isomer upon exposure to simulated sunlight. *Photochemistry and photobiology*, 51(2):161–167, Feb. 1990.

[226] M. Tian, R. Shinkura, N. Shinkura, and F. W. Alt. Growth Retardation, Early Death, and DNA Repair Defects in Mice Deficient for the Nucleotide Excision Repair Enzyme XPF. *Molecular and Cellular Biology*, 24(3):1200–1205, Jan. 2004.

[227] A. Toker. The biology and biochemistry of diacylglycerol signalling. Meeting on molecular advances in diacylglycerol signalling. *EMBO reports*, 6(4):310–314, Apr. 2005.

[228] M. Tresini, D. O. Warmerdam, P. Kolovos, L. Snijder, M. G. Vrouwe, J. A. A. Demmers, W. F. J. van IJcken, F. G. Grosveld, R. H. Medema, J. H. J. Hoeijmakers, L. H. F. Mullenders, W. Vermeulen, and J. A. Marteijn. The core spliceosome as target and effector of non-canonical ATM signalling. *Nature*, 523(7558):53–58, July 2015.

[229] V. G. Tusher, R. Tibshirani, and G. Chu. Significance analysis of microarrays applied to the ionizing radiation response. *Proceedings of the National Academy of Sciences*, 98(9):5116–5121, Apr. 2001.

[230] S. H. Um, F. Frigerio, M. Watanabe, F. Picard, M. Joaquin, M. Sticker, S. Fumagalli, P. R. Allegrini, S. C. Kozma, J. Auwerx, and G. Thomas. Absence of S6K1 protects against age- and diet-induced obesity while enhancing insulin sensitivity. *Nature*, 431(7005):200–205, Sept. 2004.

[231] C. Van Buskirk and P. W. Sternberg. Epidermal growth factor signaling induces behavioral quiescence in Caenorhabditis elegans. *Nature neuroscience*, 10(10):1300–1307, Oct. 2007.

[232] M. van de Ven, J. O. Andressoo, V. B. Holcomb, M. von Lindern, W. M. C. Jong, C. I. De Zeeuw, Y. Suh, P. Hasty, J. H. J. Hoeijmakers, G. T. J. van der Horst, and J. R. Mitchell. Adaptive stress response in segmental progeria resembles long-lived dwarfism and calorie restriction in mice. *PLoS Genetics*, 2(12):e192, Dec. 2006.

[233] G. T. van der Horst, H. van Steeg, R. J. Berg, A. J. van Gool, J. de Wit, G. Weeda, H. Morreau, R. B. Beems, C. F. van Kreijl, F. R. de Gruijl, D. Bootsma, and J. H. Hoeijmakers. Defective transcription-coupled repair in Cockayne syndrome B mice is associated with skin cancer predisposition. *CELL*, 89(3):425–435, May 1997.

[234] I. van der Pluijm, G. A. Garinis, R. M. C. Brandt, T. G. M. F. Gorgels, S. W. Wijnhoven, K. E. M. Diderich, J. de Wit, J. R. Mitchell, C. van Oostrom, R. Beems, L. J. Niedernhofer, S. Velasco, E. C. Friedberg, K. Tanaka, H. van Steeg, J. H. J. Hoeijmakers, and G. T. J. van der Horst. Impaired Genome Maintenance Suppresses the Growth Hormone–Insulin-Like Growth Factor 1 Axis in Mice with Cockayne Syndrome. *PLoS Biology*, 5(1):e2–16, Dec. 2006.

[235] M. R. Van Gilst, H. Hadjivassiliou, A. Jolly, and K. R. Yamamoto. Nuclear hormone receptor NHR-49 controls fat consumption and fatty acid composition in C. elegans. *PLoS Biology*, 3(2):e53, Feb. 2005.

[236] G. van Meer, D. R. Voelker, and G. W. Feigenson. Membrane lipids: where they are and how they behave. *Nature Reviews Molecular Cell Biology*, 9(2):112–124, Feb. 2008.

[237] J. Venema, L. H. Mullenders, A. T. Natarajan, A. A. van Zeeland, and L. V. Mayne. The genetic defect in Cockayne syndrome is associated with a defect in repair of UV-induced DNA damage in transcriptionally active DNA. *Proceedings of the National Academy of Sciences*, 87(12):4707–4711, June 1990.

[238] J. Vijg and Y. Suh. Genome Instability and Aging. *Annual Review of Physiology*, 75(1):645–668, Feb. 2013.

[239] J. A. Vizcaíno, A. Csordas, N. del Toro, J. A. Dianes, J. Griss, I. Lavidas, G. Mayer, Y. Perez-Riverol, F. Reisinger, T. Ternent, Q.-W. Xu, R. Wang, and H. Hermjakob. 2016 update of the PRIDE database and its related tools. *Nucleic Acids Research*, 44(D1):D447–56, Jan. 2016.

[240] T. L. Vrablik and J. L. Watts. Emerging roles for specific fatty acids in developmental processes. *Genes & Development*, 26(7):631–637, Apr. 2012.

[241] M. Wakasugi, M. Shimizu, H. Morioka, S. Linn, O. Nikaido, and T. Matsunaga. Damaged DNA-binding protein DDB stimulates the excision of cyclobutane pyrimidine dimers in vitro in concert with XPA and replication protein A. *Journal of Biological Chemistry*, 276(18):15434–15440, May 2001.

[242] D. M. Walther, P. Kasturi, M. Zheng, S. Pinkert, G. Vecchi, P. Ciryam, R. I. Morimoto, C. M. Dobson, M. Vendruscolo, M. Mann, and F. U. Hartl. Widespread Proteome Remodeling and Aggregation in Aging C. elegans. *CELL*, 161(4):919–932, May 2015.

[243] T. C. Walther and R. V. Farese. Lipid droplets and cellular lipid metabolism. *Annual review of biochemistry*, 81(1):687–714, 2012.

[244] Y. Wang and D. E. Levy. C. elegans STAT Cooperates with DAF-7/TGF-β Signaling to Repress Dauer Formation. *Current Biology*, 16(1):89–94, Jan. 2006.

[245] Y. Wang, N. Zhang, L. Zhang, R. Li, W. Fu, K. Ma, X. Li, L. Wang, J. Wang, H. Zhang, W. Gu, W.-G. Zhu, and Y. Zhao. Autophagy Regulates Chromatin Ubiquitination in DNA Damage Response through Elimination of SQSTM1/p62. *Molecular Cell*, 63(1):34–48, July 2016.

[246] G. Weeda, I. Donker, J. de Wit, H. Morreau, R. Janssens, C. J. Vissers, A. Nigg, H. van Steeg, D. Bootsma, and J. H. Hoeijmakers. Disruption of mouse ERCC1 results in a novel repair syndrome with growth failure, nuclear abnormalities and senescence. *Current Biology*, 7(6):427–439, June 1997.

[247] L. Whiley, A. Sen, J. Heaton, P. Proitsi, D. García-Gómez, R. Leung, N. Smith, M. Thambisetty, I. Kloszewska, P. Mecocci, H. Soininen, M. Tsolaki, B. Vellas, S. Lovestone,

C. Legido-Quigley, and AddNeuroMed Consortium. Evidence of altered phosphatidylcholine metabolism in Alzheimer's disease. *Neurobiology of aging*, 35(2):271–278, Feb. 2014.

[248] S. Wolff, H. Ma, D. Burch, G. A. Maciel, T. Hunter, and A. Dillin. SMK-1, an Essential Regulator of DAF-16-Mediated Longevity. *CELL*, 124(5):1039–1053, Mar. 2006.

[249] S. Wolters and B. Schumacher. Genome maintenance and transcription integrity in aging and disease. *Frontiers in Genetics*, 4, 2013.

[250] S. Wook Oh, A. Mukhopadhyay, B. L. Dixit, T. Raha, M. R. Green, and H. A. Tissenbaum. Identification of direct DAF-16 targets controlling longevity, metabolism and diapause by chromatin immunoprecipitation. *Nature Genetics*, 38(2):251–257, Dec. 2005.

[251] S. Wullschleger, R. Loewith, and M. N. Hall. TOR signaling in growth and metabolism. *CELL*, 124(3):471–484, Feb. 2006.

[252] X. Xu, P. Gopalacharyulu, T. Seppänen-Laakso, A.-L. Ruskeepää, C. C. Aye, B. P. Carson, S. Mora, M. Orešič, and A. A. Teleman. Insulin signaling regulates fatty acid catabolism at the level of CoA activation. *PLoS Genetics*, 8(1):e1002478, Jan. 2012.

[253] J. K. Yao and G. M. Rastetter. Microanalysis of complex tissue lipids by high-performance thin-layer chromatography. *Analytical biochemistry*, 150(1):111–116, Oct. 1985.

[254] Y.-j. You, J. Kim, M. Cobb, and L. Avery. Starvation activates MAP kinase through the muscarinic acetylcholine pathway in Caenorhabditis elegans pharynx. *Cell Metabolism*, 3(4):237–245, Apr. 2006.

[255] Y. H. Zeidan and Y. A. Hannun. Activation of acid sphingomyelinase by protein kinase Cdelta-mediated phosphorylation. *Journal of Biological Chemistry*, 282(15):11549–11561, Apr. 2007.

[256] Y. H. Zeidan, B. X. Wu, R. W. Jenkins, L. M. Obeid, and Y. A. Hannun. A novel role for protein kinase Cdelta-mediated phosphorylation of acid sphingomyelinase in UV light-

induced mitochondrial injury. *FASEB journal : official publication of the Federation of American Societies for Experimental Biology*, 22(1):183–193, Jan. 2008.

[257] L. Zeng, G.-Z. Wu, K. J. Goh, Y. M. Lee, C. C. Ng, A. B. You, J. Wang, D. Jia, A. Hao, Q. Yu, and B. Li. Saturated Fatty Acids Modulate Cell Response to DNA Damage: Implication for Their Role in Tumorigenesis. *PLoS ONE*, 3(6):e2329–9, June 2008.

[258] H. Zhang, N. Abraham, L. A. Khan, and V. Gobel. RNAi-based biosynthetic pathway screens to identify in vivo functions of non-nucleic acid-based metabolites such as lipids. *Nature Protocols*, 10(5):681–700, May 2015.

[259] H. Zhang, J. T. Chang, B. Guo, M. Hansen, K. Jia, A. L. Kovács, C. Kumsta, L. R. Lapierre, R. Legouis, L. Lin, Q. Lu, A. Meléndez, E. J. O'Rourke, K. Sato, M. Sato, X. Wang, and F. Wu. Guidelines for monitoring autophagy in Caenorhabditis elegans. *Autophagy*, 11(1):9–27, 2015.

[260] Y. Zhang, X. Zou, Y. Ding, H. Wang, X. Wu, and B. Liang. Comparative genomics and functional study of lipid metabolic genes in Caenorhabditis elegans. *BMC genomics*, 14(1):164, 2013.

[261] H. Zhu, H. Shen, A. K. Sewell, M. Kniazeva, and M. Han. A novel sphingolipid-TORC1 pathway critically promotes postembryonic development in Caenorhabditis elegans. *eLife*, 2:e00429–19, 2013.

[262] R. Zoncu, A. Efeyan, and D. M. Sabatini. mTOR: from growth signal integration to cancer, diabetes and ageing. *Nature Reviews Molecular Cell Biology*, 12(1):21–35, Jan. 2011.

Acknowledgements

I want to thank my supervisor Prof. Dr. Björn Schumacher for the support and guidance during my PhD path. In addition, I would like to thank my thesis committee, Prof. Dr. Siegfried Roth and Prof. Dr. Markus Krüger, for their insightful comments and suggestions, and Dr. Ashley Williams for taking the protocol. My sincere thanks also goes to Prof. Dr. Susanne Brodesser, for being an amazing guide through the "world of Lipids", always providing precious help and advice. My sincere gratitude goes to Hendrik Nolte, a priceless support for all my work and my knowledge regarding proteomics and data analysis. You have been a colleague but also a friend, thank you for being there whenever I needed you.I want to thank also Peter Frommolt, head of Bioinformatics Facility in CECAD, for the informatics support.

The funding of my PhD study comes from the european Marie Curie FP7 ITN CodeAge fellowship program. These years have been for me a unique experience of life and work. I met great persons across a well organized and supported internationsl network, and I had the opportunity to attend many training workshops and interesting conferences. My sincere gratitude goes in particular to Heike Brucherseifer, the amazing coordinator of the network, which in these years helped and supported me like a mother will do, I really felt at home.

I would like to thank all my fellow labmates, across these years many people joined, many left, but together we have always been the soul of the lab. Now I am writing sitting in a fancy office in front of two fancy screens, but I will never forget my first day in the old lab, close to the bin, behind a door, listening to the steps of the boss coming or leaving. The fridays were the most waited appointments to drink a "beer on the wall", with the bossy Maria turning always super drunk, the statuary Alex pumping his muscles while drinking proteins'milkshakes and Vip and Juju cheering with the polish beer Tiskie. But the friday evening could turn also

more exciting for special celebration, hanging out in the social room drinking the FLIMM Waldmeister from the 50 ml Falcons and litterary speaking all the languages of the world. That's the time when the nice love story between Najmeh and Markus started, four years passed and now you guys are happily married, I wish you all the best (careful Markus that Najmeh is becoming a Taekwon-do expert)! Than you Markussien for helping in the preparation of Zusammenfassung, I will reward your effort with super tiramisu', I promise.

Vip a special thanks goes to you, my mentor and my support, you have been a good teacher, while me a really annoying student (Juju will say "nothing we don't know"), although now I became a bleaching-proteomic-lipidomic-data analysis-whatelseyoucanthinkaboutit expert. We all really miss you here, now the friday beer sessions became more sporadic and when I am in the lab I am annoying the poor Juju (Ms Juliana Bianco) with my karaoke sessions: he gets music stucked in his head and hates me. Then he turns to Arturito and they discuss about movies and videogames (Arturito and Jenny are really pro, lately they did many videogames competition). Arturito spread also its Rubik cube mania to Yao (congrats for the driving licence achievement!) and introduced great manga and animation to Hui-Ling (whom I thank a lot for the amazing LaTEX support, without you I would have already freak out). I would like to thank Rania for the session of girly-chatting, the patience in guiding me through worm pathogen assays and for proof-reading my manuscript, I really appreciate.

Many many thanks goes to Jenny, you have been always a great support for all of us, and I am really sorry for annoying you with all the "Jenny may I ask you?Jenny can you order?Jenny do you know where is this/that?Jenny may you translate this?". You had next to you two amazing colleagues, that I want also to thank since I have annoyed them too: Josi and Julia, forming the JJ team! Thank you Michi and Laia for the stimulating discussions and technical support during the development of my PhD, and for the contributing to my manuscript. I would like to thank my forever neighbour Matthias and Rena, you guys have been amazing friends!Ok ok Matthias I will remove the bracelet! A great thank you to the office neighbour Ash, that is becoming more italian than me while visiting so often Bergamo, and Aakanksha, at my eyes the cells/mice goddes! Besides, I would like to thank also the new PhD students that recently joined the lab, Chara, Pavana and Simon, may your PhD be great! I also appreciate the administrative

support of Kim, and her patience in filling with me everytime all the annoying documents.

Last but not the least my heartfelt thanks goes to my girls, Flavia and Amanda, for being colleagues but also friends. You are always there when is time to go out enjoying life and also whenever problems arise: I love this multitasking friendship, is priceless!We should cheer with a Spritz!

A big hug and thank to my Italian team, blood of my blood, that constantly make me feel like home: Tiz, my Tiz, I miss you a lot, you were and are my source of inspiration, but no worries there are still Ale, Fla and Sara here to cheer me up! Ale with his funny jokes "in romanesco", Fla with our regular chatting/updating of our lives (we are 30 km apart but is still like working cheek to cheek) and Sara, my personal life/shopping/training/motivational assistant (thanks also to Giacomo for being such an amazing chef).

My greatest thanks goes to my family, to my uncle Gianluca, always on my side, and to my beloved Stefano. You believed in me since we met and you pushed me to follow my goals, to become a good scientists and a better person. I will be here to support you in the same way, thank you for being always on my side, my half-apple.

My heartfelt thanks goes to the most important pieces of this big puzzle of my life, my parents, that with their effort and stubborness allowed me to study and pushed me to become the person I am today...dad I know you are proud of me, I miss you so much.

Homo faber fortunae suae.

Erklärung

Ich versichere, dass ich die von mir vorgelegte Dissertation selbständig angefertigt, die benutzten Quellen und Hilfsmittel vollständig angegeben und die Stellen der Arbeit - einschließlich Tabellen, Karten und Abbildungen, die anderen Werken im Wortlaut oder dem Sinn nach entnommen sind - in jedem Einzelfall als Entlehnung kenntlich gemacht habe; dass diese Dissertation noch keiner anderen Fakultät oder Universität zur Prüfung vorgelegen hat; dass sie - abgesehen von unten angegebenen Teilpublikationen - noch nicht veröffentlicht worden ist sowie, dass ich eine solche Veröffentlichung vor Abschluss des Promotionsverfahrens nicht vornehmen werde. Die Bestimmungen der Promotionsordnung sind mir bekannt. Die von mir vorgelegte Dissertation ist von Prof. Dr. Björn Schumacher betreut worden.

Lebenslauf

Persönliche Daten

Name: Diletta Edifizi

Geburtsdatum: 10.09.1988

Geburtsdort: Padova, Italy

Nationalitt : italienisch

Anschrift: Sankt Vither strasse 12, 50933 Köln

E-Mail Adresse: edifizid@uni-koeln.de

Studium

2013 - 2017

Promotionsstudent im Fachgenetik

Doktorarbeit an der Universität zu Köln in der Arbeitsgruppe von Herrn Prof. Dr. Björn Schumacher.

2010 - 2012

MSc. im Molekular Biologie und Genetik

Studium an der Universität Pavia, Italien, und Praktikum an dem Neurobiologie Institut in der Arbeitsgruppe von Frau Dr.Cristina Cereda.

2007 - 2010

BSc. im Molekular Biologie

Studium an der Universität Padova, Italien, und Praktikum an dem Pharmakologie Institut in der Arbeitsgruppe von Frau Prof.Maura Floreani.

Schulbildung

2002 - 2007

Staatsexamen und Approbation, Padova, Italien.

Stipendien und Auszeichnungen

2016 - 2017

Doktorandenstipendium

Exzellenzcluster Cellular Stress Responses in Aging- associated Diseases (CECAD), Universitt zu Köln, Köln, Deutschland.

2013 - 2016

Doktorandenstipendium

Europäisch Marie Curie FP7 Initial Training Network (CodeAge 316354)

2013

Rotary Club Preise fr Master Diplomarbeit Response of SOD1 to oxidative stress in a cellular model of neurodegeneration and in ALS patients.

Konferenz-Teilnahmen

2013 - 2016

Mündliche Präsentation

CodeAge Annual Meetings: 1st in Mailand (Italy), 2nd in Heraklion (Krete), 3rd and 4th in

Kln (Deutschland) and final conference in Heraklion (Krete).

2014

Posterpräsentation

The 30th Ernst Klenk Symposium in Molecular Medicine DNA Damage Response and Repair Mechanisms in Aging and Disease, Köln, Deutschland.

Posterpräsentation

CECAD Retreat, Köln, Deutschland.

2016

Posterpräsentation

The 2nd Cologne Ageing Conference, Köln, Deutschland.

Publikationen

2015

Genome Instability in Development and Aging: Insights from Nucleotide Excision Repair in Humans, Mice, and Worms.

Biomolecules